UC San Diego

UC San Diego Electronic Theses and Dissertations

Title

Biological and molecular characterization of lifeguard : an inhibitor of the Fas apoptotic pathway

Permalink

https://escholarship.org/uc/item/9jw1g90b

Author

Hurtado de Mendoza Casaus, Tatiana

Publication Date

2009

Peer reviewed|Thesis/dissertation

eScholarship.org Powered by the California Digital Library
University of California

UNIVERSITY OF CALIFORNIA, SAN DIEGO

Biological and Molecular Characterization of Lifeguard: An Inhibitor of the Fas Apoptotic Pathway

A dissertation submitted in partial satisfaction
of the requirements for the degree
Doctor of Philosophy

in

Biology

by

Tatiana Hurtado de Mendoza Casaus

Committee in charge:

Professor Inder M. Verma, Chair
Professor Webster Cavenee
Professor Ananda Goldrath
Professor William F. Loomis
Professor Dennis O'Leary
Professor Deborah Spector

2009

Copyright ©
Tatiana Hurtado de Mendoza Casaus, 2009
All rights reserved.

The Dissertation of Tatiana Hurtado de Mendoza Casaus is approved, and it is acceptable in quality and form for publication on microfilm and electronically:

_____

_____

_____

_____

_____

_____

Chair

University of California San Diego

2009

DEDICATION

I would like to dedicate this work to my family and my husband for their continued support through all the ups and downs that characterize an experimental thesis.

To my husband Bruno for sharing with me the experience of becoming a scientist and always encouraging me and supporting me in the tough moments. For his very valuable scientific advice and perspective.

To my parents for being supportive of me coming to San Diego for my education even if that meant being far from home. For their love, support and continued interest in my research. For all the times they came to visit.

To my two sisters that have also been a great emotional support and have become part of the lab for all the time they have spent there with me.

To my grandmother that has shown us how to age successfully and water ski at 87 years old.

Lastly I wanted to make a special dedication to Jason Hwang, who was the graduate student in the lab that started the work on Lifeguard.

TABLE OF CONTENTS

Signature page ……..……... iii

Dedication …….. iv

Table of Contents …….…….. v

List of Symbols …….. vi

List of Figures ……..…….. viii

Acknowledgements ……..…….. x

Curriculum Vitae ……..……...…… xiii

Abstract of the Dissertation ……..... xv

1 Introduction ……. 1

2 Generation and validation of the LFG knockdown and knockout mouse models ……...…….. 9

3 The antiapoptotic protein LFG plays a role in cerebellar cell survival ……... 20

4 A possible neuroprotective role for LFG after cerebral ischemia …… 45

5 LFG's role in the immune system …….……... 50

6 How does LFG protect from Fas mediated cell death? ……...…. 81

7 Additional findings in LFG knockdown mice …….. 110

Appendices ……...…….....…….. 131

References ……..... 141

LIST OF SYMBOLS

AICD	Activation Induced Cell Death
AIP4	Atrophin 1 Interacting Protein 4
ATP	Adenosine Triphosphate
BACE 1	β-Secretase 1
BI-1	Bax Inhibitor 1
Bid	BH3 Interacting Domain death agonist
C’	Carboxy terminus
ΔC	Carboxy terminal deletion
CA	Cornu Ammonis
CB	Calbindin
CD	Cluster of Differentiation
CGN	Cerebellar Granule Neurons
CHX	Cyclohexamide
CNS	Central Nervous System
CRD	Cysteine Rich Domains
DD	Death Domain
DED	Death Effector Domain
DG	Dentate Gyrus
DISC	Death Induced Signaling Complex
DN	Double Negative
DNA	Deoxyribonucleic acid
DP	Double Positive
E18	Embryonic day 18
EGL	External Granular Layer
FACS	Fluorescent Activated Cell Sorter
FADD	Fas Associated Death Domain containing protein
FasL	Fas ligand
FasR	Fas receptor
FITC	Fluorescein Isothiocyanate
FLIP	FLICE inhibitor protein
GFAP	Glial Fibrillary Acidic Protein
GFP	Green Fluorescent Protein
Gr	Granulocytes
GluR2	Glutamate Receptor 2
H&E	Hematoxylin and Eosin
IGL	Internal Granular Layer
IκB	Inhibitor of kappa B
IKK	Inhibitor of kappa B Kinase
IP	Immunoprecipitation
ISH	*In situ* hybridization
JNK	Jun N terminal kinase
kDa	kilo Dalton
KO	Knockout

LCMV	Lymphocytic Choriomeningitis Virus
LFG	Lifeguard
Mac	Macrophages
MCAO	Medial Cerebral Artery Occlusion
MHC	Major Histocompatibility Complex
ML	Molecular layer
MW	Molecular Weight
N’	Amino terminus
ΔN	Amino terminal deletion
NF-κB	Nuclear Factor kappa B
NGF	Nerve Growth Factor
NMP35	Neural Membrane Protein 35
OB	Olfactory Bulb
P0	Postnatal day 0
PC	Purkinje cell
PCL	Purkinje Cell Layer
PI3K	Phosphoinositide 3 Kinase
PLAD	Pre-Ligand Assembly Domain
PV	Parvalbumin
QPCR	Quantitative Polymerase Chain Reaction
RAG	Recombination Activating Gene
RNA	Ribonucleic acid
RNAi	RNA interference
siRNA	small interfering RNA
TCR	T Cell Receptor
TNF	Tumor Necrosis Factor
TNFR	Tumor Necrosis Factor Receptor
TRADD	TNF Associated Death Domain containing protein
TRAF	TNF Receptor Associated Factor
TRAIL	TNF-Related Apoptosis-Inducing Ligand
TTC	2, 3, 5-Triphenyltetrazolium Chloride
UWB	Western Blot
WCE	Whole Cell Extract
WT	Wild type

LIST OF FIGURES

Figure 1.1- Schematic representation of the Fas signaling pathway ……..... 7
Figure 1.2- Schematic representation of lifeguard (LFG) …….. 8
Figure 2.1- Effective downregulation of overexpressed LFG by siRNA ……. 12
Figure 2.2- LFG knockdown in neuroblastoma cells NIE 115 ……. 13
Figure 2.3- Schematic representation of the lentiviral transgenesis technique and the lentiviral vector containing the LFG siRNA ……. 14
Figure 2.4- Validation of LFG knockdown *in vivo* …….. 15
Figure 2.5- Schematic representation of the knockout targeting vector and a topology map of LFG showing where the insertion takes place …….. 18
Figure 2.6- Validation of LFG knockout mice by QPCR …… 19
Figure 2.7- Expression of β-galactosidase in LFG knockout and heterozygous mice ……. 19
Figure 3.1- LFG's expression pattern in the CNS and downregulation in LFG knockdown mice …… 26
Figure 3.2- Cerebellar phenotype in early postnatal stages …….. 28
Figure 3.3- Delayed Purkinje cell differentiation ……. 31
Figure 3.4- Abnormal Purkinje cell morphology and increased apoptosis …….. 33
Figure 3.5- Definition of the Purkinje and IGL fields ……. 35
Figure 3.6- Increased apoptosis in Fas treated LFG knockout Purkinje fields ……. 36
Figure 3.7- Increased apoptosis in Fas treated LFG knockout Purkinje fields ……. 37
Figure 3.8- Increased apoptosis in LFG knockout IGL fields ……..... 38
Figure 3.9- Increased apoptosis in LFG knockout IGL fields …….. 39
Figure 4.1- TTC staining of LFG knockout and wild type brains after stroke ……. 49
Figure 5.1- Schematic representation of T cell development ……... 55
Figure 5.2- LFG's expression pattern in T cell subsets …… 57
Figure 5.3- LFG's expression pattern in T cell subsets …… 58
Figure 5.4- LFG's expression pattern in DN T cell subpopulations ……. 59
Figure 5.6- Increased cell death in Fas treated siLFG thymocytes ……... 64
Figure 5.7- LFG expression in wild type thymus is variable …… 68
Figure 5.8- Thymocyte subsets of 5 week-old mice, comparison between strains .. 69
Figure 5.9- Schematic representation of the generation of the bone marrow chimeras ……. 71
Figure 5.10- Representative FACS plot of peripheral blood analysis …… 74
Figure 5.11- Decrease of CD4 and CD8 T cell knockout vs wild type ratio overtime ……. .75
Figure 5.12- Increase of knockout vs wild type ratio of B cells overtime …… .76
Figure 5.13- Decrease of granulocyte and macrophage knockout vs wild type ratio overtime ……. 77
Figure 5.14- Schematic representation of the phases of the immune response …….. 80
Figure 6.1- Testing of LFG siRNAs ……..… 85
Figure 6.2- Functional test of LFG siRNAs ……..…… 86
Figure 6.3- Caspase 8 activation is decreased in the presence of LFG ……..……... 89
Figure 6.4- Caspase 3 activation is decreased in the presence of LFG ……..……... 90

Figure 6.5- DISC immunoprecipitation ……..…… 91
Figure 6.6- LFG interacting partners ……..…… 94
Figure 6.7- LFG is ubiquitinated ……..…..... 97
Figure 6.8- LFG interacts with AIP4 ……..….. 98
Figure 6.9- LFG downregulates AIP4 expression ……..….. 99
Figure 6.10- Map of LFG deletion mutants ……..… 103
Figure 6.11- Expression levels of LFG deletion mutants ……..... 104
Figure 6.12- Apoptosis assay of LFG deletion mutants …….. 105
Figure 6.13- LFG protects from apoptosis in a dose dependent manner ……. 106
Figure 7.1- siLFG mice have underdeveloped lungs at birth ……. 112
Figure 7.2- LFG expression in the kidneys ……..... 113
Figure 7.3- siLFG mice have underdeveloped kidneys ……. 114
Figure 7.4- Validation of LFG knockdown in the kidney ……. 114
Figure 7.5- siLFG mice have delayed follicle formation in the spleen ……. 116
Figure 7.6- LFG expression in spleen by QPCR ……..... 117
Figure 7.7- LFG expression in thymus by QPCR ……. 118
Figure 7.8- Increased apoptosis in siLFG P0 thymus …… 119
Figure 7.9- LFG expression pattern in the brain and knockdown validation …… 121
Figure 7.10- Cytoarchitechtural analysis of the brain by Nissl staining ……. 122
Figure 7.11- Cytoarchitechtural analysis of the cerebellum by Nissl staining …… 123
Figure 7.12- Analysis of cortical layers by ISH …….. 125
Figure 7.13- siLFG mice have brain hemorrhages and larger blood vessels …….. 128
Figure 7.14- Astrocyte recruitment to blood vessels in siLFG mice …….. 129
Figure 7.15- Analysis of blood vessel leakiness ……. 130
Table 5.1- T cell subpopulations in wild type and siLFG mice at P0 ……..... 60
Table 5.2- T cell subpopulations in wild type and siLFG mice at 5 weeks ….…. 61
Table 5.3- Absolute number of total T cells, DP cells, thymus and body weight of 5 week-old wild type and siLFG mice …… 62
Table 5.4- DN T cell subpopulations in wild type and siLFG mice at 5 weeks ... 62
Table 5.5- Apoptosis in the different T cell subpopulations of wild type and siLFG mice at 5 weeks ……...… 63

ACKNOWLEDGEMENTS

I would like to acknowledge Professor Inder M. Verma for his support as the chair of my committee and my advisor. His guidance has been very valuable for my work and he has opened up many doors for collaborations in several different areas of research.

I would also like to acknowledge Professor William F. Loomis who was my first mentor and gave me the opportunity to start research in his laboratory, teaching me how to become a scientist.

I would like to thank Professor Ananda Goldrath and Professor Dennis O'Leary for helpful discussions and advice.

Carlos Perez-Garcia for his contribution to the characterization of the brain phenotype, I have learned a lot from him and it has been a great personal and professional experience to collaborate with him.

Bjarne Woods and Fei Liu were my collaborators in the immune system project, their contribution to this part of the project has been very important and we have had a great time working together.

Nien Hoong, thanks to his expertise we could generate the LFG knockdown mice.

I also want to thank all the members of the Verma lab for providing a great environment to work. I have learned a lot from everyone and I really appreciate your friendship.

Chapter 2, in part is currently being prepared for submission for publication of the material. Hurtado de Mendoza, Tatiana; Perez-Garcia, Carlos G; Kroll, Todd; Hoong, Nien; O'Leary, Dennis and Verma, Inder M. The Antiapoptotic Protein Lifeguard Plays a Role in Cerebellar Cell Survival. The dissertation author was the primary investigator and author of this material.

Chapter 3, in full is currently being prepared for submission for publication of the material. Hurtado de Mendoza, Tatiana; Perez-Garcia, Carlos G; Kroll, Todd; Hoong, Nien; O'Leary, Dennis and Verma, Inder M. The Antiapoptotic Protein Lifeguard Plays a Role in Cerebellar Cell Survival. The dissertation author was the primary investigator and author of this material.

Chapter 4, in part will be prepared for submission for publication of the material. Li Yang and Scott McKercher are contributing to this ongoing work. The dissertation author was the primary investigator and author of this material.

Chapter 5, in part is currently being prepared for submission for publication of the material. Hurtado de Mendoza, Tatiana; Woods, Bjarne; Liu, Fei and Verma, Inder M. The Role of Lifeguard in the Immune System. The dissertation author was the primary investigator and author of this material.

Chapter 6, in part is currently being prepared for submission for publication of the material. Hurtado de Mendoza, Tatiana; Perez-Garcia, Carlos G; Kroll, Todd; Hoong, Nien; O'Leary, Dennis and Verma, Inder M. The Antiapoptotic Protein Lifeguard Plays a Role in Cerebellar Cell Survival. The dissertation author was the primary investigator and author of this material.

Chapter 7, in part will be prepared for submission for publication of the material. Sara Weiss contributed to this work. The dissertation author was the primary investigator and author of this material.

CURRICULUM VITAE

EDUCATION

2002-2009 Doctor of Philosophy in Biology, University of California, San Diego

1994-2000 Bachelor of Science, Universidad Autonoma de Madrid
Major- Biochemistry and Molecular Biology

RESEARCH EXPRERIENCE

2003-2009 Dr. Inder M. Verma.
Laboratory of Genetics, The Salk Institute for Biological Studies

2000-2003 Dr. Wiliam F. Loomis.
Division of Biology, University of California, San Diego

TEACHING EXPERIENCE

University of California, San Diego, Division of Biology:

2003 Biochemistry, Laboratory Instructor

2004 AIDS in Science and Society, Teaching Assistant

2005 Molecular Biology of Disease, Teaching Assistant

MEETINGS

2006 Division of Biology Retreat Speaker

2007 Society for Neuroscience meeting. Lifeguard knockdown suggests specific roles in the survival of certain cell populations in the CNS and brain angiogenesis.

2009 Society for Neuroscience meeting. The antiapoptotic protein lifeguard plays a role in cerebellar cell survival.

FELLOWSHIPS

2004-2006 Legler Benbough Foundation

2007 The Chapman Charitable Trust

PUBLICATIONS

Hurtado de Mendoza, T., Perez-Garcia, C.G., Kroll, T., Hoong, N., O'Leary, D.M, and Verma, I.M. The Antiapoptotic Protein Lifeguard Plays a Role in Cerebellar Cell Survival (In preparation).

Hurtado de Mendoza, T., Woods, N.B., Liu, F., and Verma I.M. The Role of Lifeguard in the Immune System (In preparation).

Xia, Y., Padre, R.C., **Hurtado de Mendoza, T.**, Bottero, V., Tergaonkar, V.B., and Verma, I.M. (2009). Phosphorylation of p53 by IkappaB kinase 2 Promotes its Degradation by beta-TrCP. **Proc Natl Acad Sci**, 106, 2629-34.

ABSTRACT OF THE DISSERTATION

Biological and Molecular Characterization of Lifeguard: An Inhibitor of the Fas Apoptotic Pathway

by

Tatiana Hurtado de Mendoza Casaus

Doctor of Philosophy in Biology

University of California, San Diego, 2009

Professor Inder M. Verma, Chair

Apoptosis or programmed cell death participates in several biological processes, including embryonic development, tissue remodeling, tumor surveillance and immune system regulation. The Fas pathway is among the most studied apoptotic

pathways. Its misregulation can contribute to many diseases including autoimmunity and cancer.

Lifeguard (LFG) is a membrane protein isolated as an inhibitor of the Fas apoptotic pathway. LFG has wide tissue distribution with highest expression in the brain, predominantly in neurons of hippocampus and cerebellum. In order to study the biological role of LFG, we used two different models; mice with reduced LFG expression by siRNA lentiviral transgenesis and LFG null mice. Phenotypic characterization of these mice indicated that loss of LFG affected several organs, such as lungs, kidneys, spleen, thymus and brain. The work presented here reports the investigation of LFG's role in the CNS (1), in the immune system (2) as well as the molecular and biochemical characterization of LFG (3).

1. We focused in the study of LFG's biological role in the brain, especially in cerebellum, where the phenotype was most severe. LFG affected cerebellar size in early development, internal granular layer size, and Purkinje cell differentiation, morphology and susceptibility to apoptosis.

In the last decade there has been increasing evidence for an involvement of the Fas apoptotic pathway in cerebral ischemia. Therefore, we have started to test the hypothesis that LFG could have a neuroprotective role against stroke, by inhibiting Fas induced apoptosis.

2. We also investigated the role of LFG in the immune system, especially in T cell development. Based on LFG's expression pattern and on the phenotypical characterization of the T cell subpopulations in the thymus of siLFG mice we

hypothesized that LFG is a survival factor whose expression is upregulated after the major selection checkpoints in T cell development.

3. We demonstrated that LFG blocks the Fas apoptotic cascade at the level of caspase 8 activation. We also showed that LFG is ubiquitinated and it interacts with the E3 Ubiquitin ligase AIP4. Finally, deletion mutant studies revealed that the last intracellular loop and transmembrane domain of LFG are essential for its antiapoptotic function.

1

INTRODUCTION

Lifeguard and the Fas apoptotic pathway

INTRODUCTION

Apoptosis is a mechanism of programmed cell death (Kerr et al., 1972). This process is evolutionarily conserved and is defined by morphological changes and biochemical events that differ from those of necrotic cell death.

Programmed cell death is involved in embryonic development, tissue remodeling, tumor surveillance and regulation of the immune system. Dysfunction of this process can lead to serious developmental defects, oncogenesis as well as autoimmune and degenerative diseases.

Apoptosis can be triggered by intrinsic or extrinsic pathways. The intrinsic pathway can be initiated by oxidative stress, perturbed calcium homeostasis, alkylating agents, or ultraviolet and ionizing radiation, leading to cell death via the release of cytochrome c from the mitochondria and subsequent activation of caspases. The extrinsic pathway is mediated by specific cell surface receptors (death receptors) that, upon binding to their ligands, will also lead to the activation of caspases and ultimately to the death of the cell. One example of the extrinsic pathway is that mediated by the superfamily of the tumor necrosis factor receptors (TNFR) (for review see (Dempsey et al., 2003)). Upon binding to their specific ligands, multiple signal transduction pathways can be activated by recruiting different intracellular adaptors, an event that can lead to different outcomes. For instance, apoptosis will occur if death domain containing adaptors, such as Fas associated death domain containing protein (FADD) are recruited, while survival, differentiation, immune or inflammatory responses will occur if proteins from the TNF Receptor Associated factor (TRAF) family of adaptors are recruited.

Fas receptor (FasR) (also called Apo-1 or CD95) is one of the better characterized TNFR family members (Peter and Krammer, 2003). It is a type I transmembrane protein whose extracellular domain consists of three repeats of cysteine rich domains (CRD), formed by disulfide bonds; the interaction with Fas ligand (FasL) occurs mainly in the second and third CRD (from the N'). A preligand assembly domain (PLAD) in CRD 1 is necessary for the formation of Fas trimers, required for signal transduction (Golstein, 2000; Siegel et al., 2000). The intracellular domain of Fas, called death domain (DD), serves as a protein-docking site that will transduce the conformational changes induced by the binding of the ligand (Weber and Vincenz, 2001). Several adaptor proteins, including FADD or the Fas death domain–associated protein DAXX interact with the death domains of Fas to transduce the apoptotic signals (Nagata, 1999; Wallach et al., 1999). More recently, Fas signaling has also been associated with non-apoptotic outcomes, but the pathways involved are poorly understood.

In the canonical Fas-induced apoptosis, binding of FasL to the FasR is followed by the recruitment of FADD. In turn, FADD interacts with the protease caspase 8 via a death effector domain (DED) common to both proteins, to form the so-called death induced signaling complex (DISC). DISC formation results in autoproteolytic processing of caspase 8 and the release of its active form (Boatright et al., 2003; Earnshaw et al., 1999). Subsequently, the apoptotic signal can follow two pathways (Krammer, 2000): 1) Activated caspase 8 directly activates caspase 3 with subsequent activation of other proteases, lipases and DNAses (Figure 1.1). Cells in which this cascade occurs are referred to as type I cells. 2) Activated caspase 8 cleaves

the BH3 interacting domain death agonist (Bid) inducing the mitochondrial pathway that will lead to the release of cytochrome c and activation of effector caspases, an event occurring in cells referred to as type II (Li et al., 1998; Luo et al., 1998).

Lifeguard (LFG) is a molecule that inhibits Fas mediated apoptosis. LFG was cloned in our laboratory while searching for factors that could confer resistance to Fas mediated cell death (Somia et al., 1999). For this purpose, a retroviral based cDNA library from the human lung fibroblast FasL-insensitive cell line, MRC-5, was generated and used to transduce the human cervical adenocarcinoma cell line HeLa, which is sensitive to FasL. Transduced HeLa cells were treated for two weeks with the Fas agonistic antibody CH11. LFG was isolated as the most frequently occurring MRC-5 cDNA in the surviving cells.

Sequence analysis revealed a long open reading frame encoding a 316 aminoacid protein with a molecular weight of 34.6 kDa. Hydropathy plots predicted that LFG is a seven transmembrane protein, and PFAM assigned it to an uncharacterized family that shares a common signature in the region beginning with the third transmembrane domain until the middle of the fourth one (Figure 1.2).

The C terminal half of LFG has homology to a rat glutamate binding protein, the Drosophila NMDA receptor associated protein and two *C. elegans* proteins of unknown function. LFG was mapped to chromosome 12q13 by fluorescent *in situ* hybridization. Immunohistochemistry and Western blotting after cellular fractionation showed that LFG localized to the ER and plasma membrane.

The expression pattern of LFG in adult mice was determined by Northern blot on different tissues. LFG mRNA was found to be widely expressed with its highest

level in the brain. Within the brain, Northern blot and *in situ* hybridization showed expression in all the brain regions examined, predominantly in neurons from the hippocampus (mostly CA3) and cerebellum, while cells with glial morphology did not seem to express LFG.

Mouse and rat LFG homologues have been described. In rat, LFG was originally named neural membrane protein 35 (NMP35), as it was isolated from a screening searching for genes involved in the development of rat sciatic nerve. NMP35 transcripts and protein are strongly upregulated during postnatal development. *In situ* hybridization shows that it is widely distributed in the brain and spinal cord with a neuronal expression pattern. Within the neurons NMP35 is localized in dendrites and colocalizes with glutamate receptor 2 (GluR2) in the postsynaptic membrane, suggesting a possible role in synapses of the adult central nervous system (Schweitzer et al., 2002; Schweitzer et al., 1998b).

More recently a paper from Beier *et al* describes that the resistance to Fas mediated cell death observed in rat cerebellar granule neurons (CGNs) is mediated by PI3K-Akt dependant expression of LFG (Beier et al., 2005). Another group that studied the role of mouse LFG in cortical neurons and CGN reports that RNAi mediated downregulation of LFG sensitized CGNs and to a lesser extent cortical neurons to Fas mediated cell death. The same group also reported that LFG is found in lipid rafts. Upon FasL activation FasR is recruited to the lipid rafts together with caspase 8, but in the presence of LFG caspase activity is reduced (Fernandez et al., 2007a).

FasR belongs to the TNFR family and the apoptotic cascade from this group of receptors is very similar. Thus it was hypothesized that LFG may confer protection form TNF-mediated apoptosis. Surprisingly LFG did not provide any protection from TNF induced apoptosis, indicating its specificity for the Fas/FasL system. The TNFR and FasR signaling differ only in the requirement of TRADD for the TNFR pathway. Accordingly, three possible mechanisms of action were proposed and tested. 1) Downregulation of FasR in the cell surface; 2) Interference with FasL binding to the receptor; 3) Interference with the recruitment of FADD. None of these hypotheses proved to be correct (Somia et al., 1999).

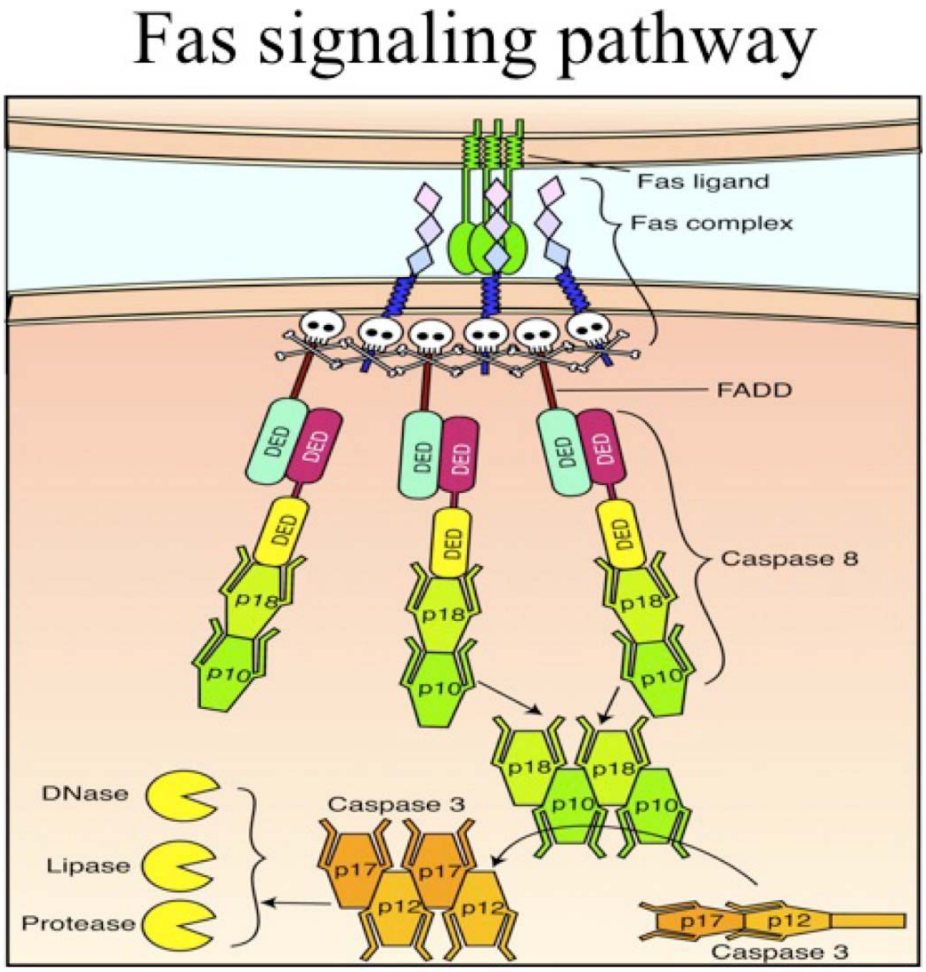

Figure 1.1- Schematic representation of the Fas signaling pathway. In the canonical Fas-induced apoptosis, binding of FasL to the FasR is followed by the recruitment of FADD. In turn, FADD interacts with the protease caspase 8 via a death effector domain (DED) common to both proteins, to form the so-called death induced signaling complex (DISC). DISC formation results in the autoproteolytic processing of caspase 8 and the release of its active form. Activated caspase 8 directly activates caspase 3 with subsequent activation of other proteases, lipases and DNAses, leading to the death of the cell.

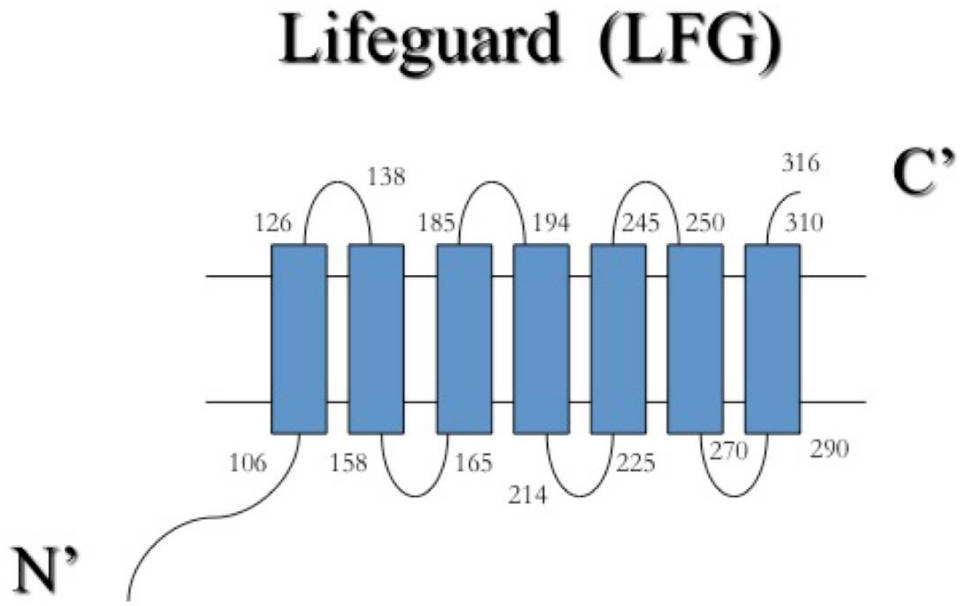

Figure 1.2- Schematic representation of Lifeguard (LFG). Hydropathy plots predict that LFG is a seven transmembrane protein with a cytosolic amino terminal (N') part and an extracellular carboxy terminal (C') part.

2

Generation and validation of the LFG knockdown and knockout mouse models

LFG knockdown mouse model

We generated mice with reduced LFG expression by lentiviral transgenesis and siRNA technology. Several siRNAs against mouse LFG were designed and cloned under the mouse U6 Pol III promoter into the U3 region of a lentiviral vector containing an eGFP cassette driven by the mouse PGK promoter. These constructs plus a control vector with a siRNA against GFP were tested by transfection into HEK293T cells together with a mouse LFG cDNA tagged in the C' with V5. Effective downregulation of the LFG protein was evaluated by Western blot with V5 antibody and demonstrated to be virtually complete (Figure 2.1). The validated siLFG lentiviral constructs and another one containing a siRNA that targets β-Secretase 1 (BACE 1) as a control, were used to generate lentiviruses and transduce NIE 115 mouse neuroblastoma cells that have endogenous LFG expression. Knockdown was assessed by QPCR. We used two different sets of LFG specific primers and cyclophilin primers as normalizers. Both LFG specific siRNAs successfully downregulated endogenous LFG expression (90-95%) (Figure 2.2).

Transduction of B6D2 fertilized eggs at the two-cell stage was performed with the virus expressing the LFG siRNA. After development to blastocyst stage they were implanted into ICR pseudopregnant females and progeny were born and bred to generate the siLFG line. A schematic representation of the design and procedure for the generation of LFG siRNA mice is shown in Figure 2.3.

In order to verify *in vivo* knockdown, radioactive *in situ* hybridization (ISH) with a LFG probe was performed in whole body sagittal sections of P0 wild type and siLFG mice. At this developmental stage the highest LFG expression in wild type

mice was found in the liver; where a significant reduction of the signal was observed in the siLFG mice (Figure 2.4).

The characterization of these mice revealed several interesting phenotypes affecting primarily lungs, heart, kidneys, spleen, thymus and brain. We also observed a high mortality after birth.

We decided to focus on the study of LFG's biological role in the brain and in the immune system. Within the brain the cerebellum showed the most interesting phenotype so we focused on cerebellar cell development and survival (Chapter 3). With respect to the immune system we investigated the role of LFG in T cell development and homeostasis (Chapter 5). A brief description of the other phenotypes observed in the LFG knockdown mice is presented in Chapter 7.

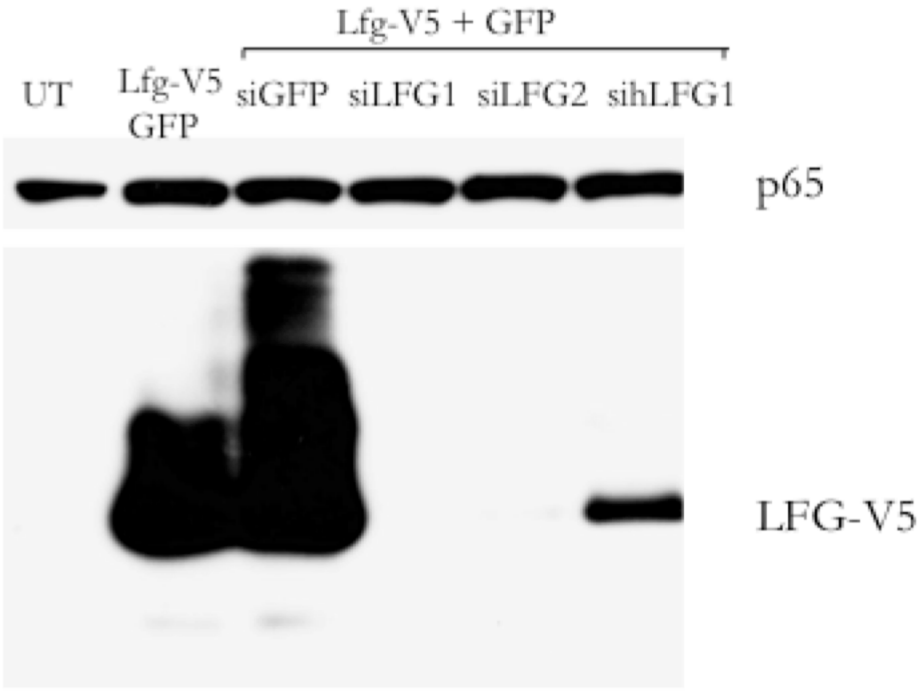

Figure 2.1- Effective downregulation of overexpressed LFG by siRNA. Western blot of protein extract from 293T cells untransfected (UT) or transfected with LFG-V5 and GFP alone or in combination with different siRNAs. The upper part is probed with p65 antibody as a loading control and the lower part with V5 antibody to detect LFG-V5.

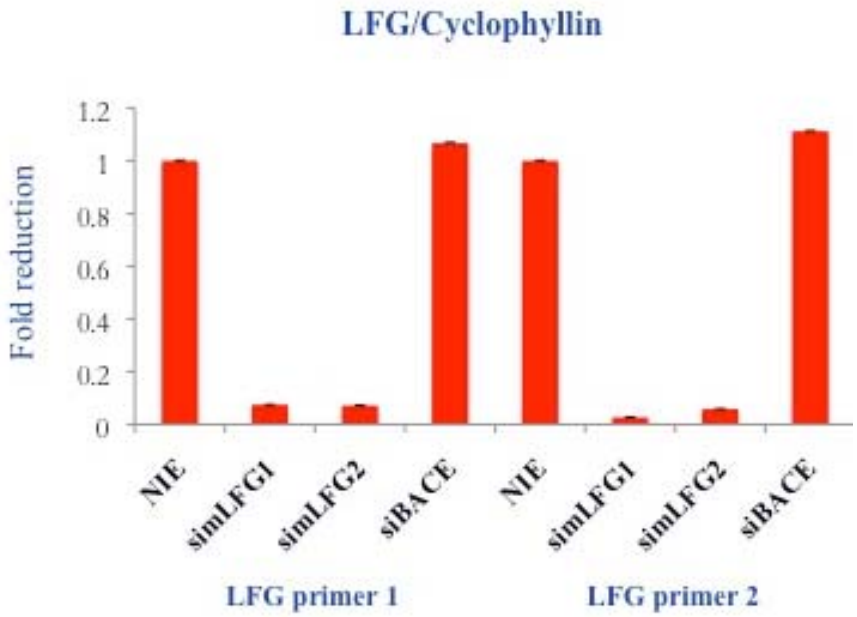

Figure 2.2- LFG knockdown in neuroblastoma cells NIE 115. Histograms showing the level of LFG expression by QPCR in NIE-115 cells, either uninfected (NIE) or infected with lentiviruses expressing the LFG specific siRNAs or and siRNA to BACE-1 as a control. Cyclophilin was used as a normalizing control.

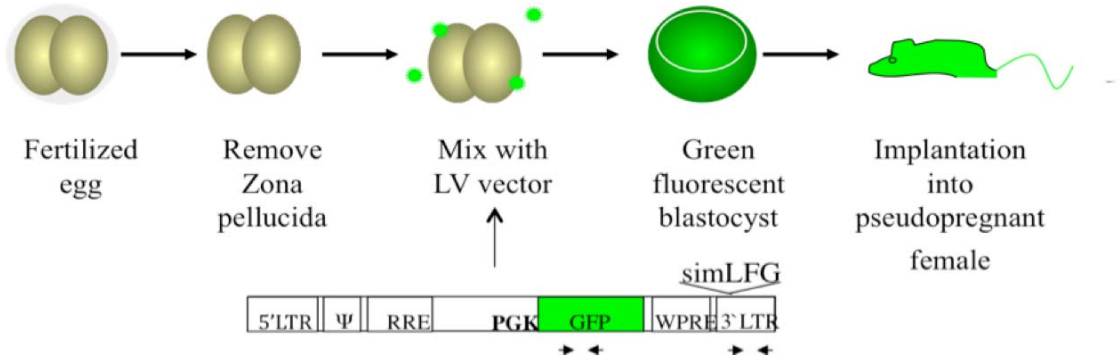

Figure 2.3- Schematic representation of the lentiviral transgenesis technique and the lentiviral vector containing the LFG siRNA. Fertilized eggs at the two-cell stage are isolated and their zona pellucida is removed in order to infect the cells with the lentivirus. Forty-eight hours after transduction, blastocysts are transplanted into the uterus of ICR pseudopregnant females.

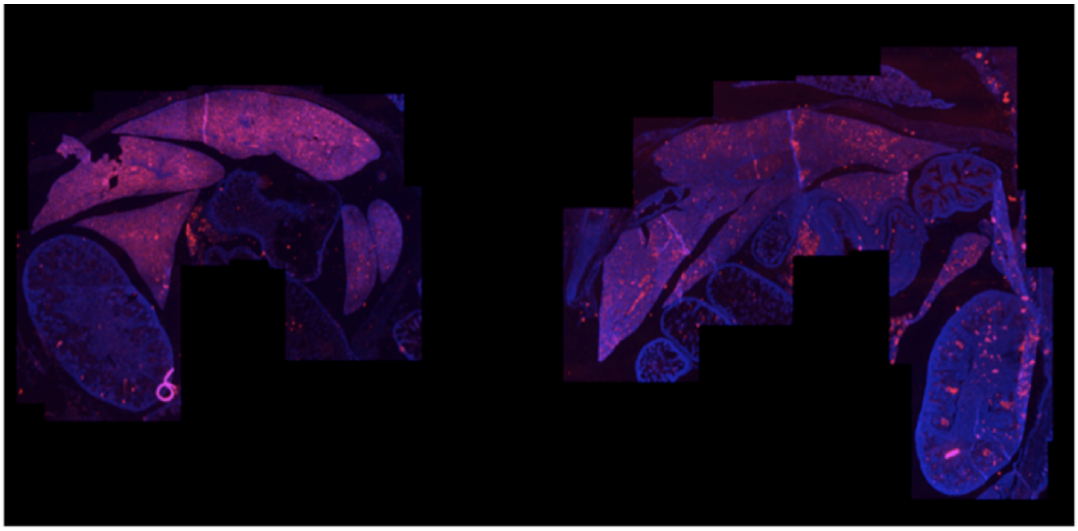

Figure 2.4- Validation of LFG knockdown *in vivo*. Radioactive *in situ* hybridization (ISH) of sagittal sections from P0 wild type and siLFG liver and kidneys. LFG probe in red and counterstaining with DAPI in blue.

LFG knockout mice

Our first approach to study LFG's biological function *in vivo* was to generate conventional LFG knockout mice, but after several attempts we failed to generate a viable mouse line. Therefore we decided to take the lentiviral siRNA approach.

By the time LFG knockdown mice were successfully generated and their phenotypic characterization was initiated, one LFG null mouse line was reported to be generated by Deltagen. This line eventually became commercially available and was purchased from Jackson laboratories in order to compare it with the siRNA knockdown model. The targeting strategy consisted in inserting a LACZ-Neomicin cassette between exons four and five of the LFG genomic sequence. This insertion generated a fusion protein with the Beta galactosidase acting as a reporter to study the tissue distribution of LFG. As shown in Figure 2.5 the insertion disrupts the first transmembrane domain of LFG.

Validation of the LFG knockout mice was carried out by QPCR of brain cDNAs, using primers that amplify the region downstream of the insertion and by Western blot detection of beta-galactosidase in brain lysates. LFG null mice showed a complete reduction of LFG when normalized to cyclophilin (Figure 2.6). Expression of beta-galactosidase was confirmed by Western blot (Figure 2.7).

These mice have been characterized in order to do a comparative study with the siLFG mice. Since the line has a pure C57Bl6 background it has also been a great tool to perform experiments that require a pure background, such as the bone marrow chimeras generated for the immune system studies described in Chapter 5 or the cerebral ischemia study described in Chapter 4.

Chapter 2, in part is currently being prepared for submission for publication of the material. Hurtado de Mendoza, Tatiana; Perez-Garcia, Carlos G; Kroll, Todd; Hoong, Nien; O'Leary, Dennis and Verma, Inder M. The Antiapoptotic Protein Lifeguard Plays a Role in Cerebellar Cell Survival. The dissertation author was the primary investigator and author of this material.

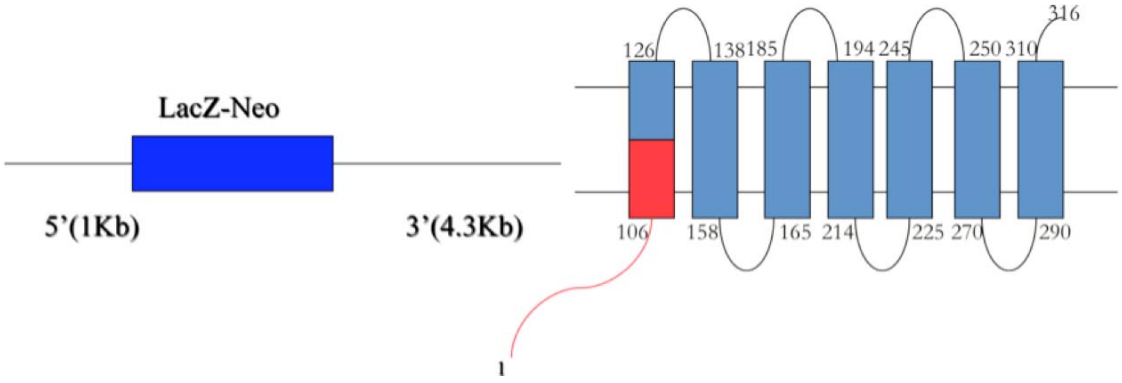

Figure 2.5- Schematic representation of the knockout targeting vector and a topology map of LFG showing where the insertion takes place. The targeting strategy consists in a LacZ-Neo cassette inserted between exons 4 and 5 of LFG, disrupting the first transmembrane domain and generating a fusion protein between the first 115 aminoacids of LFG (red) and LacZ.

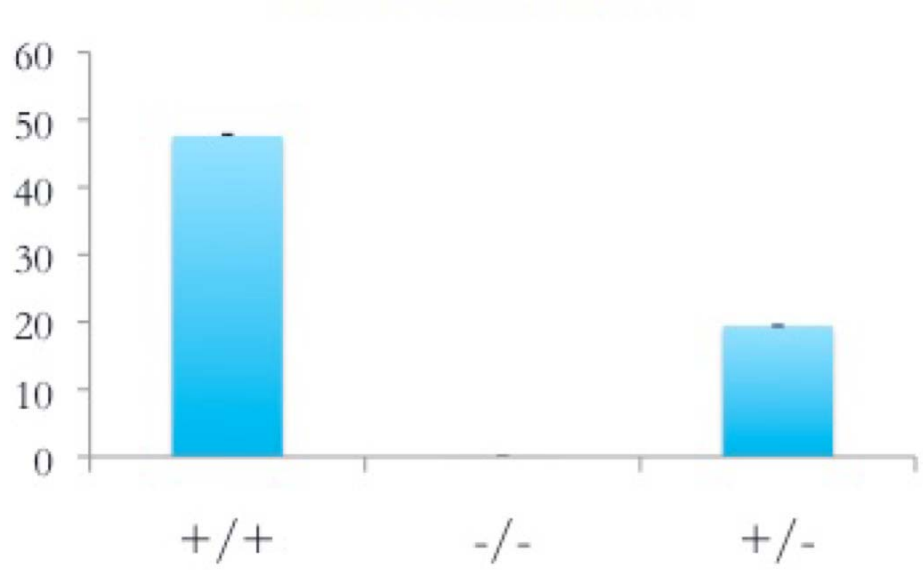

Figure 2.6- Validation of LFG knockout mice by QPCR. Histograms representing the QPCR performed on brain cDNA from wild type, heterozygous and knockout mice. LFG levels were normalized against cyclophilin.

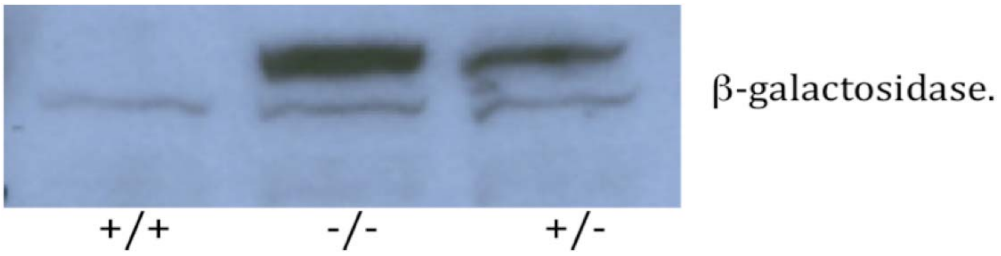

Figure 2.7- Expression of β-galactosidase in LFG knockout and heterozygous mice. Western blot of brain protein extracts from wild type, heterozygous and null mice probed with the β-galactosidase antibody.

3

The antiapoptotic protein Lifeguard plays a role in cerebellar cell survival

INTRODUCTION

Programmed cell death plays an important role in the development of the central nervous system (CNS). This process regulates the final number of neurons and glial cells observed in the adult brain by use of the apoptotic machinery of the cell. Two major periods of apoptosis have been identified during the development of the CNS in mice. The first one occurs between embryonic days E10 to E18 and is related to cell cycle regulation; it affects mainly progenitor cells and young postmitotic neuroblasts. The second apoptotic period occurs during the early postnatal stages and affects postmitotic neurons establishing neuronal connections (Lossi and Merighi, 2003). During this same postnatal period most of the cerebellar structural development takes place. There are three main neuronal types in the cerebellum; Cerebellar granular neurons (CGN), Purkinje cells (PC) and deep cerebellar neurons. Programmed cell death occurs during the development of all these cell types (Ghoumari et al., 2000) (Kitao et al., 2004) (Janowsky and Finlay, 1983) (Bourrat and Sotelo, 1984) (Delhaye-Bouchaud et al., 1985) (Suzuki, 1999).

During the first postnatal weeks there is a proliferative phase of cerebellar granular neurons that migrate from the external granular layer (EGL) across the Purkinje cell layers, guided by the radial glia, to form the internal granular layer (IGL) (Rakic, 1971) (Hatten, 1990). Purkinje cells are generated in the ventricular zone of the cerebellar primordium and then migrate to the cerebellar plate aggregating in a layer 6-10 cells thick (Luo et al., 2004) (Miale and Sidman, 1961) that will evolve into a monolayer located between the internal granular layer and the molecular layer of the cerebellum during the early postnatal stages.

The proliferation of external granular cells is regulated by Purkinje cell secretion of sonic hedgehog (Wallace, 1999) and in turn the external granule cells, by secreting factors such as Reelin, promote the migration of the Purkinje cells (Jensen et al., 2002). The ratio of these two cerebellar cell types is tightly regulated, as demonstrated by several examples of mutant mice, including the Reelin knockout mice that have a reduced proliferation of external granular cells caused by a defect in Purkinje cell migration (Yuasa et al., 1993). Another example is the lurcher mice, that have a gain of function of glutamate receptor ionotropic delta 2 (GRID2), resulting in death of Purkinje cells that lead to a massive loss of cerebellar granular cells, due to target deprivation (Selimi et al., 2000) (Doughty et al., 2000).

Mutations in apoptosis related genes have proven the involvement of this process in the regulation of cell numbers in the CNS. Within the cerebellum, transgenic mice overexpressing the antiapoptotic protein Bcl2 as well as mice that have the proapoptotic protein Bax deleted, show an increase in Purkinje cell numbers (Zanjani et al., 1996) (White et al., 1998) (Jung et al., 2008). Many different mechanisms have been shown to trigger apoptosis of nerve cells. However, the exact underlying mechanisms triggered during programmed cell death in the nervous system are not clear. One of these apoptotic mechanisms involves cell surface receptors, known as death receptors. Upon binding to their ligands, death receptors activate signaling cascades that activate caspases and ultimately lead to the death of the cell. The Fas receptor (FasR) (also called Apo-1 or CD95) is one of the better characterized death receptor family members (Peter and Krammer, 2003). CNS expression of FasR

and FasL is well established, as is their involvement in programmed cell death related to trophic factor deprivation although the exact mechanisms are not completely understood (Raoul et al., 2000). The best evidence comes from the fact that Fas-Fc, a chimeric decoy that blocks the FasR-FasL interaction, is able to reduce death induced by trophic factor deprivation in cultured spinal motor neurons, cerebellar granular cells and PC12 cells (Le-Niculescu et al., 1999) (Raoul et al., 1999) (Brunet et al., 1999). Furthermore, cerebellar granular cells from gld/gld mice, which have a mutated FasL, are also more resistant to trophic factor deprivation in culture (Le-Niculescu et al., 1999).

LFG is an antiapoptotic protein that specifically inhibits the Fas pathway. LFG expression analysis shows wide tissue distribution with the highest expression in the brain. Within the brain, LFG is expressed in all cortical layers (II-VI) with the exception of layer I; in the hippocampus, mainly in the CA3 and the granular cells from the dentate gyrus (DG), the piriform cortex and within the cerebellum in the granular and Purkinje cell layers (Schweitzer et al., 1998a; Somia et al., 1999). LFG's transcripts and protein are strongly upregulated during postnatal development, colocalizing in the dendrites with glutamate receptor 2 (GluR2) in the postsynaptic membrane, suggesting a possible role in synapses of the adult central nervous system (Schweitzer et al., 1998a) (Schweitzer et al., 2002).

Cerebellar granular neurons are known to be resistant to Fas mediated apoptosis. This resistance was attributed to the expression of LFG in cultured cerebellar granular neurons (Beier et al., 2005). In contrast, cortical neurons in which the expression of LFG was reduced, showed increased sensitivity to Fas mediated cell

death, but these neurons do not seem to depend as much as the cerebellar granular neurons on LFG for their protection against Fas mediated apoptosis (Fernandez et al., 2007b).

While these in vitro studies indicated a role of LFG in modulating Fas mediated apoptosis, its significance *in vivo* with respect to development and neuronal survival remains to be investigated. Therefore, we generated a mouse model in which LFG levels were reduced by siRNA lentiviral transgenesis.

While this study was in progress LFG null mice became commercially available, so we analyzed this new line and made a comparative study that validated the data obtained from the knockdown mice.

Analysis of LFG expression by *in situ* hybridization (ISH)

LFG expression in the brain was determined by radioactive *in situ* hybridization (ISH) performed at different embryonic and postnatal stages. Our results showed little or no expression during early embryonic stages, although during late cortical plate formation (E18.5) the expression pattern of LFG is high in the developing cortical layers. Postnatally, LFG was expressed in all cortical layers (II-VI) with the exception of layer I; hippocampus, where its level was highest in the CA3 and the granular cells from the dentate gyrus (DG), piriform cortex, olfactory bulb and in the internal granular layer and Purkinje cells of the cerebellum (Figure 3.1).

In situ hybridization for LFG on brains from P10 wt and siLFG animals demonstrated successful downregulation of LFG expression in all the laminar structures such as cerebellum, caudal cortex, hippocampus and olfactory bulb (Figure

3.1). However, LFG's downregulation did not present a uniform pattern, since we observed a greater reduction of LFG expression in the medial to caudal part of the cortex, while its rostral expression was retained. In order to correlate the levels of LFG in the siRNA model with those in the knockout mice, QPCR was performed with cDNA prepared from cerebellum of wild type, knockdown and null mice. LFG knockdown mice showed an average reduction of 80% compared to the complete loss of LFG in the null mice.

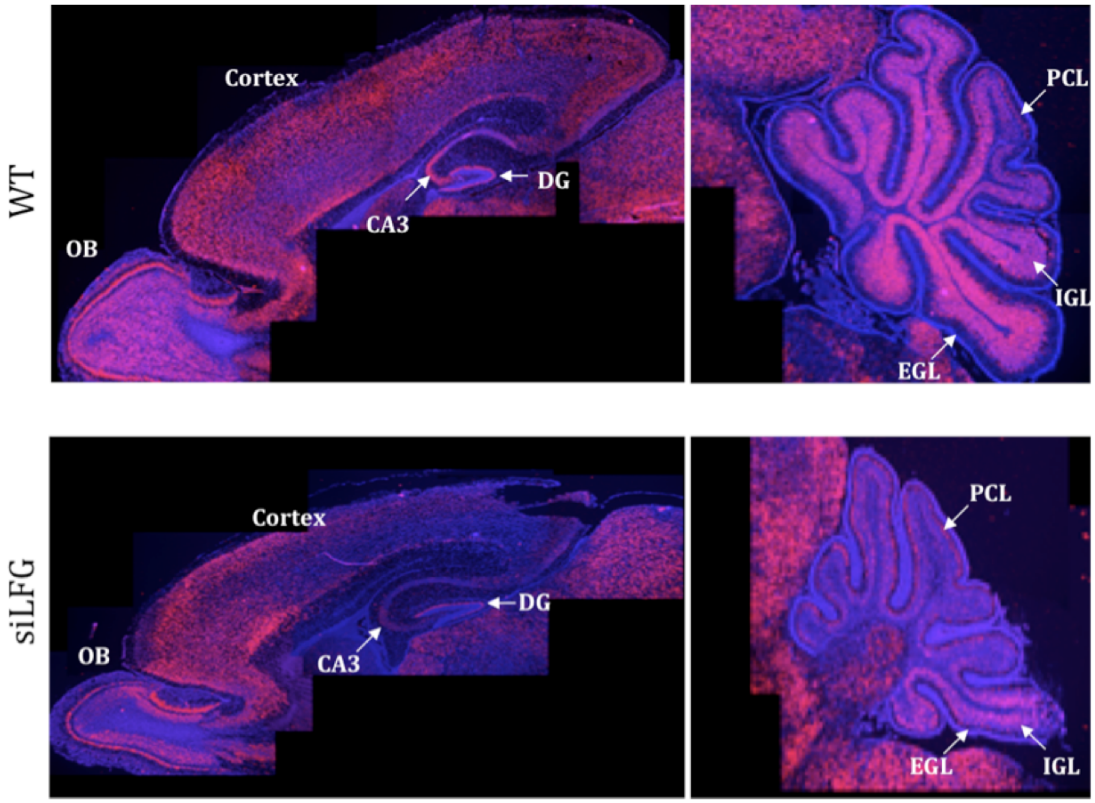

Figure 3.1- LFG's expression pattern in the CNS and downregulation in LFG knockdown mice. *In situ* hybridization of sagittal sections from P10 wild type and siLFG brain, using the LFG probe (red) and counter-stained with DAPI (blue).

Cytoarchitechtural analysis of the cerebellum

Neuroanatomical analysis of the cerebellum of wild type, null and siLFG mice was performed at different developmental stages by Cresyl Violet staining. The overall structure was mostly normal, but we observed a decrease in cerebellar size at the earlier developmental stages. Downregulation caused a more severe phenotype than the complete lack of LFG; both models had smaller cerebella at P5 (Figure 3.2 A), but they had a normal size cerebellum by P35. An important observation is that the internal granular layer was much thinner in siLFG mice than in the wild type or null mice (Figure 3.2 B).

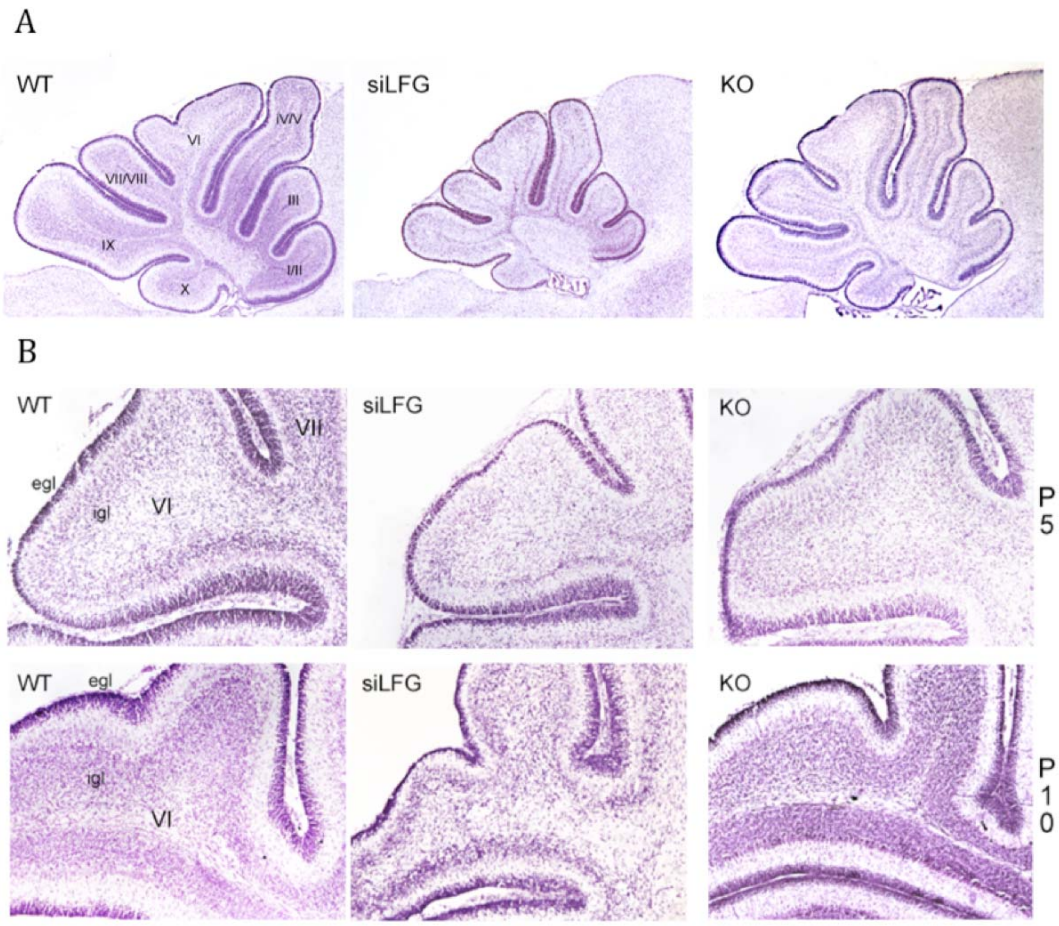

Figure 3.2- Cerebellar phenotype in early postnatal stages. Nissl staining of sagittal sections of wild type, null and siLFG cerebella.

Delay in differentiation and monolayer organization of the Purkinje cells

In order to study the development of the Purkinje cells in siLFG and wild type mice, sagittal sections of P5, P10 and P35 wild type, null and siLFG brains were immunostained for two Purkinje cell markers, Parvalbumin (PV) and Calbindin (CB).

Parvalbumin has been characterized as a differentiation marker for Purkinje cells (Andressen et al., 1995; Baurle et al., 1998) so we examined the level of differentiation of the Purkinje cells based on their PV expression. Purkinje cells from wild type mice showed strong PV staining at P5, P10 and in young adult. In contrast siLFG and null mice had no PV expression at P5 in the cerebellum. As a control for the PV staining the reticular cells of the thalamus were positive and CB staining of adjacent sections demonstrated the presence of the Purkinje cells, even if they were not expressing PV.

By P10 the staining was weak and restricted to few Purkinje cells in siLFG mice, but normal in the knockout. All the mice showed strong PV staining at P35 (Figure 3.3 A). These results indicate that there is a delay rather than a lack of Purkinje cell differentiation, since in both the siLFG and knockout mice Purkinje cells express normal levels of PV once they are young adults. From the CB immunostaining we observed that the organization of Purkinje cells was affected. Purkinje cells initially form a layer 6-10 cells thick, which by P10 is organized into a monolayer in wild type mice. Purkinje cells in the cerebellum of siLFG mice were still disorganized at P10; only a fraction of Purkinje cells was organized in a monolayer while the majority was distributed over several layers (Figure 3.3 B) and reached monolayer organization by P35.

Taken together, these data suggest a delay in Purkinje cell differentiation and organization into a monolayer. We observed again that this phenotype was more severe in siLFG mice than in the knockout mice.

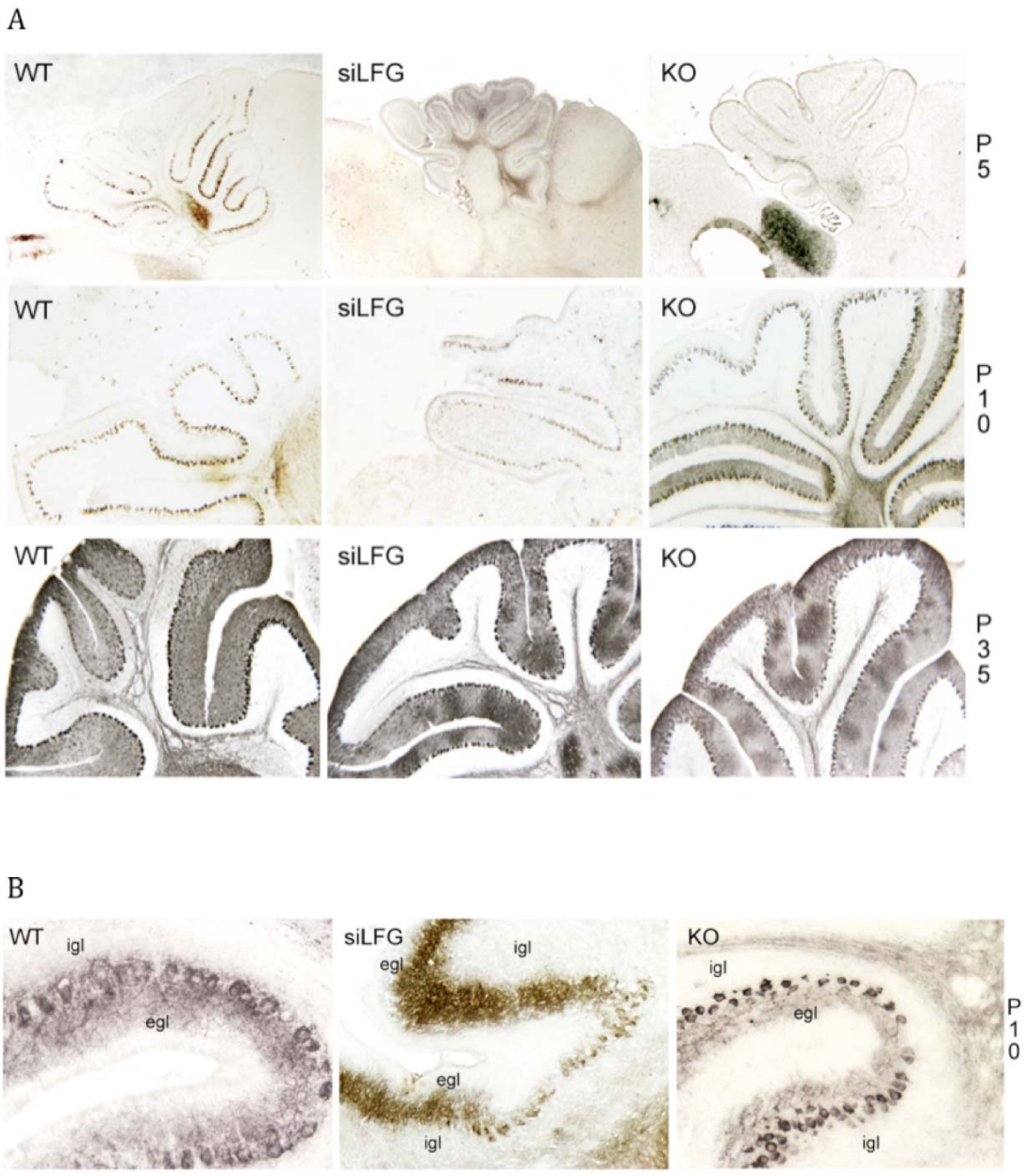

Figure 3.3- Delayed Purkinje cell differentiation. (A) Parvalbumin immunostaining of Purkinje cells in sagittal sections of P5, P10 and P35 wild type, null and siLFG cerebella. (B) Calbindin immunostaining of P10 saggital sections of wild type, siLFG, and knockout cerebella.

Purkinje cells show abnormal cell morphology and increased apoptosis compared to wild type mice

An important observation was that LFG downregulation or ablation affected Purkinje cell morphology as shown by PV staining (Figure 3.4). The cell bodies of Purkinje cells were elongated and more sparse in siLFG and LFG null mice than in the wild type.

Since LFG protects cells from Fas mediated apoptosis (Somia et al., 1999), we also hypothesized that lack of LFG could cause the Purkinje cells to undergo apoptosis. For this purpose we performed active caspase 3 immunoassay and the results revealed increased levels of apoptosis in siLFG and null Purkinje cells at P35, compared to wild type (Figure 3.4 B).

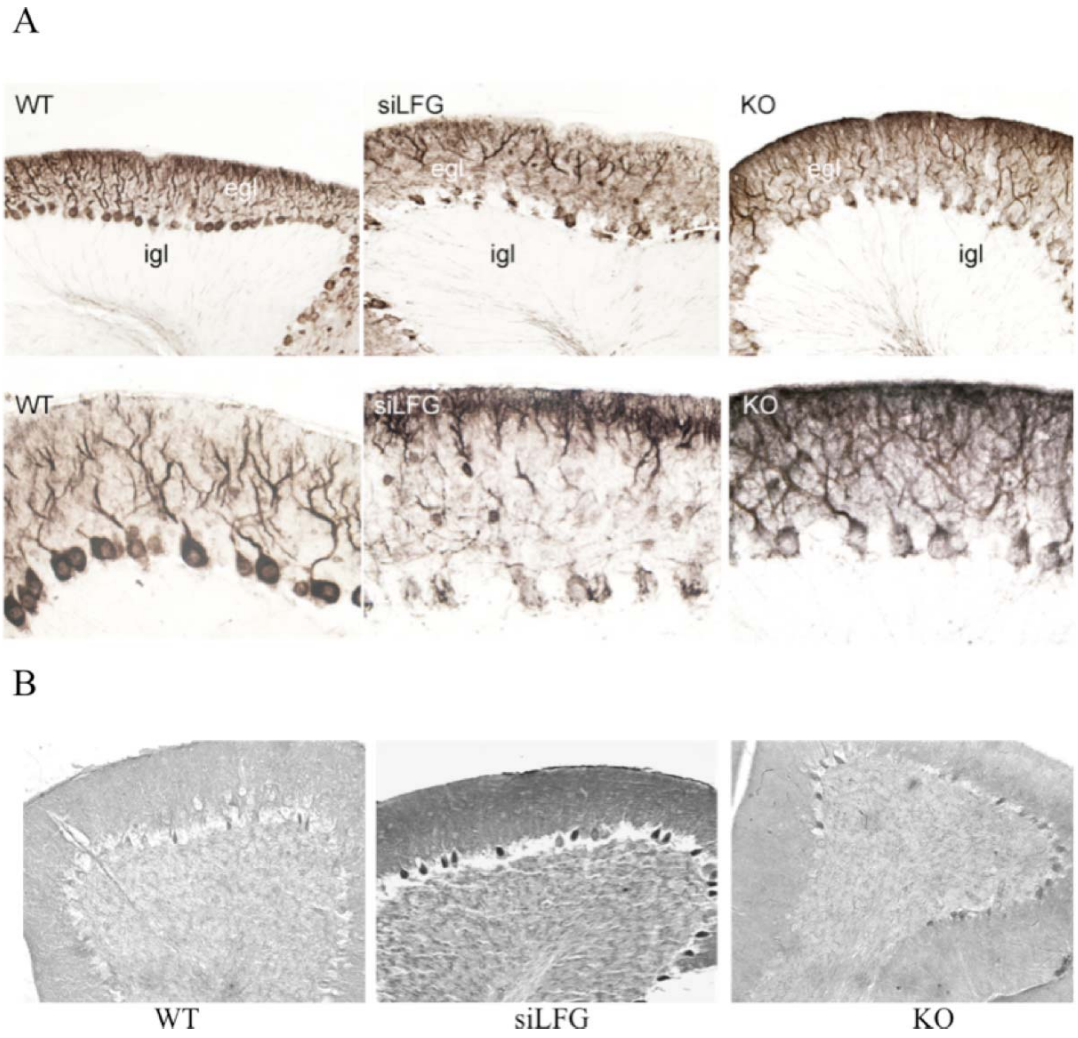

Figure 3.4- Abnormal Purkinje cell morphology and increased apoptosis. (A) Parvalbumin staining and (B) Active caspase 3 immunostaining of sagittal sections of 5-week old wild type, siLFG and knockout cerebella.

Organotypic cerebellar cultures: LFG protects Purkinje cells from Fas mediated apoptosis.

Cerebella from LFG null and wild type mice were sagittally sectioned at 400 μm using a vibratome. The cerebellar slices were cultured for five days and then treated with a Fas agonistic antibody in order to induce apoptosis. After 24 hours of incubation with Fas the cerebellar slices were fixed, permeabilized and stained for the Purkinje cell marker Calbindin and TUNEL to determine the level of cell death (Figures 3.6 and 3.8). Apoptotic cells were counted in two different fields; 1-The Purkinje cell field, defined by the expression of calbindin. 2- the internal granular layer (IGL) field, adjacent to the Purkinje field with no calbindin positive cells (Figure 3.5). We observed that LFG null cells in the Purkinje field showed a significant increase in cell death in response to the treatment with Fas (genotype X treatment: $F(1,16) = 6.034$, $p = 0.026$ by two-way ANOVA). Tukey's *post hoc* multiple comparison gave a $p < 0.001$ for the factor genotype, $p = 0.706$ for Fas treatment within wild type, $p = 0.004$ for Fas treatment within knockout, $p = 0.09$ for genotype within untreated and $p < 0.001$ for genotype within Fas treatment (Figure 3.7). These data suggest that wild type Purkinje cells are resistant to Fas mediated cell death and that the loss of LFG makes them become Fas sensitive.

On the other hand, LFG null cells in the internal granular layer showed an increased apoptosis compared to wild type, but the Fas treatment did not have a significant effect (genotype X treatment: $F(1,16) = 3.614$, $p = 0.075$ by two-way ANOVA) (Figure 3.9).

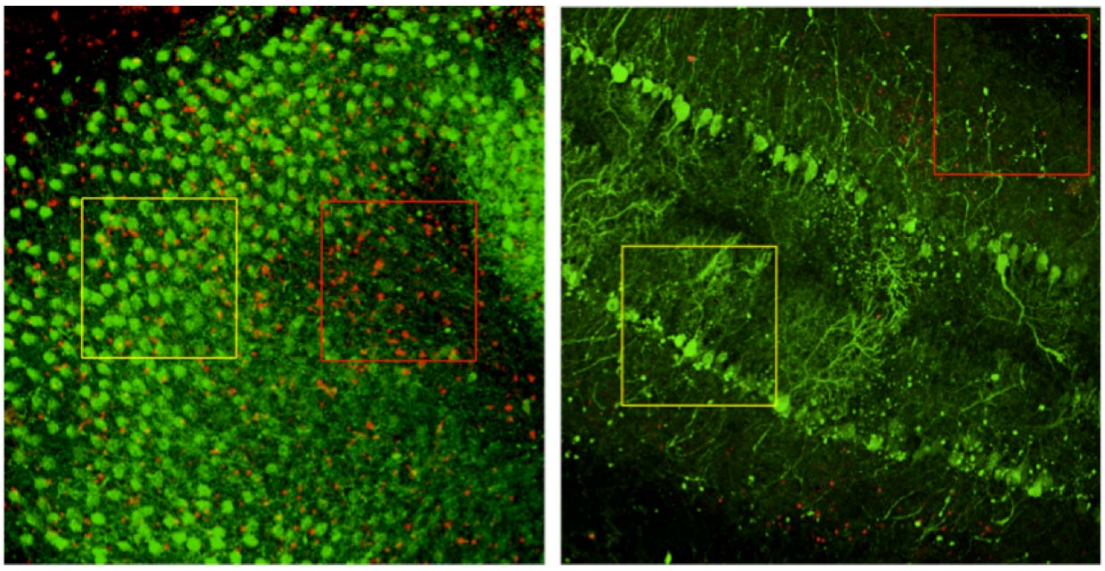

Figure 3.5- Definition of the Purkinje and IGL fields. Representative images of cerebellar slices immunostained with Calbindin (green) and TUNEL (red). The yellow squares represent the Purkinje cell fields and the red squares represent the IGL fields.

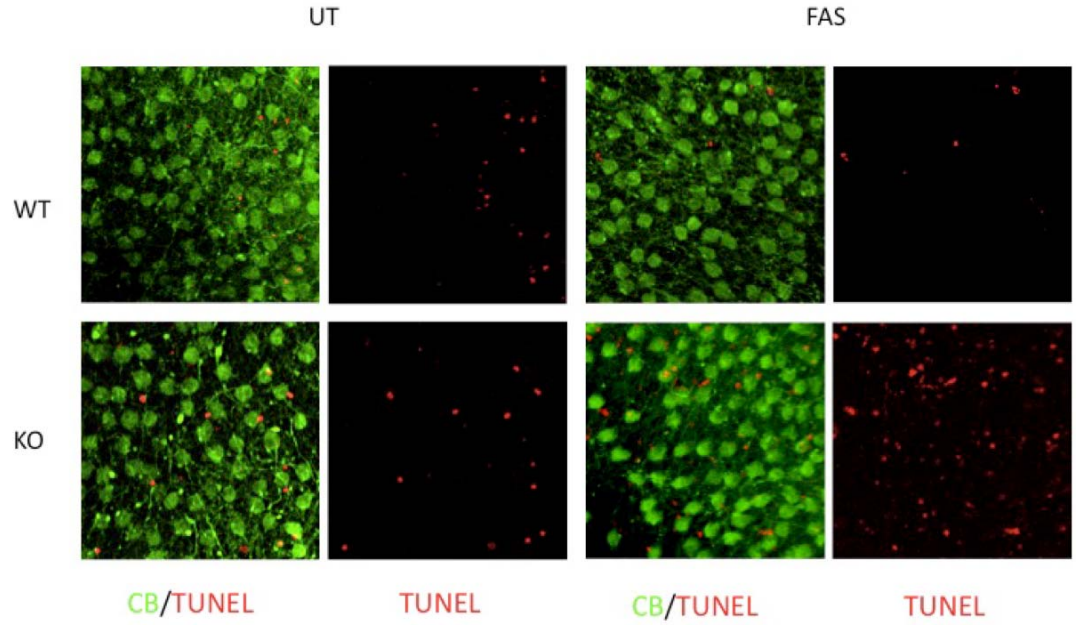

Figure 3.6- Increased apoptosis in Fas treated LFG knockout Purkinje fields. Representative images of wild type and knockout Purkinje cell fields immunostained with Calbindin (green) and TUNEL (red) untreated (UT) or Fas treated.

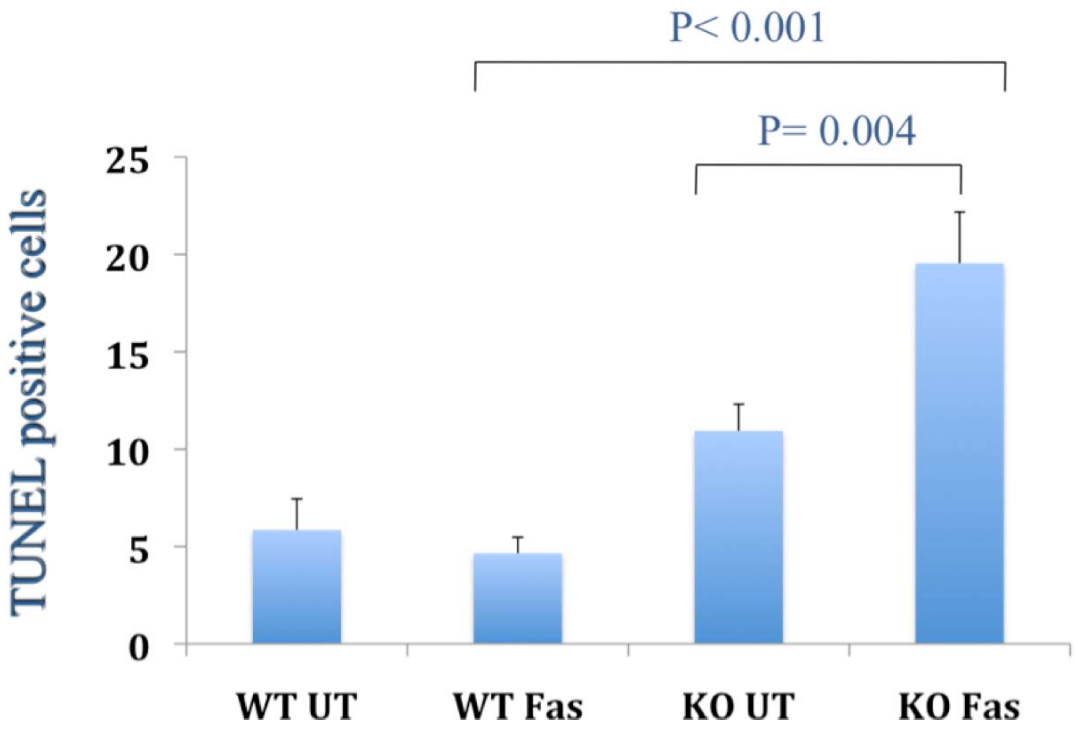

Figure 3.7- Increased apoptosis in Fas treated LFG knockout Purkinje fields. Histogram representing the number of TUNEL positive cells per Purkinje cell field across the two genotypes and Fas treatment. (n = 72 knockout fields per condition, n = 48 wild type fields per condition).

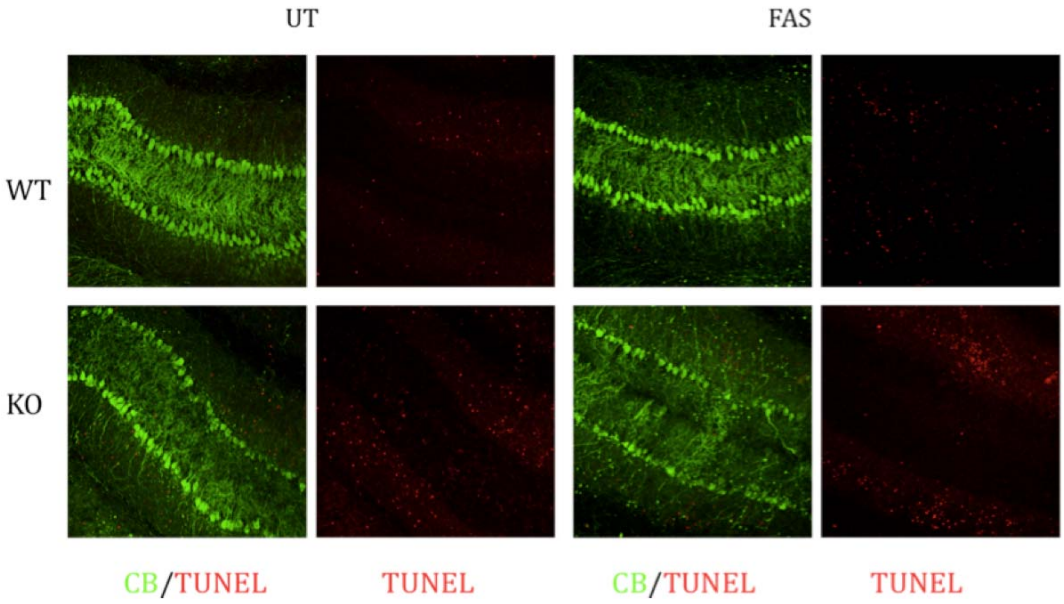

Figure 3.8- Increased apoptosis in LFG knockout IGL fields. Representative images of wild type and knockout internal granular layer fields immunostained with Calbindin (green) and TUNEL (red) untreated (UT) or Fas treated.

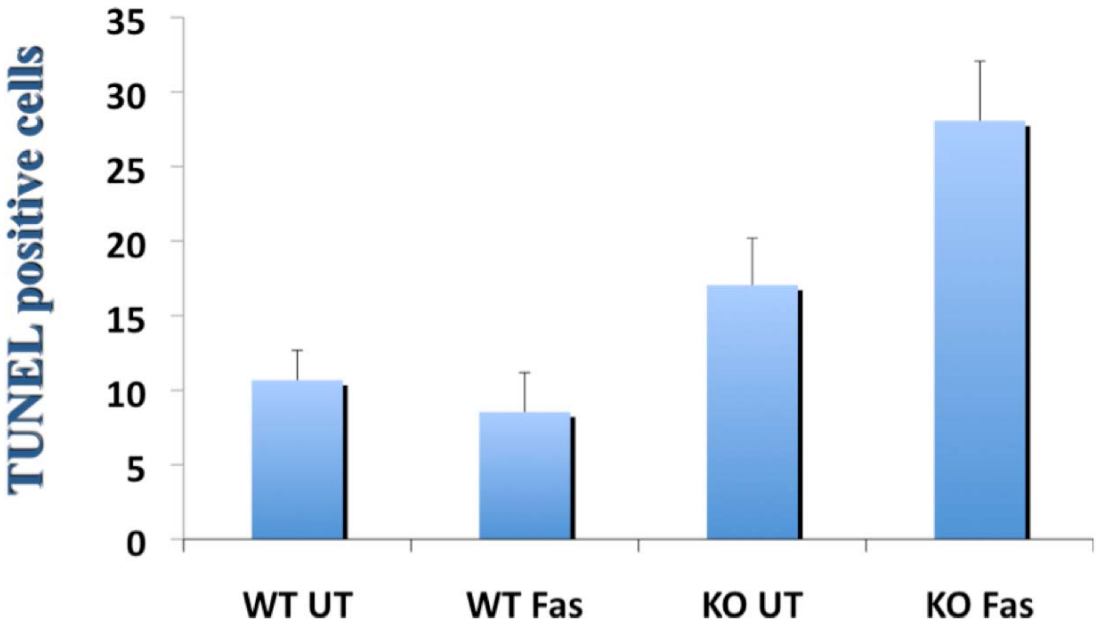

Figure 3.9- Increased apoptosis in LFG knockout IGL fields. Histogram representing the number of TUNEL positive cells per internal granular layer field across the two genotypes and Fas treatment. (n = 72 knockout fields per condition, n = 48 wild type fields per condition).

CONCLUSIONS AND DISCUSSION

This is the first study addressing the role of LFG in the cerebellum *in vivo*. We found that siLFG mice have a reduced cerebellar size in early developmental stages, decreased internal granular layer size and a delay in Purkinje cell development, with an abnormal morphology and increased apoptosis. LFG null mice showed the same Purkinje cell phenotype, even though it was less severe, but did not show any significant phenotype in the internal granular layer. Since this model is more uniform than the siLFG model it was used to demonstrate that the lack of LFG has a direct effect in the survival of Purkinje cells and that the Fas pathway plays a role in Purkinje cell survival.

LFG was isolated as an inhibitor of the Fas apoptotic pathway (Somia et al., 1999), but its mechanism of action remains unknown. Programmed cell death is involved in embryonic development, tissue remodeling, tumor surveillance and regulation of the immune system. Dysfunction of this process can lead to serious developmental defects, oncogenesis as well as autoimmune and degenerative diseases. Our results are consistent with the antiapoptotic role of LFG. The loss of Purkinje cells was correlated with an increased apoptosis measured by TUNEL and active caspase 3 immunostaining *in vivo* and by increased sensitivity to Fas mediated apoptosis in organotypic cerebellar cultures. We also observed a severe reduction of the granular cell layer in the LFG knockdown mice that correlates with the *in vitro* studies performed by Beier, *et al,* and Fernandez *et al, in* which cerebellar granular cells died from Fas mediated apoptosis when LFG was downregulated.

The fact that the siLFG model exhibits a more severe phenotype than the knockout was unexpected. Nevertheless, there are similar examples in the literature, such as the doublecortin or doublecortin-like kinase cases. In humans mutations in the doublecortin gene cause neocortical malformations, but mice with a targeted mutation in the doublecortin gene had normal neocortical lamination. Instead, mice with reduced doublecortin levels by siRNA did show the same phenotype observed in the human pathology (Bai et al., 2003; Corbo et al., 2002; Koizumi et al., 2006). As discussed in the doublecortin papers it is possible that in the knockout model, where there is a complete lack of protein, there are compensatory effects that make the phenotype less severe. In the case of LFG the compensatory effects may cause upregulation of other antiapoptotic proteins. Another possible explanation is that in the LFG knockout the amino terminal part of the protein is still intact and it could still retain some function, producing a less severe phenotype, but deletion mutants of most of the amino terminal part of LFG still provide protection from Fas mediated cell death. We still cannot rule out the possibility of off-target effects of the siRNA, especially in the case of the internal granular layer, whose phenotype was observed only in the siLFG mice, but there are already two publications of *in vitro* studies where cerebellar granular cells loose their resistance to Fas mediated apoptosis after downregulation of LFG mediated by siRNA (Beier et al., 2005; Fernandez et al., 2007b). The phenotype we found in siLFG mice would be supported by these two independent studies. This means five different siRNA sequences against LFG can give rise to the same effect on CGNs. In addition the phenotypes observed in the siLFG mice and the knockout are similar enough that makes it unlikely to be due to off target

effects of the siRNA. In order to completely rule out this possibility, a rescue experiment would be necessary.

Having a phenotype that affects both granular and Purkinje cells raises the question: Is LFG directly affecting the survival of both cell types? Or does LFG have a major effect in one population and a secondary effect in the other? These two cell populations depend on each other for their survival. There are many examples in which the mutation of a certain gene primarily affects one of them and the other population dies as a consequence. A good example is the Reelin knockout mice that have a reduced proliferation of external granular cells caused by a defect in Purkinje cell migration (Yuasa et al., 1993). Or the lurcher mice, that have a gain of function of glutamate receptor ionotropic delta 2 (GRID2), resulting in death of Purkinje cells that lead to a secondary loss of granular cells (Wullner et al., 1995).

Cerebellar granular cells have been shown to be resistant to Fas mediated apoptosis, based on their AKT dependant expression of LFG. Reduction of LFG expression by siRNA makes these cells become sensitive to Fas induced cell death in culture (Beier et al., 2005). Taking this data into account, we can expect a direct effect of the downregulation of LFG in the survival of the cerebellar granular cells, but we do not have any evidence that leads us to think that the loss of LFG would also have a direct effect in Purkinje cells. The delay in Purkinje cell differentiation and establishment of a monolayer could be a consequence of the reduced granular cell population; the death of the Purkinje cells could then be explained by a lack of synaptic connections leading to apoptosis.

If we take into account the fact that the knockout has a normal granular cell population but still displays the Purkinje cell phenotype, we could think that the effect of LFG on Purkinje cell survival is a direct effect. However, in order to confirm our observation we performed organotypic cerebellar cultures and examined the sensitivity of wild type and knockout Purkinje cells to Fas mediated apoptosis. Our results show an increased sensitivity of LFG null Purkinje cells to Fas induced apoptosis, suggesting a direct effect of LFG in Purkinje cell survival.

Interestingly, the phenotype we are describing here is quite similar to that of mice with missexpression of the homeobox gene engrailed 2 (L7En2 mice) (Jankowski et al., 2004). Like siLFG mice, L7En2 mice have hypoplastic cerebellum with delayed Purkinje cell differentiation and organization in a monolayer. There is suggestive evidence that the engrailed 2 locus is linked to autism spectrum disorder (ASD) and indeed L7En2 mice display anatomic features similar to those reported for individuals with autism (Benayed et al., 2005). It will be interesting to investigate whether LFG might also be a gene whose mutation correlates with the neurodevelopmental defect hypothesis of the etiology of autism.

While LFG is highly expressed in the cerebellum, it was also found in other brain regions. These include the cortex, the olfactory bulb and the hippocampus, that like the cerebellum are laminated structures but whose development is not significantly affected by LFG. With this respect it is important to notice that cerebellar development occurs primarily post-natally and correlates with an increase in LFG expression (Schweitzer et al., 1998a). On the other hand, the cortex and the hippocampus, develop during embryonic stages, when LFG's expression is lower.

Therefore, while LFG appears to play an important role in cerebellar development, its role in cortical and hippocampal neurons appears not to be developmental and remains to be determined. One interesting hypothesis to be tested is that in these structures LFG may play a role in post-developmental neuronal maintenance and survival, specifically during brain injury and trauma such as stroke and traumatic brain injury as well as in neurodegenerative diseases.

In conclusion, we found that LFG plays an important role in cerebellar development and survival of granular and Purkinje cells.

Chapter 3, in full is currently being prepared for submission for publication of the material. Hurtado de Mendoza, Tatiana; Perez-Garcia, Carlos G; Kroll, Todd; Hoong, Nien; O'Leary, Dennis and Verma, Inder M. The Antiapoptotic Protein Lifeguard Plays a Role in Cerebellar Cell Survival. The dissertation author was the primary investigator and author of this material.

4

A possible neuroprotective role for LFG after cerebral ischemia

INTRODUCTION

Cerebral ischemia or ischemic stroke is a condition in which insufficient blood supply to the brain leads to poor oxygenation (hypoxia). Hypoxia can cause the death of the brain tissue directly affected. In addition, cellular damage can occur following restoration of the blood supply, a process known as reperfusion injury that produces inflammation and oxidative damage causing cell death. Stroke typically results in the loss of neurological functions regulated by the region affected.

The degree of neurological damage caused by a stroke determines if the loss of brain functions will be transient, permanent or even fatal. Stroke is the second most common cause of death worldwide and the leading cause of adult disability in the United States and Europe.

Cell death after cerebral ischemia was for long considered to be only necrotic. However, there is now increasing evidence that apoptotic cell death also occurs after stroke. In fact, the core of brain tissue that suffered the most severe hypoxia undergoes necrotic cell death. Instead its surrounding region is less severely affected and remains metabolically active: it is called the ischemic penumbra. Cells in the penumbra may undergo apoptosis several hours or even days after the stroke determining the so-called secondary damage and the severity of the neurological consequences of stroke. Secondary damage occurs also after hemorrhagic stroke or traumatic brain injury and represents an attractive therapeutic target.

The apoptotic pathways involved in secondary damage after stroke include the intrinsic and extrinsic pathways as well as caspase independent pathways. So far the death receptors that have been implicated in apoptotic cell death after stroke are

TNFR-1, Fas and p75 NTR. Fas, FasL and TNF-related apoptosis-inducing ligand (TRAIL) are upregulated in the postischemic brain and mice expressing dysfunctional FasL as well as TNF knockout mice have significantly reduced infarct volumes after middle cerebral artery occlusion (MCAO). To further support the involvement of Fas and TNF in the damage after stroke, treatment with neutralizing antibodies against FasL and TNF remarkably reduced the infarct volume (Broughton et al., 2009; Martin-Villalba et al., 1999; Rosenbaum et al., 2000).

Since LFG protects cells against Fas mediated apoptosis we hypothesized that LFG could play an important role in neuroprotection after stroke. We predicted that if our hypothesis was correct mice lacking LFG would suffer a more severe brain damage after cerebral ischemia.

LFG knockout mice have larger infarct volumes after stroke induced by medial cerebral artery occlusion

A well-established model to induce cerebral ischemia is the medial cerebral artery occlusion (MCAO). In this model a surgical filament is introduced into the external carotid artery and forwarded until its tip occludes the origin of the middle cerebral artery, causing a cessation of blood flow and subsequent brain infarction in its area of supply. The occlusion can be permanent or transient if the filament is removed after a certain amount of time to restore blood-flow.

To test our hypothesis wild type as well as LFG knockout mice were subject to MCAO for two hours and 24 hours after occlusion they were sacrificed. Brains were collected and the infarct size was revealed by 2, 3, 5-triphenyltetrazolium chloride (TTC) histology. TTC is oxidized by intact mitochondrial dehydrogenases of healthy

tissue, yielding a red colored product called formazan. By contrast, lack of dehydrogenase activity prevents staining of the infarcted tissue: the red live area can be easily distinguished from the dead white one. Our preliminary data shows that the infarct volumes are 25.5% in wild type and 48% in LFG knockout mice (Figure 4.1). Another parameter analyzed after stroke was the neurological score measuring the motor deficit of the mouse 24 hours after occlusion. Motor functions were scored from 0 to 4 where 0 = no deficit; 1 = forelimb weakness and torso turning to the ipsilateral side when held by tail; 2 = circling to affected side; 3 = unable to bear weight on affected side; and 4 = no spontaneous locomotor activity. In this aspect we also observed more severe neurological scores in LFG knockout (score = 4) compared to wild type (score = 1).

This data is still very preliminary so we need to increase the number of mice per group to know if the differences observed are statistically significant. So far it suggests that our hypothesis of the neuroprotective role of LFG after stroke could be valid. For future experiments we should also look at the Fas pathway related apoptotic events, such as caspase 8 and caspase 3 activation or DISC formation, to see if the LFG knockout mice show a more severe damage because they are less protected from Fas mediated cell death.

Chapter 4, in part will be prepared for submission for publication of the material. Li Yang and Scott McKercher are contributing to this ongoing work. The dissertation author was the primary investigator and author of this material.

	LFG KO	WT
Score	4	1
Infarct size	48%	25.5%

Figure 4. 1- TTC staining of LFG knockout and wild type brains after stroke. Coronal brain sections (1mm thick) of knockout and wild type brains stained with TTC, the red area is the healthy tissue and the white one is the infarcted tissue.

5

Lifeguard’s role in the immune system

INTRODUCTION

Fas or CD95 is an important molecule in many aspects of the immune system, including the killing of pathogen-infected cells and the death of obsolete and potentially dangerous lymphocytes, acting as a guardian against autoimmunity and tumor development. Since LFG is an inhibitor of this pathway, we hypothesized that LFG may play a role in the immune system. In this study we focused on T cell development and immune response.

T cell development is an elaborated process consisting of several stages that can be summarized as follows:

1. Multipotent precursors enter the thymus where the specification to the T cell pathway begins.

2. Proliferative expansion and T cell receptor (TCR) gene rearrangement commits the cell to the T lineage within the thymus.

3. β-selection: This process selects cells that have successfully rearranged the β chain of the TCR.

4. TCR dependant selection: Once the TCR is functional after the rearrangement of the α chain; those T cells that react strongly to self-antigen presented by the Major Histocompatibility Complex (MHC) are deleted while the ones reacting with low or moderate affinity are selected for.

5. Developmental divergence between CD4+ and CD8+ T cells.

6. Mature T cells migrate to the periphery and continue to differentiate by exposure to antigen and cytokines (for review see (Krammer, 2000; Rothenberg and Taghon, 2005)).

T cells are divided in 4 populations depending on the expression of two specific coreceptors for the T cell receptor (TCR) known as cluster of differentiation 4 (CD4) and 8 (CD8). CD4 restricts T cell interaction with the major histocompatibility complex II (MHC II) expressed and utilized by antigen presenting cells to present antigens to the immune system. CD8 restricts the interaction to MHC I utilized to present antigens by all nucleated cells.

- DN or CD4-/CD8-: double negative cells expressing neither CD4 nor CD8. DN cells are further subdivided in 4 groups (DN1-DN4) depending on the expression of the cluster of differentiation antigen 44 (CD44) and 25 (CD25). During these stages the progenitor cell is specified and committed to the T cell lineage. At the DN3 stage β-selection occurs, so the cells that were not able to rearrange correctly the β chain of the TCR are eliminated, the rest progress to DN4.

-DP or CD4+/CD8+: At this stage cells start to express CD4 and CD8 and positive selection occurs. This process depends on the TCR interaction with MHC presenting self antigen, so cells that react with very high affinity will be deleted (negative selection) and only those who have an intermediate affinity will be selected for (positive selection), while the ones that didn't recognize at all the peptides presented by MHC will die by neglect.

-CD4+ or CD8+ single positive cells: The surviving cells from the positive selection are now differentiated into CD4 or CD8 cells depending on their interaction with MHC class II or class I respectively. Then these mature cells migrate out of the thymus to continue their differentiation in the periphery.

The role of the Fas pathway in this process has remained very controversial. Fas is expressed at low levels in DN T cells, while high levels are detected in DP and CD4 or CD8 positive thymocytes. The sensitivity of these two types of T cells to Fas is different; DP T cells are sensitive to FasL but single positive thymocytes are not (Drappa et al., 1993; Nishimura et al., 1995).

Fas deficient mice (lpr) suffer from lymphadenopathy and autoimmunity (lupus erythematosus) (Watanabe et al., 1995). The best evidence against Fas involvement in negative selection comes from this mouse model, in which the negative selection process is not altered. On the other hand there is data suggesting that Fas is involved in negative selection, but only when T cells encounter high antigen concentration (for review see (Sprent and Kishimoto, 2002)).

In the periphery a role for Fas has been shown in activation induced cell death (AICD) that constitutes a second line of defense against autoimmunity. In the spleen, Fas levels are low in resting T cells but its expression is upregulated upon activation (Drappa et al., 1993). After T cells are activated there is a clonal expansion dependant on IL-2, followed by an effector phase after challenging with antigen and then a down phase that eliminates most of these cells except for some that will become memory cells. During the expansion cells are resistant to apoptosis but in the down phase they become sensitive to it in the presence of IL-2 except for the memory cells. The Fas pathway is known to play an important role in the initial phases of AICD, but it is not the only apoptotic mechanism involved (Krammer, 2000).

The Bcl2 family has been reported to influence survival of immature T lymphocytes, therefore playing a role in positive selection. Bcl2 expression in

thymocytes is biphasic, being high in DN cells, low in DP except for a small percentage that correspond to the cells surviving the positive selection and it goes back up in CD4 and CD8 mature T cells. TCR and Bcl2 expression are regulated independently (Gratiot-Deans et al., 1994).

Bcl2 deficient mice have fulminant lymphoid apoptosis, polycystic kidneys and hipopigmented hair. Lymphocyte differentiation is initially normal but thymus and spleen undergo massive apoptotic involution. The phenotype is not 100% penetrant; at 7 weeks some mice become ill and show a marked reduction of DP thymocytes with a reciprocal increase in DN cells. CD4 and CD8 single positives were also reduced, in some cases CD8 T cells were more affected. Thymocytes of these mice were more sensitive to dexamethasone and ionizing radiation than wild type ones (Veis et al., 1993).

Within this scenario we hypothesized that LFG may participate in the regulation of T cell development and differentiation. To test our hypothesis we examined LFG's expression pattern in the thymus and analyzed the different T cell populations and their sensitivity to Fas in wild type and siLFG mice (Chapter 5A).

The availability of LFG knockout mice in a pure C57Bl6 background has allowed us to generate LFG bone marrow chimeras. With these chimeras it becomes possible to do competitive repopulation studies and antiviral immune response studies. Preliminary data and future directions for this part are discussed in part B of this chapter.

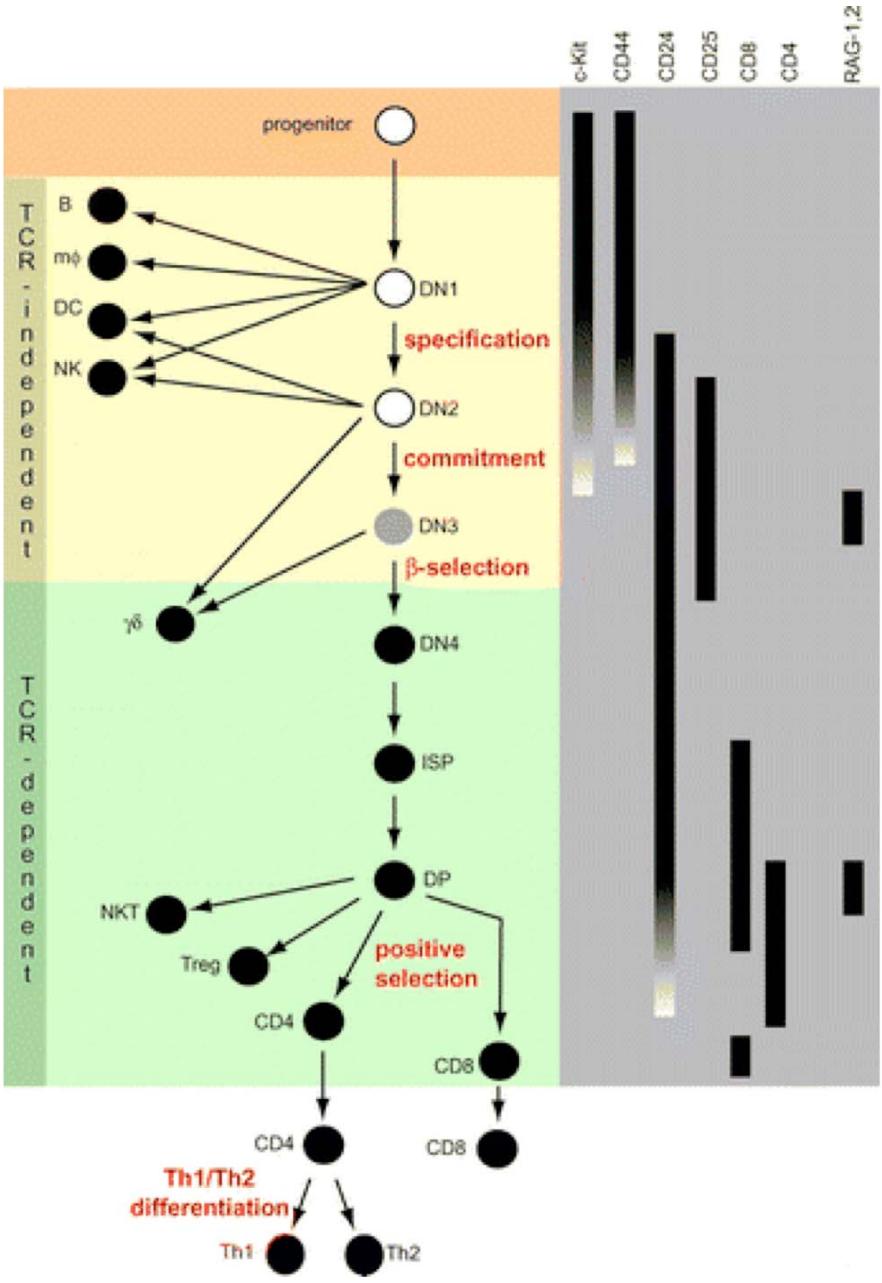

Figure 5.1- Schematic representation of T cell development. This figure illustrates the different steps of differentiation that a progenitor cell undergoes before it becomes a mature T cell, indicating the markers and selection processes at each developmental stage.

A-LFG and T cell development

LFG expression pattern in T cell subpopulations in the thymus

To determine LFG's expression pattern in the different T cell subtypes we isolated thymocytes from wild type 5 week-old mice and performed three-color immunostaining with LFG, CD4 and CD8 antibodies. The highest levels of LFG expression were found in DN and CD8 T cells. CD4 T cells also expressed LFG but at lower levels than CD8. DP cells expressed the lowest amounts of LFG of all subtypes, although a subset of DP cells expressed LFG at much higher levels than the rest of the subpopulations (Figure 5.2). In order to determine if the fraction of DP cells that expressed high levels of LFG was corresponding to cells that had survived the positive selection, we immunostained thymocytes with LFG, CD4, CD8 and CD3 antibodies. (co-expression of CD3 with LFG in the DP cells would indicate that LFG is upregulated in cells that survive the positive selection). The results presented in Figure 5.3 show that all CD3 high DP T cells are also LFG positive. However LFG expression was not restricted to this subset. We still find some DP cells that express LFG at lower levels than the CD3 high DP T cells.

We also analyzed the different DN subsets for LFG expression. DN1 and DN2 showed high LFG expression. DN3 cells were subdivided into two populations, DN3 and DN3b, depending on the level of LFG expression that was reduced in DN3, increased in DN3b and decreased in DN4 (Figure 5.4). Since the β selection happens in the transition from DN3 to DN4, it is possible that the cells that rearrange correctly their TCR β-chain upregulate LFG as a positive survival signal.

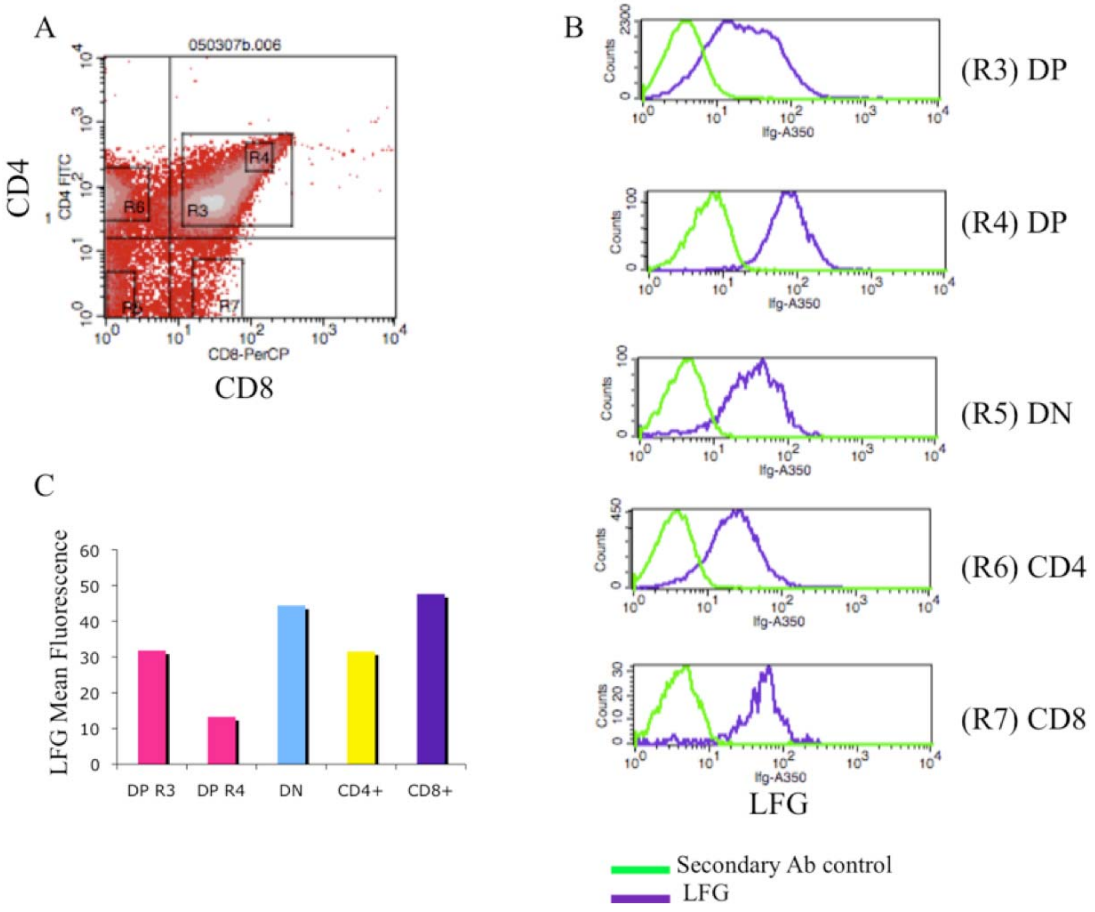

Figure 5.2- LFG's expression pattern in T cell subsets. (A) Dot plot of wild type thymus from 5 week-old mice stained with CD4 and CD8. (B) Histograms showing LFG staining overlayed with the secondary antibody control for the different populations coming from the gates in figure A. (C) Representative histogram showing the mean fluorescence of LFG staining for the different populations in a wild type mouse.

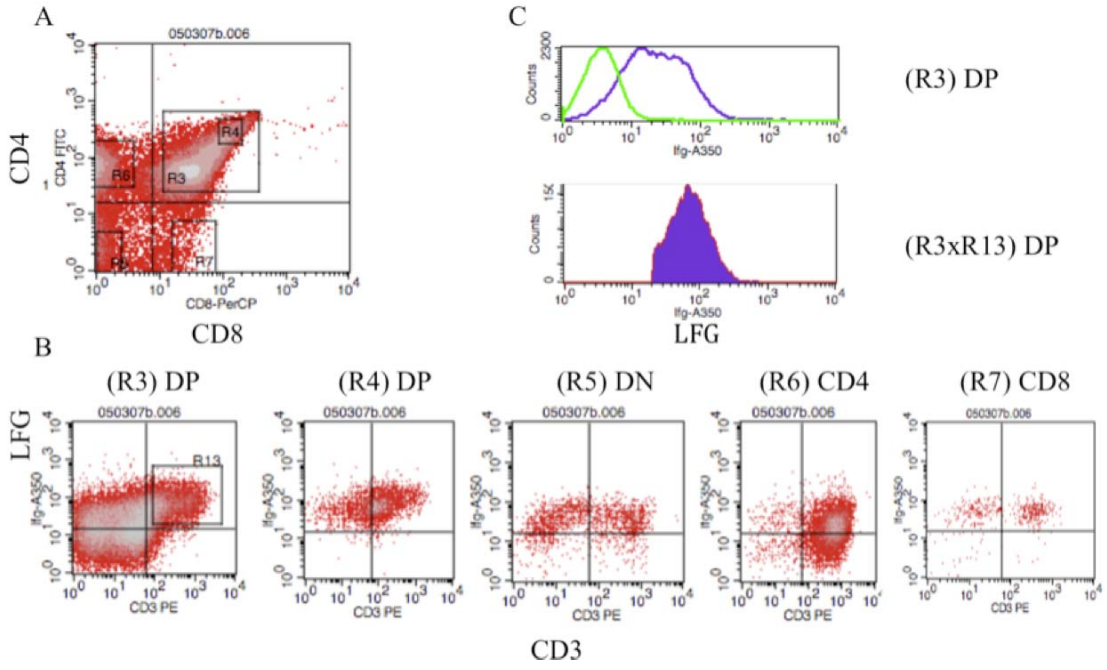

Figure 5.3- LFG's expression pattern in T cell subsets. (A) Dot plot of wild type thymus from 5 week-old mice stained with CD4 and CD8. (B) Dot plots of the regions established in A and their staining with LFG and CD3. (C) Histograms showing LFG expression in (R3) DP cells (top) or in the (R3) DP cells that fall in R13 corresponding to high CD3 expression.

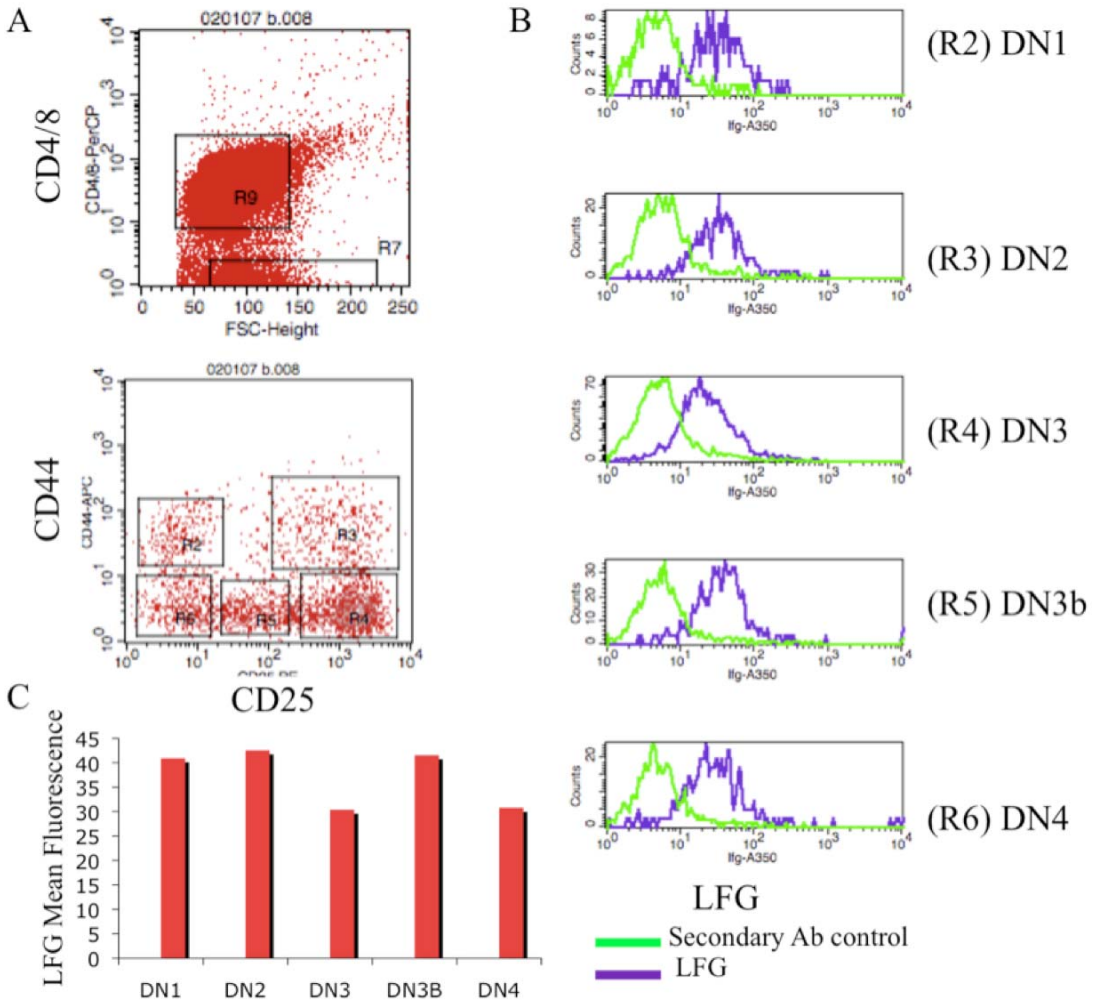

Figure 5.4- LFG's expression pattern in DN T cell subpopulations. (A) Dot plots of thymocytes from 5 week-old mice stained with CD4 and CD8. R7 represents the DN population and R9 DP and single positives (top). Based on the R7 gate cells were examined for their CD25 and CD44 staining establishing the different DN populations (bottom). (B) Histograms showing LFG staining overlayed with the secondary antibody control for the different populations coming from the gates in figure A (bottom). (C) Representative histogram showing the mean fluorescence of LFG staining for the different DN populations in a wild type mouse.

Distribution of the thymocyte subpopulations in siLFG mice

We tested weather the downregulation of LFG had any effect on the distribution of thymocyte subpopulations. For this purpose thymocytes from mice at P0 and 5 weeks of age from wild type and siLFG mice were harvested. Immunostaining was performed using CD4, CD8, CD25 and CD44 antibodies followed by FACS analysis.

The rationale for choosing the P0 timepoint was that the phenotype at this age can be more severe, since several siLFG mice die soon after birth. For this timepoint we analyzed nine wild type and seven siLFG mice. A reduction in DP cells and an increase in DN cells was observed, with only the increase in DN cells being statistically significant (Table 5.1). No significant differences were observed within the DN subpopulations.

Table 5.1- T cell subpopulations in wild type and siLFG mice at P0. Percentage of the T cell subpopulations in wild type (WT) and siLFG mice at P0 as indicated. The percentage values from the siLFG mouse showing the largest difference with the wt are also shown (siLFG C). n = 9 WT, n = 7 siLFG.

	% DP	%DN	%CD4	%CD8
WT (Std dev)	82.43 (2.82)	6.18 (1.68)	8.94 (2.59)	2.45 (0.78)
siLFG (Std dev)	77.86 (3.82)	**11.24** (2.79)	8.81 (1.75)	2.08 (0.77)
siLFG C	**72.31**	**16.79**	7.85	3.05
p-value	0.1060	**0.0032**	0.3894	0.1213

At 5 weeks of age, 8 wild type and 10 siLFG mice were analyzed. The results showed that siLFG mice had a reduced percentage of DP T cells that resulted in an increased percentage of DN as well as of CD4 and of CD8 cells (Table 5.2). The value in absolute numbers showed that the decrease in DP cells was significant and the overall cell number in the thymus was reduced in siLFG mice compared to wild type. On the other hand no significant differences were found in thymus or body weight apart from the most severe cases like siLFG 883 (Table 5.3).

Table 5.2- T cell subpopulations in wild type and siLFG mice at 5 weeks. Percentage of the T cell subpopulations in wild type (WT) and siLFG mice at 5 weeks of age. The values of the siLFG mouse with the largest difference with the WT are also shown (siLFG 883). n = 8 WT, n = 10 siLFG mice.

	% DP	%DN	%CD4	%CD8
WT	82.18	3.44	11.40	2.99
(Std dev)	(3.54)	(0.70)	(2.44)	(0.96)
siLFG	**71.60**	**6.13**	**16.49**	**5.78**
(Std dev)	(6.54)	(1.66)	(3.92)	(2.37)
siLFG 883	**56.41**	**7.83**	**25.06**	**10.7**
p-value	**0.0008**	**0.0006**	**0.0056**	**0.0065**

Table 5.3- Absolute number of total T cells, DP cells, thymus and body weight of 5 week-old wild type and siLFG mice. The values of the siLFG mouse with the largest difference with the WT are also shown (siLFG 883). n = 8 WT, n = 10 siLFG mice.

	Total cell #	Absolute # DP	Thymus weight (mg)	Body weight (g)
WT	1.34E8	1.10E8	61.62	17.32
siLFG	**8.4E7**	**6.06E7**	54.95	14.49
siLFG 883	**5.17E7**	**2.92E7**	36.70	11.33
p-value	**0.0084**	**0.0026**	0.2502	0.084

When the DN subpopulations were analyzed a significant reduction in the DN3b cells was observed (Table 5.4) suggesting the possibility that these cells may utilize LFG upregulation as a survival signal after β selection.

Table 5.4- DN T cell subpopulations in wild type and siLFG mice at 5 weeks. Percentage of the different DN T cell subpopulations in 5 week-old wild type and siLFG mice. The values of the siLFG mouse with the largest difference with the WT are also shown (siLFG 883). n = 8 WT, n = 10 siLFG mice.

	% DN1	% DN2	% DN3	% DN3b	% DN4
WT (Std dev)	3.61 (0.43)	17.83 (5.32)	44.61 (4.28)	11.58 (2.56)	12.22 (7.98)
siLFG (Std dev)	3.32 (1.28)	23.10 (6.44)	43.18 (9.03)	**8.10** (1.26)	11.48 (11.01)
siLFG 883	1.97	25.94	**51.69**	**8.15**	**3.4**
p-value	0.5586	0.0812	0.6873	**0.0016**	0.8747

Apoptosis in the different subpopulations of 5 week-old wild type and siLFG mice was analyzed by staining with Annexin V, DAPI, CD4 and CD8. The results showed that apoptosis was significantly increased in siLFG DP and CD8+ T cells. The total amount of apoptosis was also significantly increased in siLFG mice (Table 5.5).

Table 5.5- Apoptosis in the different T cell subpopulations of wild type and siLFG mice at 5 weeks. Percentage of apoptotic cells within the different T cell subpopulations in wild type and siLFG mice at 5 weeks. The values of the siLFG mouse with the largest difference with the WT are also shown (siLFG 820). n = 6 WT, n = 6 siLFG mice.

% Apoptotic cells	DP	DN	CD4	CD8	Total
WT (Std dev)	6.21 (2.16)	14.86 (4.14)	8.53 (1.06)	1.05 (0.43)	4.23 (0.72)
siLFG (Std dev)	**14.37** (8.09)	14.10 (4.22)	10.59 (3.10)	**2.01** (0.53)	**7.20** (2.89)
siLFG 820	**26.65**	19.85	13.90	**2.79**	**10.81**
p-value	**0.0272**	0.7586	0.1532	**0.0061**	**0.0348**

LFG downregulation increased thymocyte sensitivity to Fas mediated cell death

Thymocytes from wild type and siLFG mice were cultured in the presence or absence of the anti-Fas antibody Jo2. Viability was measured at 0, 6, 8, 12 and 24 hours after treatment using a luciferase assay that measured the levels of ATP as an index of metabolical activity. Dexamethasone treatment was also used as a control for specificity, since Bcl2 deficient cells are more sensitive to this treatment and Bcl2 and Fas represent two different pathways (Van Parijs et al., 1998) (Figure 5.6).

Our results indicate that siLFG thymocytes are more sensitive to Fas mediated cell death, but equally sensitive to dexamethasone treatment, showing the specificity of LFG for the Fas pathway.

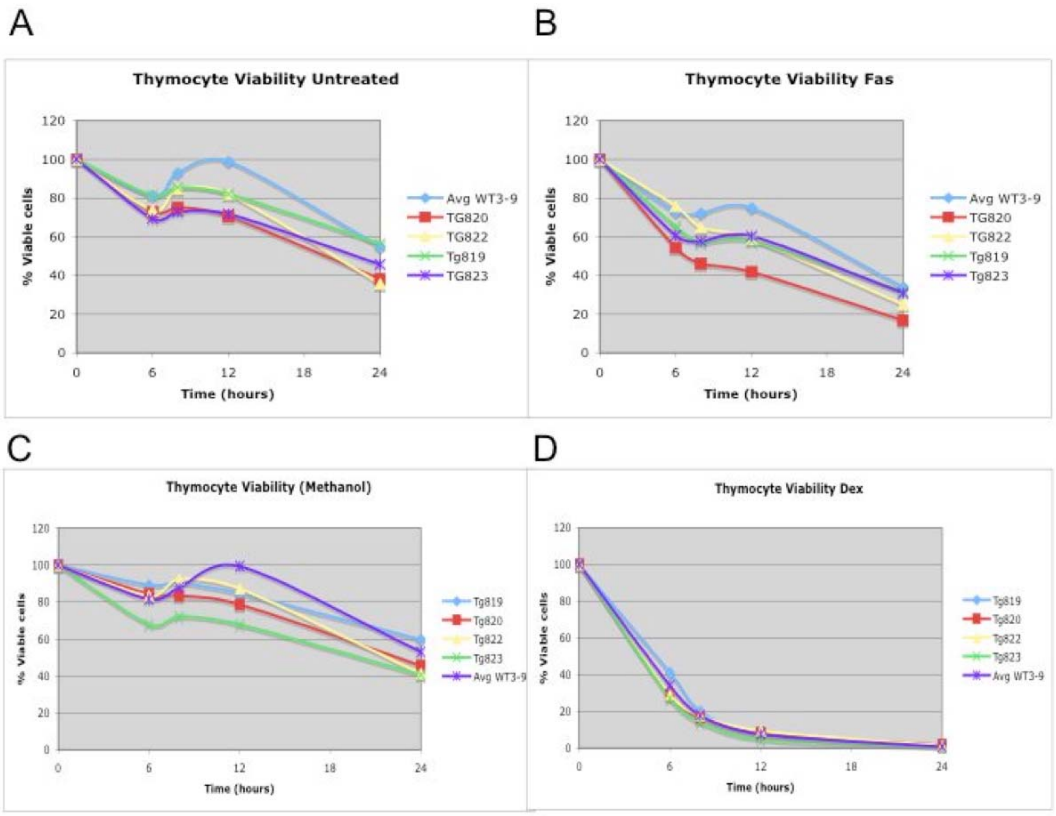

Figure 5.6- Increased cell death in Fas treated siLFG thymocytes. Viability curves from thymocytes of 5 week-old wild type and siLFG mice cultured in the absence (A) or presence of 0.5 micrograms/ml of the anti Fas antibody Jo2 (B). Dexamethasone dissolved in methanol was used as a control: thus methanol (C) and 1 micromolar dexamethasone (D) were assayed. The curve for wt (n=6) is blue in A and B and purple in C and D. Curves from siLFG mice are represented individually.

CONCLUSSIONS AND DISCUSSION

LFG presents an interesting pattern of expression in the different T cell subsets. When considering the role of LFG as a protective antiapoptotic molecule it is possible to hypothesize that LFG would be upregulated providing a survival factor to those cells that have undergone a selection process either for the correct rearrangement of the T cell receptor (TCR) or for not reacting strongly to self antigen presented by MHC. The first checkpoint at the double negative stage is the correct rearrangement of the TCR β chain between the DN3 and DN4. Based on our LFG expression data we decided to subdivide the DN3 subpopulation into DN3 and DN3b. The latter presented an upregulation of LFG that could represent the cells that have correctly rearranged their TCR β chain. The DN3b group was also included in our DN subpopulation analysis and we found that it was the only group significantly reduced in siLFG mice. These data suggest a functional connection between the upregulation of LFG in DN3b cells and their survival.

The next important selection process occurs at the double positive stage, where only about 5% of the cells survive for having a functional TCR that does not strongly react to our self-antigen. According to our hypothesis, LFG should be upregulated in these cells that were positively selected. This group of DP cells can be distinguished from the rest for their high expression of CD3; our data showed that they also express high levels of LFG. The T cell subpopulation data showed a reduced number and increased apoptosis of double positive cells in siLFG mice, correlating the upregulation of LFG expression with the survival of this cells.

Taken together, these data support the hypothesis that LFG has a role as a survival factor upregulated after the β selection and positive selection stages.

We also found an increased sensitivity to Fas but not Dexamethasone treatment in T cells derived from siLFG mice. Nevertheless, the fact that LFG inhibits the Fas pathway doesn't necessarily imply its involvement in the phenotype we observed; LFG could also have Fas independent functions.

It is also important to discuss the mouse model we have used for this study. At first we attempted to generate a conventional LFG knockout but did not succeed. Thus, we opted instead for generating mice with reduced LFG levels by lentiviral transgenesis and siRNA technology. This represents a novel approach to investigate the biological function of molecules *in vivo* with important differences from the knockout. For instance it is important to consider that the level or degree of downregulation may determine the severity of the phenotype observed and that this may vary in different tissues. A certain degree of variability in the severity of the phenotypes described was found in mice from the siLFG colony. Since it was not known what degree of LFG downregulation might result in an observable phenotype, and since the possibility exists that LFG downregulation differed among individuals of the siLFG colony, attempts were made to correlate the severity of the phenotype with the levels of LFG. Such task turned out to be hampered by the finding that there is a considerable variation in the levels of LFG in the thymus of wt mice at the mRNA level (Figure 5.7) and the fact that all the different LFG antibodies we tried did not recognize endogenous levels of LFG in Western blot of thymus lysates.

The siLFG line is generated in a hybrid background; from all the strains tested for the procedure of generating transgenic mice by lentiviral transgenesis the best results were obtained with the first generation (F1) of C57Bl6 and DBA2 mice. The mixed background was a concern since different strains of mice can show variability in various immunological aspects. In order to rule out the possibility that the phenotype observed could be due to the mixed background of the mice, we analyzed the T cell subpopulations in the two parental strains and compared them with our results. Figure 5.8 shows that even if there are small differences between the two parental strains in terms of the percentages of the T cell subpopulations, our data was still significant. In this figure each mice is represented individually, so it also allows us to see the variability in the severity of the phenotype observed in the siLFG colony.

To further investigate the role of LFG in the immune system, we attempted to generate bone marrow chimeras with wild type and siLFG cells. These experiments were not successful due to the mixed background of the siLFG mice. While this study was in progress, LFG knockout mice became commercially available. Since these mice have been backcrossed into the C57Bl6 background, it became possible to generate the LFG bone marrow chimeras that will allow us to do competitive repopulation assays as well as immune response studies.

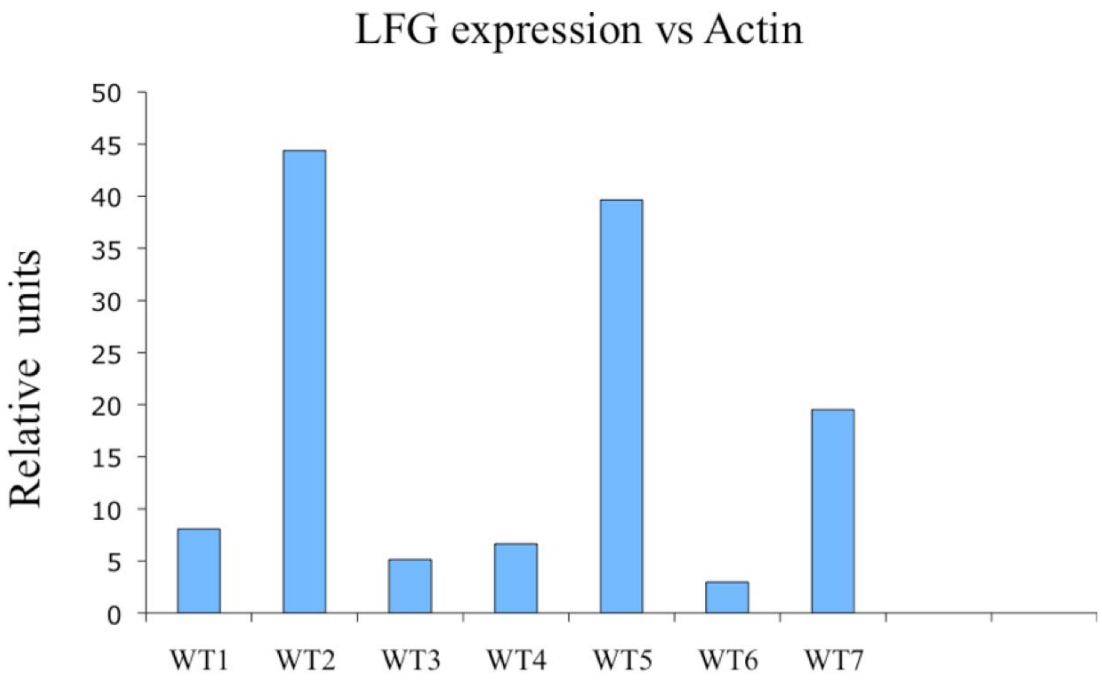

Figure 5.7- LFG expression in wild type thymus is variable. Histogram showing QPCR data of LFG expression level normalized to actin in seven wild type mice.

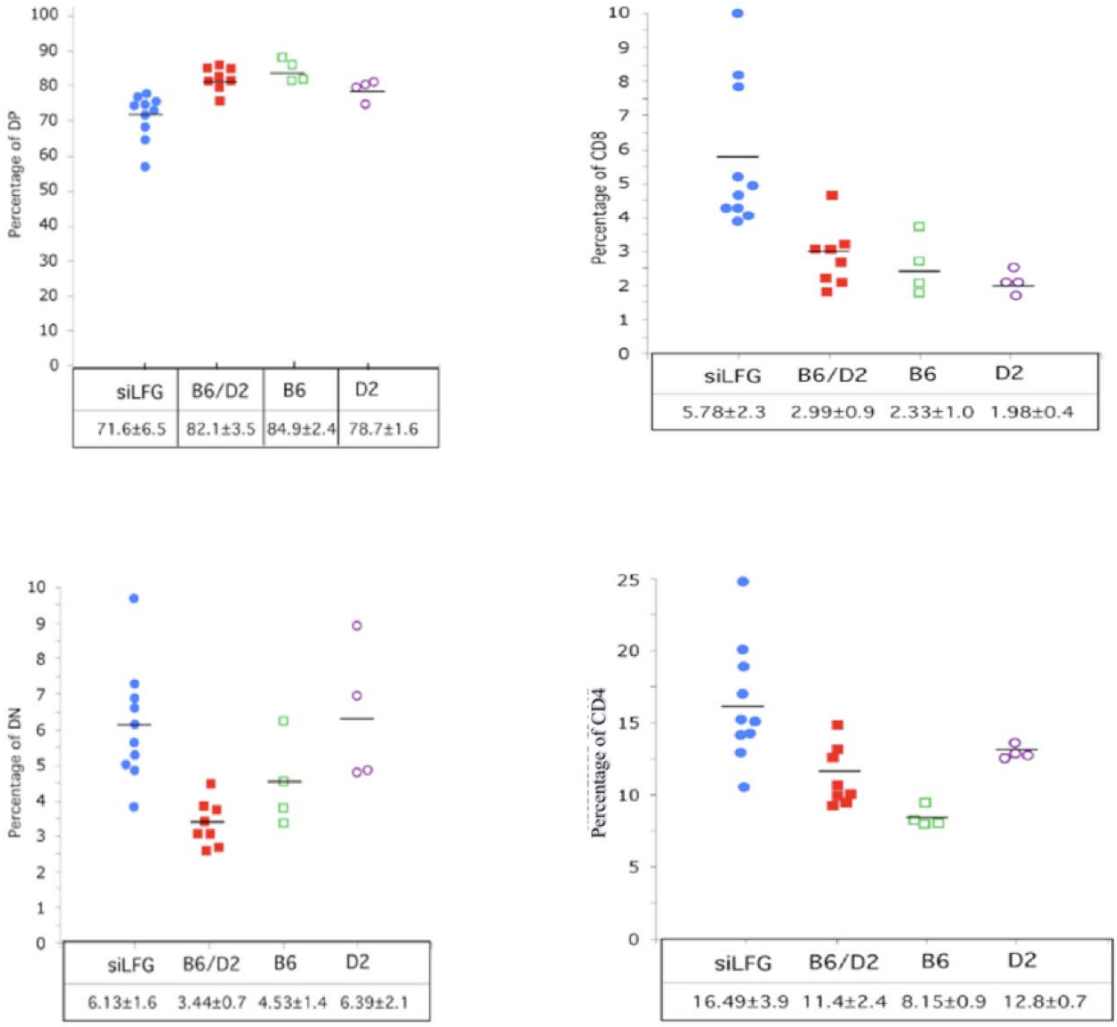

Figure 5.8- Thymocyte subsets of 5 week-old mice, comparison between strains. The graphs show the percentage and corresponding standard deviations of DP, CD8 (top), DN and CD4 T cells (bottom) in the siLFG, wild type (B6D2) and parental strains C57Bl6 (B6) and DBA2 (D2) mice. Each mouse is plotted individually.

B-LFG bone marrow chimeras

Generation of LFG bone marrow chimeras

The term chimera in genetics refers to an organism that contains different populations of genetically distinct cells. Bone marrow chimeras constitute a very useful tool to study, in the same animal, how two genetically different populations behave. In our study we have generated bone marrow chimeras combining wild type cells that have the CD45.1 marker and LFG knockout cells that have the CD45.2 marker. As a host we chose the RAG knockout mice; RAG stands for recombination activating gene and it is essential for immunoglobulin and T cell receptor gene recombination. The loss of the RAG protein means that the mice have no mature T cells or B cells and are therefore immunocompromised. To generate our bone marrow chimeras we lethally irradiated 10 RAG knockout mice and transplanted CD45.1 wild type and CD45.2 LFG null bone marrow cells in a 1:1 ratio by tail vain injection. Two of the irradiated mice did not receive a bone marrow transplant and died approximately ten days after irradiation, serving as irradiation controls to ensure that the dose was lethal.

The bone marrow chimeras were used for two different experiments: 1- Competitive repopulation assay. 2- Immune response.

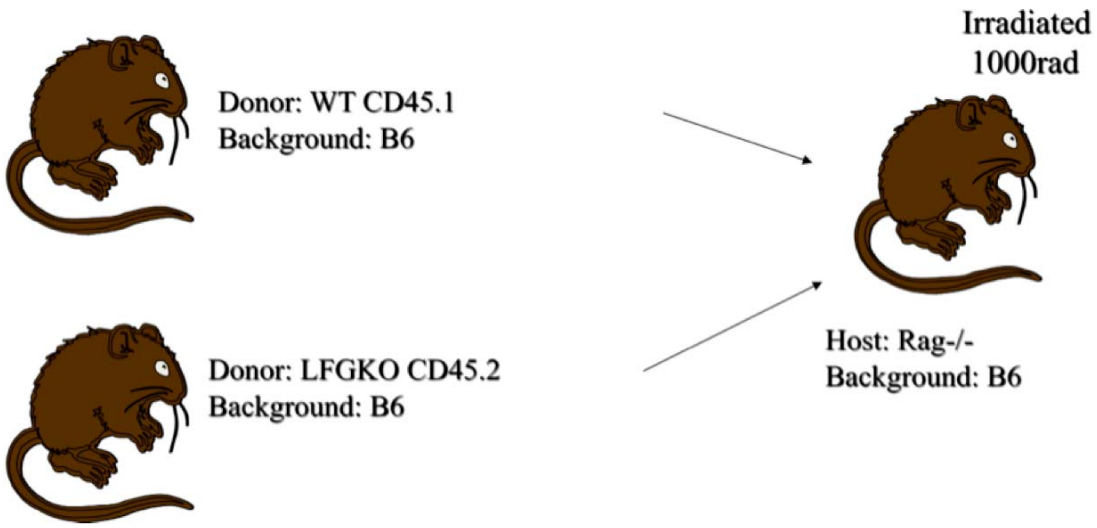

Figure 5.9- Schematic representation of the generation of the LFG bone marrow chimeras. Rag knockout mice were lethally irradiated prior to receive a bone marrow transplant with wild type (CD45.1) and LFG null (CD45.2) cells in a 1:1 ratio.

Competitive repopulation assay

The competitive repopulation assay allows us to pinpoint any selective advantage or disadvantage that the LFG knockout cells might have in repopulating the hematopoietic compartment. With this assay it is possible to determine whether the lack of LFG affects the development, differentiation or survival of any of the hematopoietic cell types. For this purpose peripheral blood at five, ten and fifteen weeks was analyzed by FACS staining with antibodies specific for the different hematopoietic cell types, together with the CD45.1 and CD45.2 markers to distinguish the cells originated from wild type or LFG knockout cells respectively (Figure 5.10).

Interestingly, we found that even if LFG null cells were able to generate all the different hematopoietic cell types, over time there was a pronounced decrease of CD4 and CD8 T cells (Figure 5.11), granulocytes and macrophages (Figure 5.13) compared to wild type. On the other hand the percentage of B cells originated from the LFG null cells was increased compared to the percentage of B cells of wild type origin (Figure 5.12). Statistical analysis was performed using a paired T-Test and all the observed changes were significant ($p<0.05$).

We also performed bone marrow transplants of wild type or LFG KO cells into the RAG knockout mice and performed the same analysis of their peripheral blood at 5 and 10 weeks after transplant, but saw no significant differences. This suggested that the hematopoietic system is able to compensate for the loss of LFG and only in a context of competition with a wild type cell we can see the effects of the lack of LFG.

It remains to be determined if the effects we see are developmental or homeostatic. The observation that the differences were not found at 5 weeks after

transplant but only over time suggests that a homeostatic rather than a developmental mechanism may be at play. Mice lacking Fas or FasL are known to accumulate several fold increases in B cells and CD4 and CD8 T cells indicating a role for this pathway in immune system homeostasis.

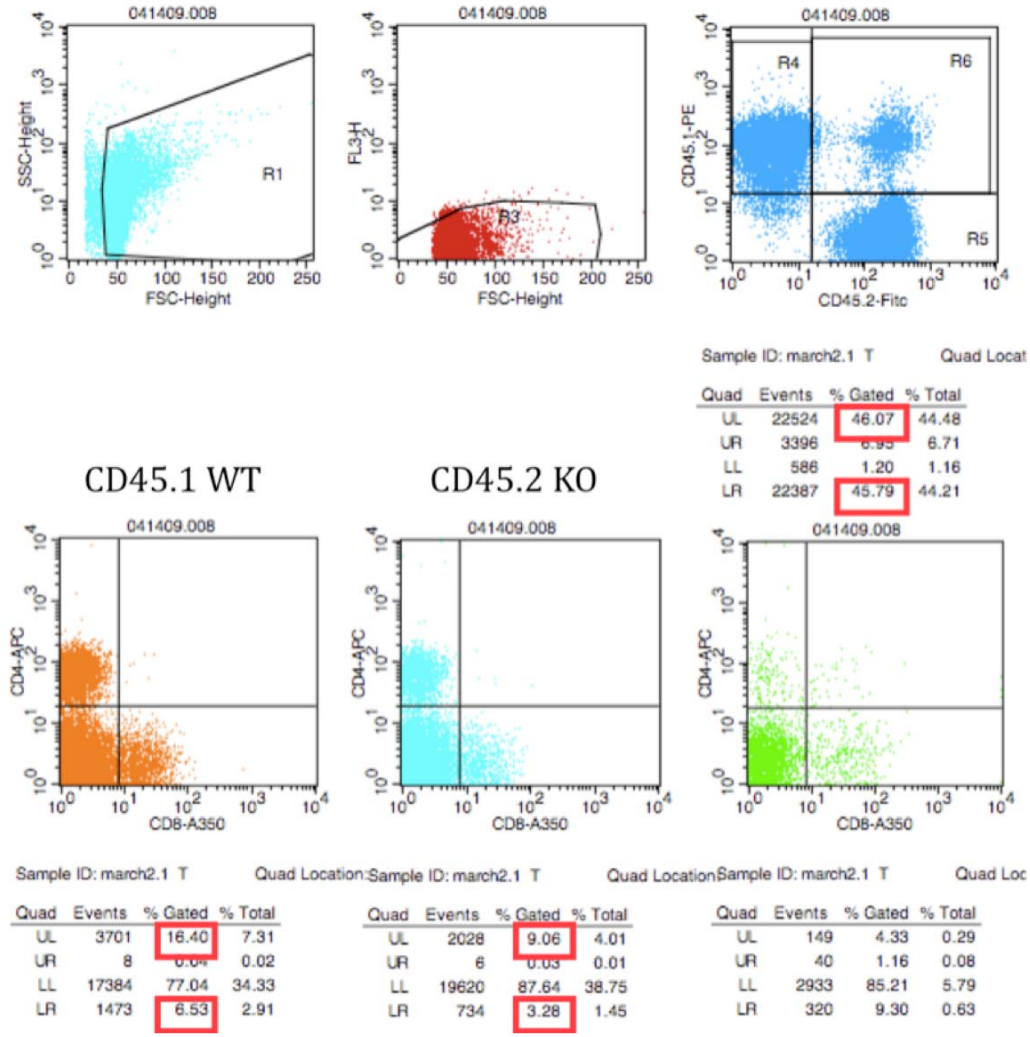

Figure 5.10- Representative FACS plot of peripheral blood analysis. Peripheral blood was collected and stained with markers for the different hematopoietic cell types (CD4 and CD8 for T cells in this case) plus CD45.1 and CD45.2 to determine the percentages of the different cell types originated from wild type or LFG knockout cells respectively.

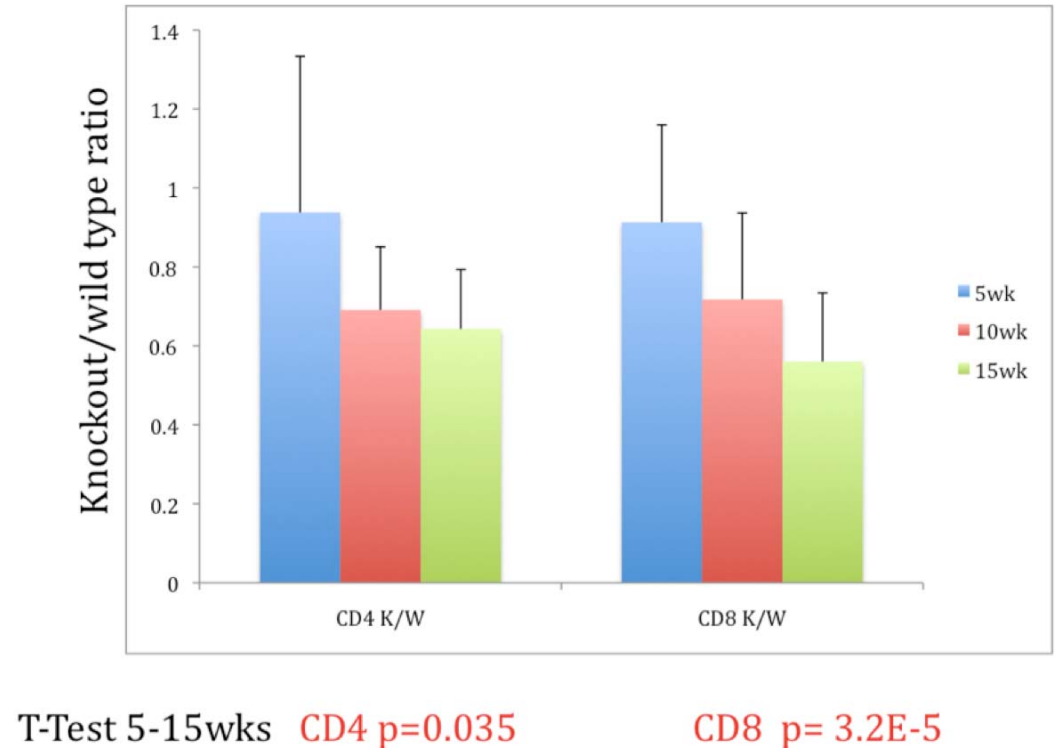

Figure 5.11- Decrease of CD4 and CD8 T cell knockout vs. wild type ratio overtime. Histograms representing the ratios between the percentages of CD4 or CD8 knockout versus wild type cells (n = 8 mice).

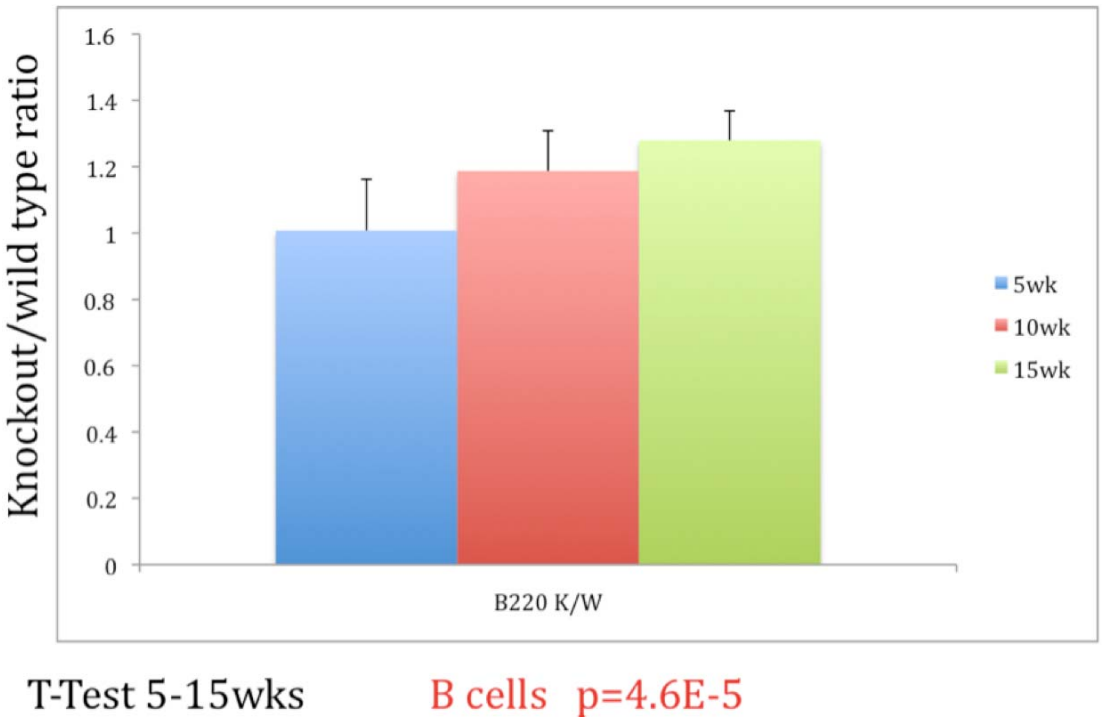

Figure 5.12- Increase of knockout vs. wild type ratio of B cells overtime. Histograms representing the ratio between the percentages of knockout versus wild type B cells (n = 8 mice).

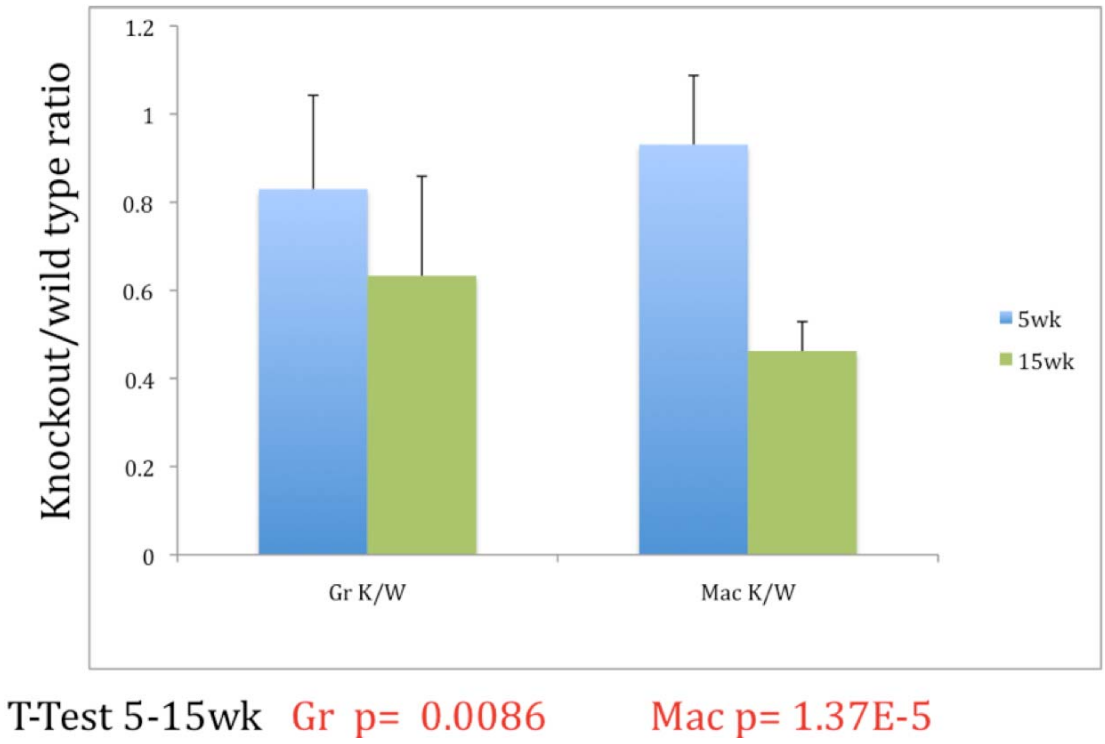

Figure 5.13- Decrease of granulocyte and macrophage knockout vs. wild type ratio overtime. Histograms representing the ratio between the percentages of granulocytes and macrophages in knockout versus wild type cells (n = 8 mice).

Immune response

We were also interested in a possible role of LFG in the immune response. Upon antigen encountering and proper co-stimulation from antigen presenting cells, naïve T cells can quickly expand into effector T cells. The effector T cells are pre-programmed to contract rapidly through a process called activation induced cell death (AICD). Only ~10% of these cells are selected to enter memory phase to ensure a rapid secondary response in case the same pathogen is encountered again. B cells also go through AICD during contraction phase (Figure 5.14). Since the Fas pathway has been implicated in AICD, we hypothesized that lack of LFG would lead to increased apoptosis during this process. This could possibly lead to a defective secondary or memory response if memory cells loose their ability to survive AICD in the absence of LFG

To test this hypothesis we utilized the Lymphocytic Choriomeningitis Virus (LCMV) infection model. LCMV has been the Rosetta stone for studies of the antiviral immune response. The virus belongs to the Arenavirus family of single-stranded RNA virus. It has a small and well-characterized genome. Intraperitoneal injection of LCMV-armstrong strain in mice potently induces an acute CD8, CD4 as well as B cell responses, followed by a stable memory phase. Since the dominant epitopes of this virus were mapped antigen specific T cells can be detected by ex-vivo stimulation with peptide and staining for interferon-gamma. The antigen specific B cells can also be enumerated by Elispot-based limited dilution assay.

The study of the immune response to LCMV infection in our LFG bone marrow chimeras as well as in mice transplanted with wild type or LFG null cells will indicate at which level LFG plays a role in the antiviral immune response.

Chapter 5, in part is currently being prepared for submission for publication of the material. Hurtado de Mendoza, Tatiana; Woods, Bjarne; Liu, Fei and Verma, Inder M. The Role of Lifeguard in the Immune System. The dissertation author was the primary investigator and author of this material.

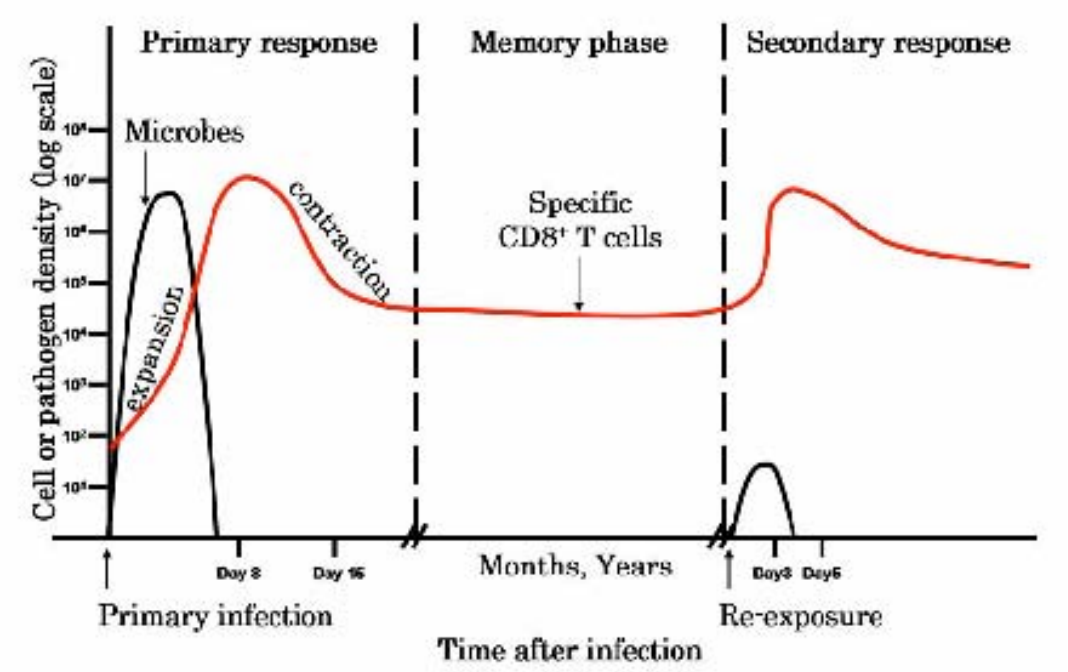

Figure 5.14– Schematic representation of the phases of the immune response.
The graph represents in red the density of immune cells over time along the different phases of the immune response. The pathogen density is represented in black.

6

How does LFG protect from Fas mediated cell death?

INTRODUCTION

How does LFG protect from Fas mediated apoptosis? Three hypotheses that could explain how LFG interferes with apoptosis mediated by Fas but not by TNF were already tested and ruled out (Somia et al., 1999) : 1) LFG does not downregulate FasR levels in the cell surface. 2) LFG does not interfere with FasL binding to FasR. 3) LFG does not interfere with FADD recruitment.

In 2005 Beier *et al*, showed that LFG expression was dependant on the PI3K pathway. Using cerebellar granular cells (CGNs) that express LFG and are resistant to Fas mediated cell death, they tested the effects or PI3K inhibitors, such as wortmanin, in combination with FasL and found out that CGNs died by apoptosis. They also determined that the signal required AKT and used a constitutively active form or a dominant negative. This group also isolated the LFG promoter and performed luciferase reporter assays showing that LFG's expression was inhibited by PI3K inhibitors and to a lesser degree by I-κB. On the other hand nerve growth factor (NGF) was a potent activator of LFG expression (Beier et al., 2005).

In 2007 Fernandez *et al*, published a similar study in CGNs and cortical neurons. This group demonstrated that LFG was present in lipid rafts microdomains and suggested that this could be the site of interaction with the Fas receptor in order to regulate the pathway (Fernandez et al., 2007b).

Sequence analysis of LFG revealed that it belongs to a cytoprotective family with evolutionarily conserved functions in the prevention of programmed cell death. One of the members of this family is Bax inhibitor 1 (BI-1) that protects cells from endoplasmic reticulum (ER) stress by interacting with proteins of the Bcl2 family. The

interaction of LFG and the Bcl2 family of proteins was tested showing an interaction with Bax in coimmunoprecipitation studies (Reimers et al., 2006).

In order to find out the mechanism of action of LFG we started by constructing two systems that will allow a comparison of how Fas mediated cell death is affected in the presence or absence of LFG. The first model was made by introducing LFG in HeLa cells, that are sensitive to Fas and do not express LFG. The second model was to use a cell line that expressed endogenous LFG and use RNAi to create a LFG knockdown condition. In both models we used LFG cDNA or short interfering RNAs (siRNAs) against LFG cloned into lentiviral vectors for the purpose of making stably transduced cell lines. The markers to study the apoptotic pathway were caspase 8, to determine the initiation of the death-signaling cascade, and caspase 3 to follow up the apoptotic events.

We also decided to generate LFG deletion mutants to find out what part of the protein was essential for its antiapoptotic function and lastly we searched for LFG interacting partners to see if they could offer some clues on LFG's mechanism of action.

Generation of a HeLa-LFG stable cell line and testing of siRNAs against LFG

In order to generate a HeLa-LFG stable cell line, a flag tagged LFG cDNA was cloned into a lentiviral vector and was transfected into 293T together with the packaging plasmids to make virus. HeLa cells were infected with this virus. Four days after infection the Fas agonistic antibody CH11 was added to the culture media in

order to select for resistant cells. After two weeks of selection cells were tested for LFG expression by Western blot and quantitative PCR (Figure 6.1).

Since this model was well established, testing first the siRNAs in this system became the best option. Therefore, siRNAs against LFG were designed and cloned into lentiviral vectors that contained a green fluorescent protein (GFP) cassette driven by the CMV promoter used as a marker. After testing the ability of the siRNAs to reduce LFG mRNA and protein levels (Figure 6.1), the next step was to make the viruses to infect HeLa-LFG cells with siLFG1, siLFG5, and siβ-secretase (BACE) as a control virus, and perform the functional assay to test if the siRNAs against LFG could interfere with its antiapoptotic function. The results showed that the uninfected HeLa-LFG cells and the ones infected with si-BACE, had a 75% survival, while HeLa-LFG cells transduced with si-LFG1 and si-LFG5 were more sensitive to treatment with a Fas agonistic antibody for 24 hours (Figure 6.2).

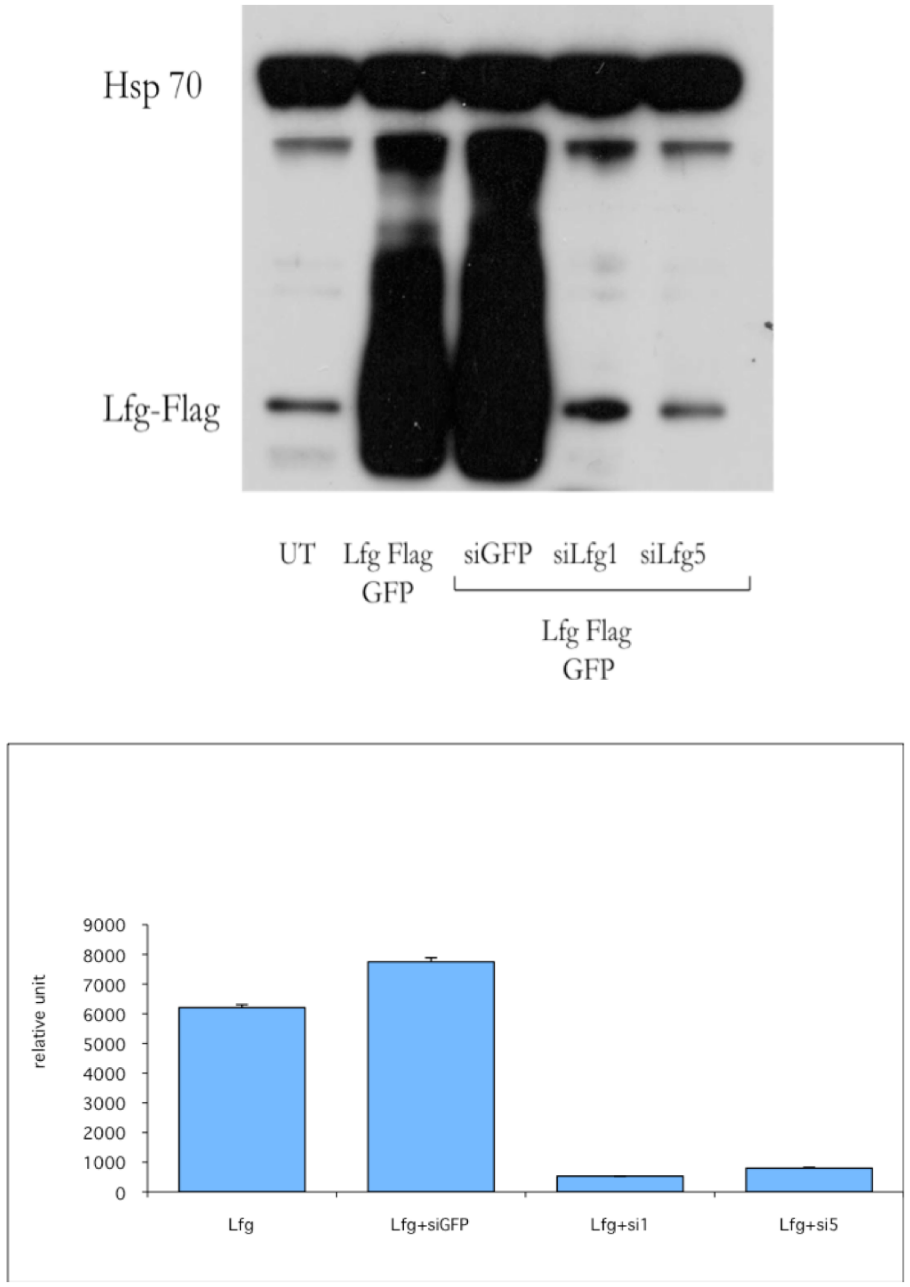

Figure 6.1- Testing of LFG siRNAs. 293 T cells were either untransfected (UT) or transfected with LFG-Flag cDNA alone or in combination with siGFP, siLFG1 or siLFG5. Downregulation of LFG was assessed by Western blot with the Flag antibody and Hsp 70 as a loading control (top) or by QPCR normalized to cyclophillin (bottom).

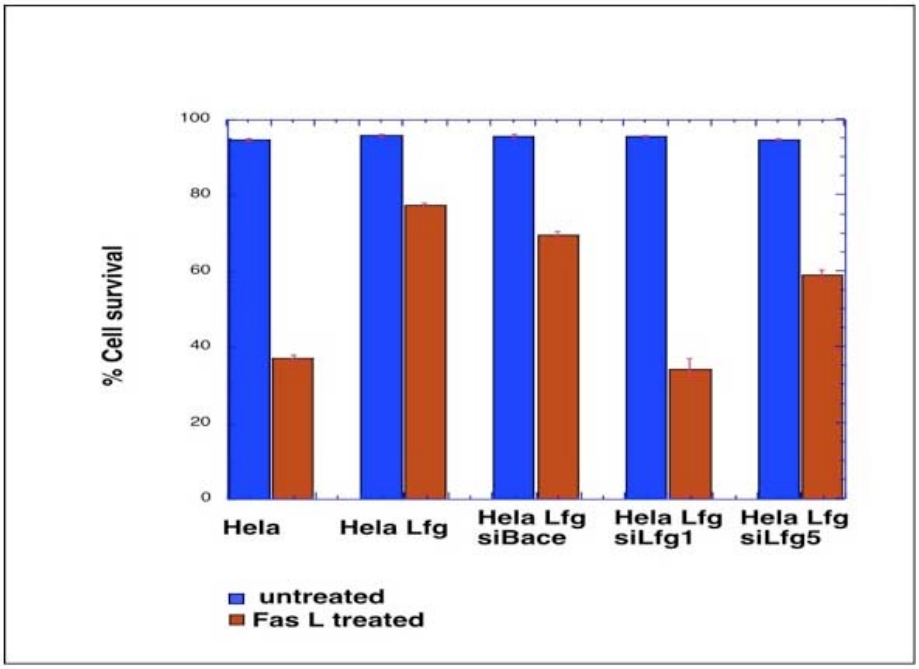

Figure 6.2- Functional test of LFG siRNAs. Histograms representing the percentage of surviving cells after 24 hours of Fas stimulation of cells infected with virus expressing siRNAs for LFG or BACE as indicated. The viability of the cells was assessed by Annexin V and DAPI staining.

Analysis of the Fas apoptotic signaling cascade

The HeLa and HeLa-LFG cell lines were chosen to perform the initial experiments to investigate the anti-apoptotic mechanism of LFG. We started by looking at the effects of LFG expression on caspase 8 and caspase 3 activation in order to evaluate the initiation and the progression of the apoptotic cascade respectively. Apoptosis was induced by incubation with the CH11 Fas agonist for 24 hours, and cells were collected separating the dead fraction (floating cells) from the live one (attached cells). Western blot analysis with caspase 8 and caspase 3 antibodies revealed that HeLa cells expressing LFG had reduced levels of both caspase 8 and caspase 3 cleavage, indicating that LFG was acting upstream of caspase 8 cleavage (Figures 6.3 and 6.4). These experiments were also performed in the SHSY5Y neuroblastoma cell line transduced with either a control siRNA or a LFG siRNA. Since caspase 8 expression could not be detected, experiments were continued with HeLa cells as the main model.

Next, we decided to investigate the events that occur prior to caspase 8 cleavage, namely the formation of the death induced signaling complex (DISC). DISC is a multiproteic complex formed upon Fas activation whose main components are Fas receptor, FADD and caspase 8. For this purpose, DISC immunoprecipitation (IP) experiments were carried out, using an apoptosis inducing Fas antibody to IP the rest of the DISC components. By comparing HeLa to HeLa-LFG cells we observed that FADD and caspase 8 were recruited in both cell lines. However, caspase 8 was fully activated in HeLa cells while in HeLa-LFG cells it was only partially cleaved (Figure 6.5). This data was in agreement with that described by Fernandez *et al,* showing that

in cells expressing LFG, Fas and caspase 8 are recruited to lipid rafts where LFG is located, but the level of caspase 8 activation is lower. Thus, our data suggested that LFG was acting at the level of caspase 8 activation.

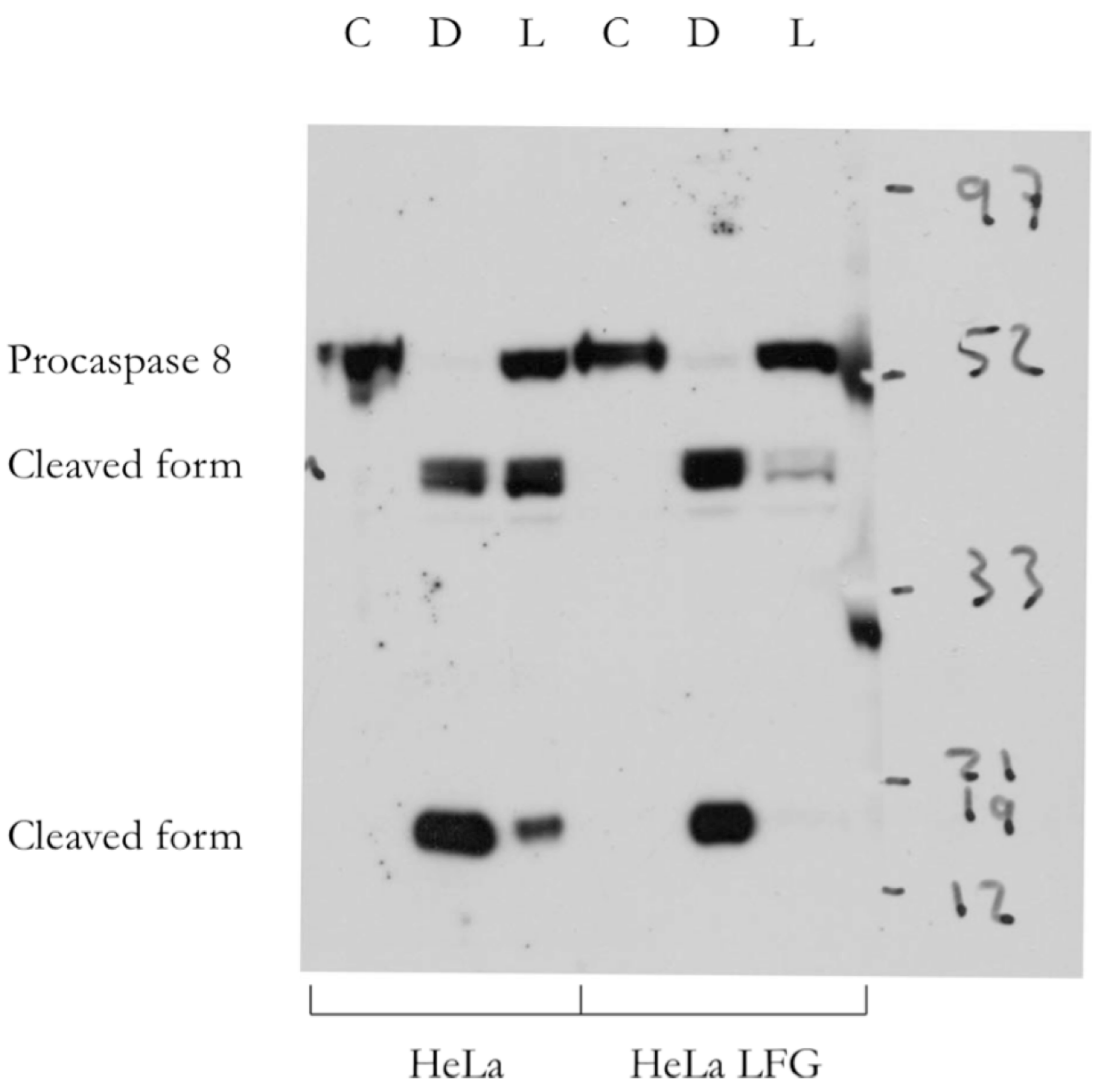

Figure 6.3- Caspase 8 activation is decreased in the presence of LFG. Western blot of protein extracts from HeLa and HeLa-LFG cells. C, untreated cells; D, floating (dead) cells, L adherent (live) cells, after treatment with CH11 (0.5 μg/ml for 24 h). The blot was probed with a caspase 8 antibody that recognizes the procaspase and the cleaved forms.

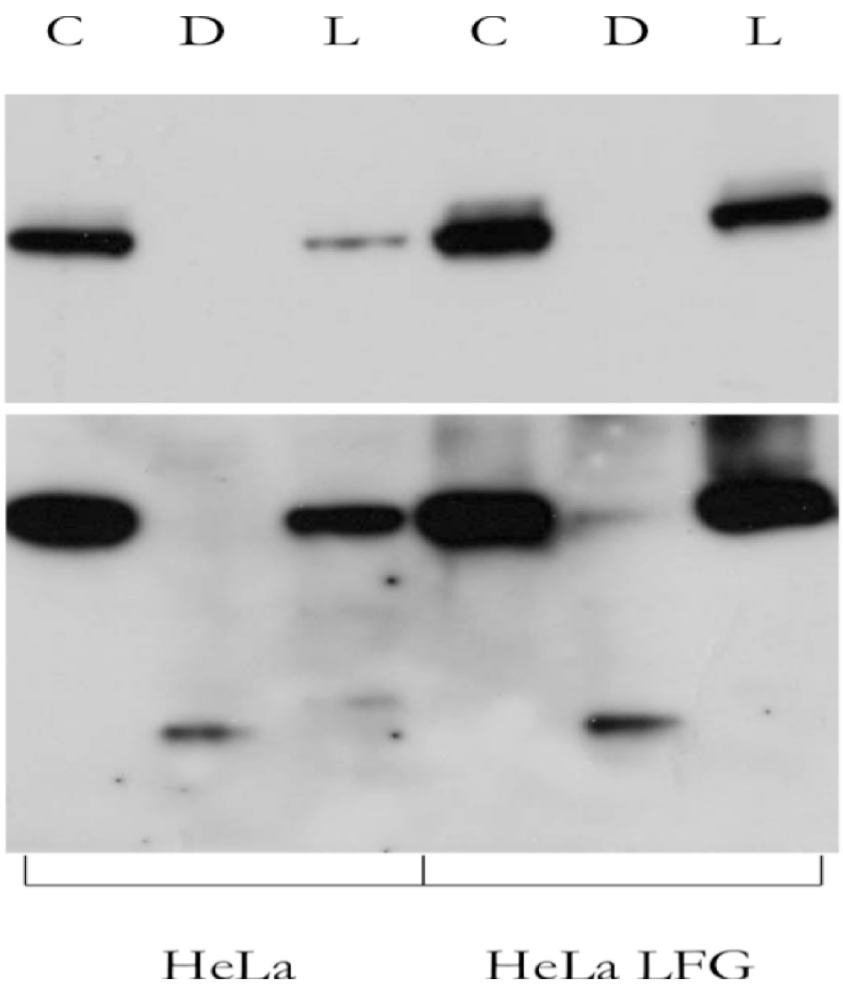

Figure 6.4- Caspase 3 activation is decreased in the presence of LFG. Western blot of protein extracts from HeLa and HeLa-LFG cells. C, untreated cells; D, floating (dead) cells, L adherent (live) cells, after treatment with CH11 (0.5 μg/ml for 24 h). The blot was probed with a caspase 3 antibody that recognizes the procaspase and the cleaved forms. The upper panel visualizes the procaspase form. The lower panel is a longer exposure showing the presence of the active form.

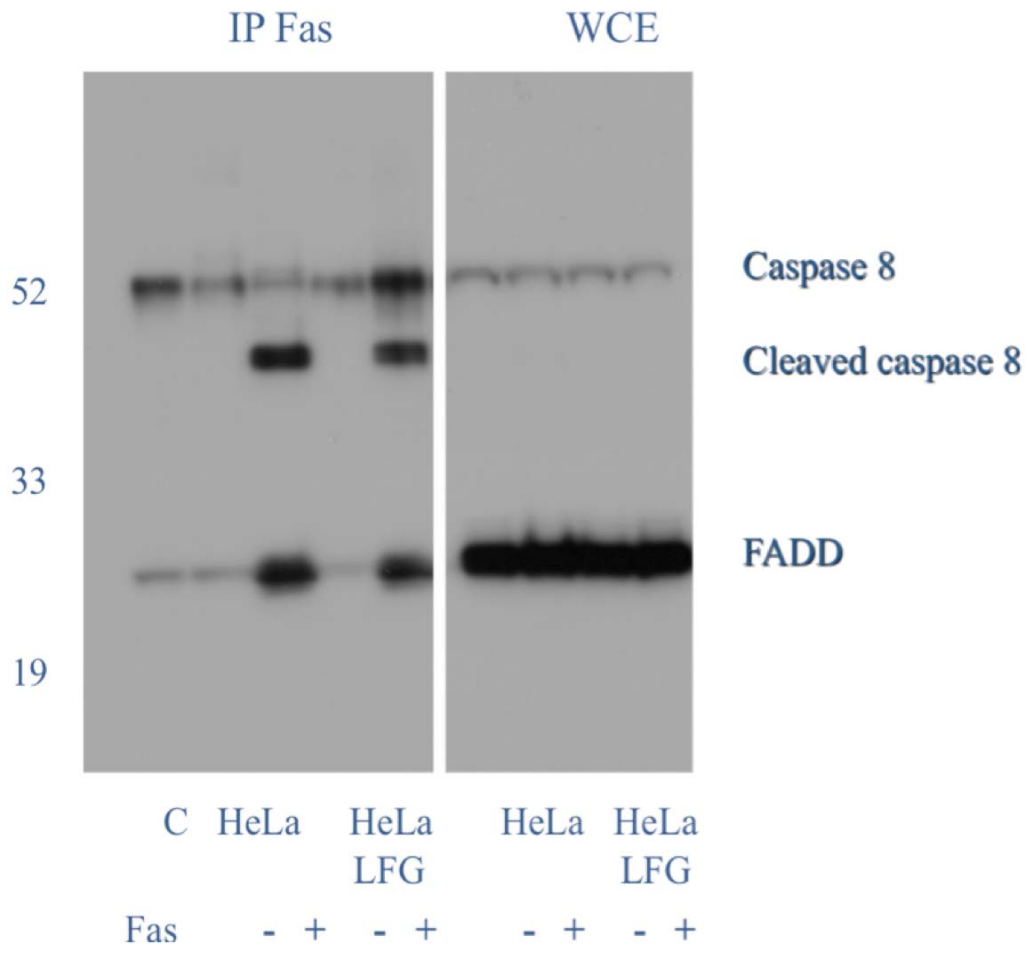

Figure 6.5- DISC immunoprecipitation. IP Western (left) and Western blot (right) of HeLa and HeLa-LFG protein extracts untreated or treated with Fas Ab and then immunoprecipitated with Fas Ab. The upper part of the blot is probed for caspase 8 and the lower part for FADD. C, control of antibody only (no cells).

Search for interacting partners of LFG

Does LFG interact with other proteins? Immunoprecipitation studies indicated that LFG and Fas interact, but it was not known weather the interaction is direct or mediated by other proteins (Somia et al., 1999). Finding out which molecules can interact with LFG can give important clues to discover its mechanism of action.

The strategy consisted in constructing a vector expressing LFG with a six histidine and a flag tag in its N terminus. The plasmid was transfected into 293T cells that were subsequently used to purify LFG using a niquel affinity column that binds the six histidines, followed by flag antibody mediated purification. As a control for non-specific background bands the same plasmid containing GFP instead of LFG was used in the process.

Potential interacting partners are identified by silver or comassie staining of the electrophoresed proteins as bands that appear in the LFG lane but are not present in the control (Figure 6.6). These bands are subject to mass spectrometry and then confirmed by co-immunoprecipitation. The fact that the level of expression of GFP is much higher than LFG makes it difficult to fish out single bands present only in the LFG lane. Therefore, both lanes are cut into 15-20 pieces and run through mass spectrometry. The results of the LFG lane are then compared to the equivalent fractions of the GFP lane and proteins that show a significant score that are not present in the control are considered as possible interacting partners, to be validated by co-immunoprecipitation.

Combining the data of three independent experiments the possible interacting partners were:

-p63: A type II transmembrane protein located in the RER. It can be reversibly palmitoylated during mitosis and when intracellular protein transport is blocked. If overexpressed it forms a tubular membrane network in the cytoplasm, rearranging the ER (Schweizer et al., 1993a; Schweizer et al., 1993b). It provides a link between ER and microtubules. It has been shown to interact with MAP2 in neurons (Farah et al., 2005).

-LFG was detected at its known MW (35 Kda) but also at around 50KDa in all experiments.

-Ubiquitin was present along the LFG sample at different molecular weights and in some cases in the same fraction as LFG (very high molecular weight (MW)).

-In one of the experiments an E3 Ubiquitin ligase was found as a possible interacting partner: Atrophin 1 interacting protein 4 (AIP4) or better known as Itch, a Nedd- 4 like Ub ligase.

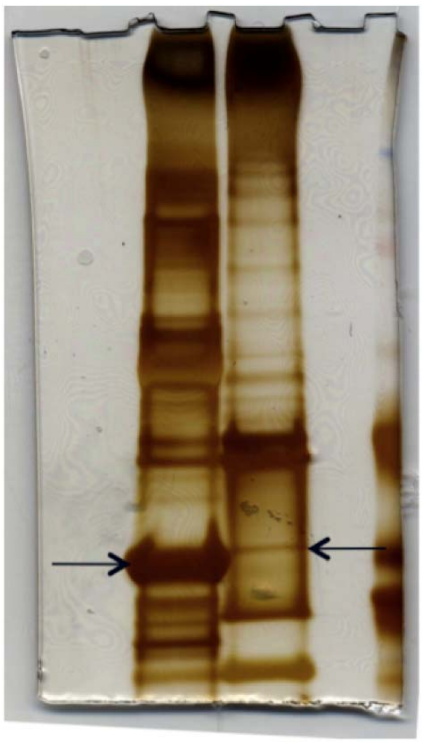

Figure 6.6- LFG interacting partners. Silver stained protein gel containing the purified cell extracts by niquel column and Flag antibody of 293T cells transfected with GFP (left lane) or LFG (right lane).

Is LFG ubiquitinated?

As a follow up of the data obtained after mass spectrometry we performed co-immunoprecipitation experiments with LFG and ubiquitin to test if LFG was ubiquitinated and if AIP4 was the E3 ubiquitin ligase.

For this purpose, 293T cells were transfected either with empty vector, LFG-Flag, Ubiquitin tagged with the HA epitope or a combination of the latter two; cells were lysed, immunoprecipitated with Flag and then run in a gel and blotted with HA and Flag antibodies. The Western blot showed a strong ubiquitination of LFG (Figure 6.7).

The next step was to test the possibility that AIP4 was the E3 ligase that ubiquitinated LFG. Therefore, we decided to confirm the interaction between LFG and AIP4 by co-immunoprecipitation. We transfected 293T cells with AIP4, GFP-Flag and LFG-Flag alone or in combination; cells were lysed, immunoprecipitated with Flag and then run in a gel and blotted with AIP4 antibody. As shown in figure 6.8, AIP4 coimmunoprecipitated with LFG-Flag when transfected together, but not with GFP-Flag.

Encouraged by the results we wanted to perform the functional test, so we generated a ligase dead AIP4 by substituting the cystein of the HECT domain for an alanine (C830A). Ubiquitination assays using the wild type or the ligase dead AIP4 showed no difference in LFG's ubiquitination, but we did not have a positive control that confirmed that our mutant AIP4 was ligase dead.

On the other hand we observed that every time we cotransfected LFG with AIP4, the levels of the ubiquitin ligase were reduced compared to cotransfection with

GFP. Titration experiments cotransfecting a constant amount of AIP4 and increasing amounts of LFG confirmed the previous observation that somehow LFG's overexpression downregulated AIP4 protein levels (Figure 6.9).

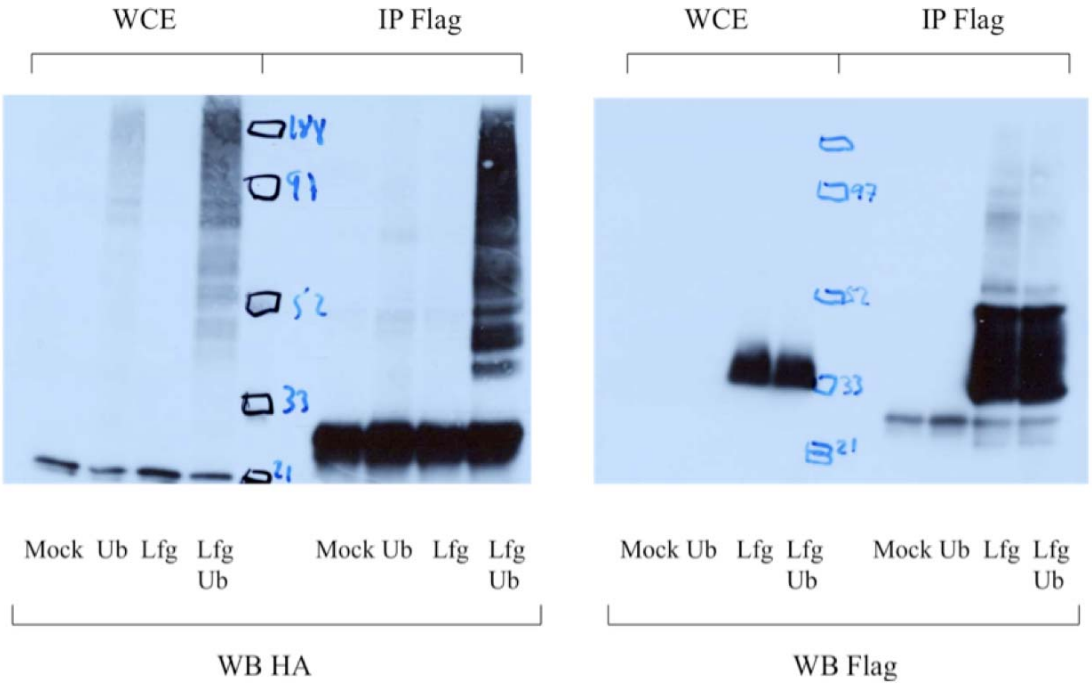

Figure 6.7- LFG is ubiquitinated. IP Western blots of 293T protein extracts transfected with empty vector (mock), Ubiquitin-HA, LFG-Flag, or a combination of LFG-Flag and Ubiquitin-HA. Flag antibody was used for IP and then HA antibody (left blot) or Flag antibody (right blot) were used to probe the blots.

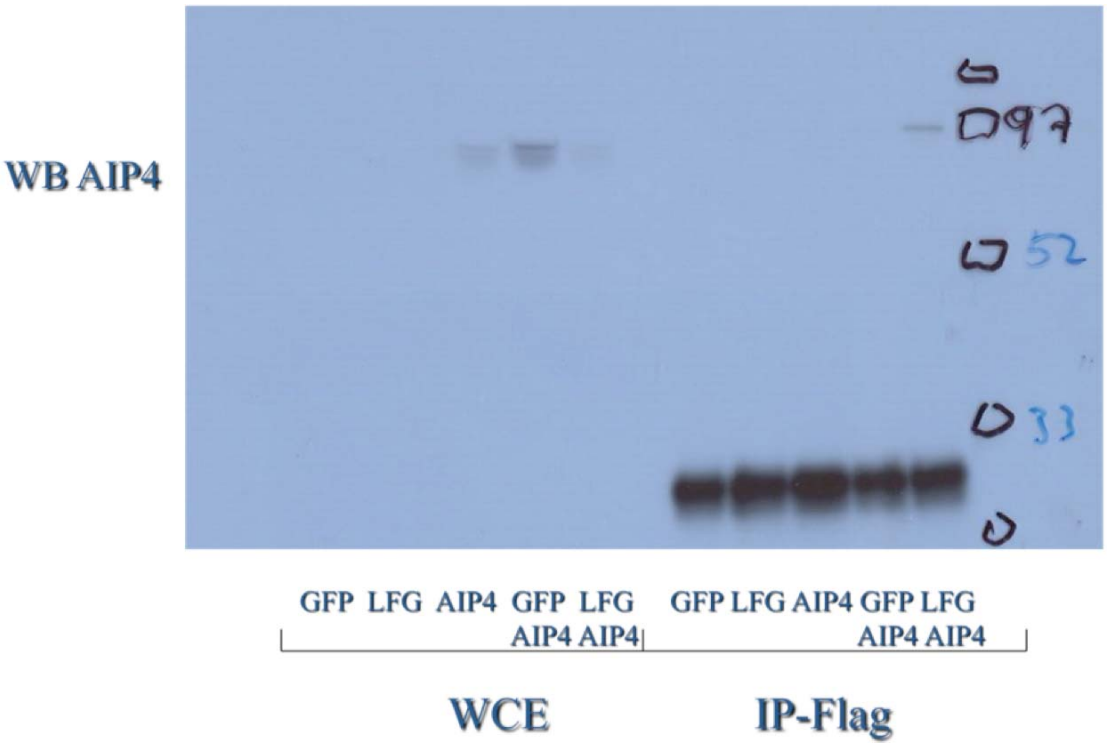

Figure 6.8- LFG interacts with AIP4. IP Western blot of 293T protein extracts transfected with GFP-Flag, LFG-Flag, or AIP4 alone or in combination. Flag antibody was used for IP and then AIP4 antibody was used to probe the blot.

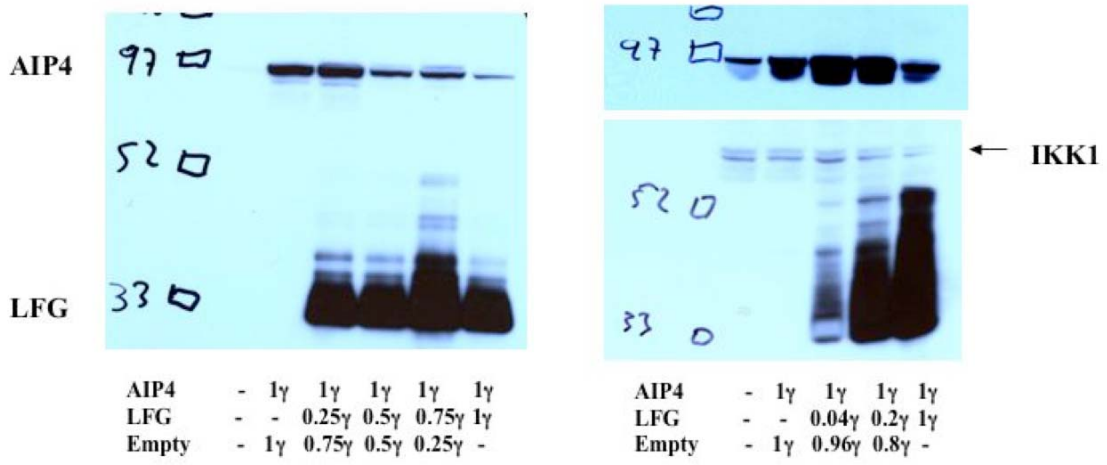

Figure 6.9- LFG downregulates AIP4 expression. Western blot of lysates from 293T cells transfected with constant amounts of AIP4 and increasing amounts of LFG-Flag. Blots were probed with AIP4, flag and IKK1 antibodies.

LFG deletion mutants

In the attempt to find out how LFG protects the cell from Fas mediated apoptosis we generated several deletion mutants with the purpose of determining what part of LFG was essential for its protective function.

Since LFG's amino terminal portion is cytosolic we reasoned that this might be an important part of the protein that could interact with other proteins and transduce a signal. Therefore we generated Δ31 that eliminated the first 31 aminoacids, Δ38 that deleted the first 38 aminoacids including the PPSY motif that was identified as a potential binding site for the E3 ubiquitin ligase AIP4 and Δ105 that eliminated the whole amino terminal part. We also wanted to delete the extracellular carboxy terminal domain, so we generated the ΔC mutant and finally we attempted to delete the last intracellular loop with its transmembrane domain and extracellular C' potion, ΔC46.

These deletion mutants were cloned into lentiviral vectors containing a 2A sequence followed by a GFP cassette that served as a transduction marker; providing the advantage of analyzing Fas mediated cell death by FACS separating Fas sensitive untransduced cells from the GFP expressing cells that were also expressing LFG or the deletion mutants.

Before performing the apoptosis assay we analyzed the expression and cellular localization of these mutants to make sure the deletion did not have an effect in them. As Figure 6.11 shows Δ31, Δ38 and ΔC had comparable expression level to wild type LFG, on the other hand ΔC46 and especially Δ105 were expressed at lower levels.

Cellular localization was normal except for the Δ105 mutant that seemed to localize correctly in some cells but not in others.

The functional assay consisted in incubating the HeLa cells transduced with LFG or with the different mutants with the Fas agonistic antibody, CH11, for 24 hours. Then the cells were harvested and analyzed by FACS after staining with annexin V to identify apoptotic cells. Since we had the GFP marker we could gate on the GFP positive population to test the effect of the expression of LFG or its mutant versions on the survival of the cell. The data from this experiment suggested that the Δ31, Δ38 and ΔC were perfectly able to protect HeLa cells from Fas mediated apoptosis while Δ105 and ΔC46 were not (Figure 6.12).

An interesting observation was that within the transduced cell population there were various levels of GFP expression probably due to the different number of viral integrations per cell, so we made four subdivisions; no GFP, low GFP, medium GFP and high GFP and analyzed the data by looking at apoptosis in this four different populations. The purpose of this was to investigate a possible dose dependent effect in LFG's protection from apoptosis, so we plotted the data for each mutant and the wild type LFG as a function of percentage of live cells versus GFP expression (Figure 6.13). The graph showed that the higher the level of GFP, the higher the percentage of live cells, reaching more than 95% live cells in the highest GFP expressing cells. This suggests a dose dependant effect of LFG in protecting cells form Fas mediated cell death. We observed that all the deletion mutants except for ΔC46 followed the dose dependent pattern. Surprisingly Δ105 showed protection at the highest expression level, suggesting that the major problem with this mutant was its low level of

expression. We also observed form the cellular localization studies that when the intensity of GFP was higher Δ105 tended to have a normal cellular distribution, therefore we may think that the amino terminal portion of LFG is not absolutely essential for its antiapoptotic function. On the other hand the ΔC46 mutant showed the opposite effect, the more it was expressed, the less it protected, suggesting that the last intracellular loop together with the last transmembrane domain play an important part in LFG's antiapoptotic function.

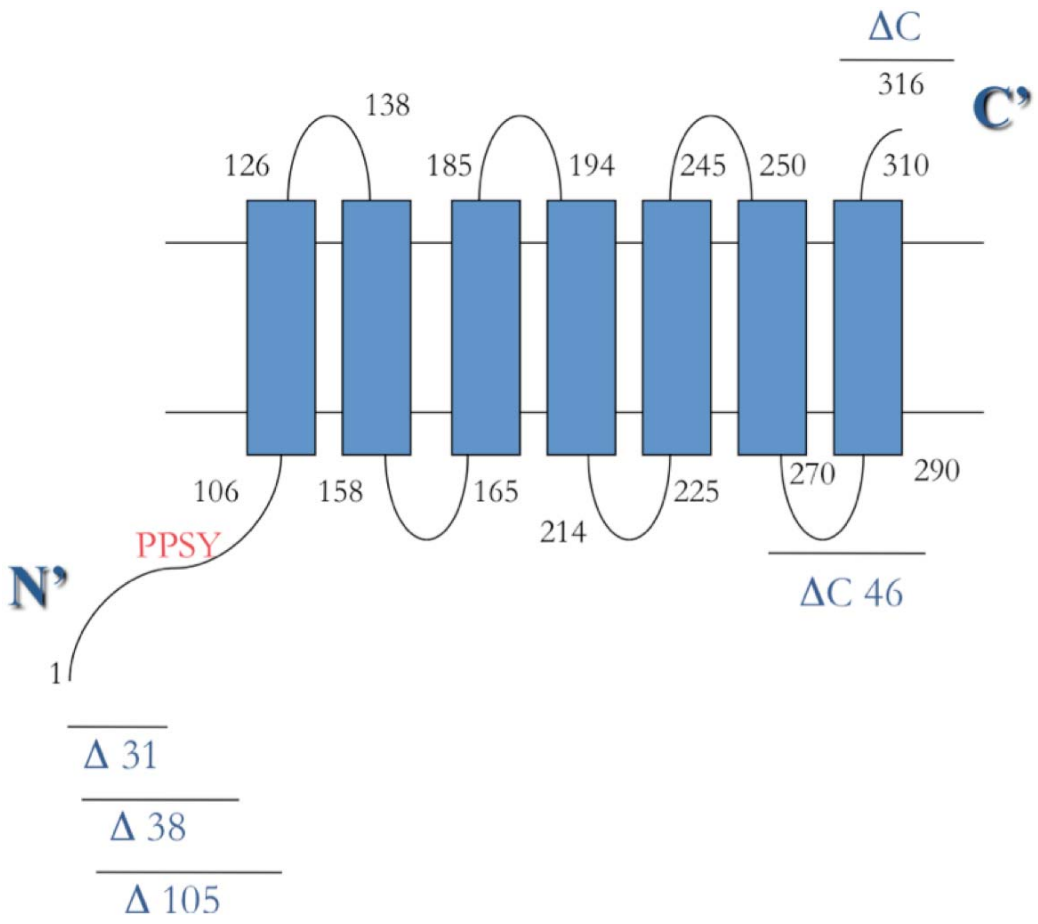

Figure 6.10- Map of LFG deletion mutants. Schematic representation of LFG and the five deletion mutants generated. The PPSY motif represented in red is a putative binding site for AIP4 E3 ubiquitin ligase.

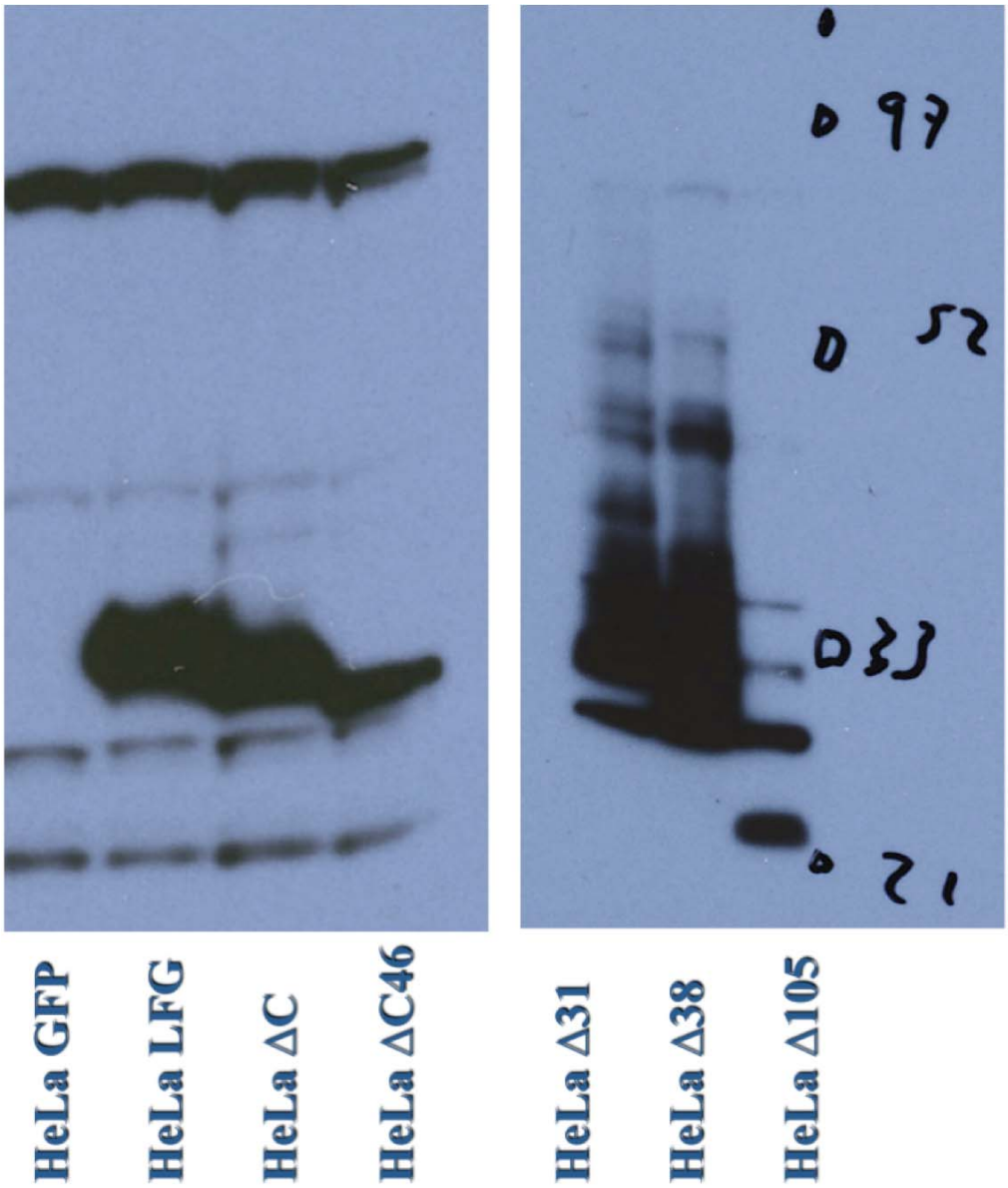

Figure 6.11- Expression levels of LFG deletion mutants. The expression of LFG deletion mutants was measured by Western blot of 293T cell lysates transfected with the wild type LFG or the different mutants.

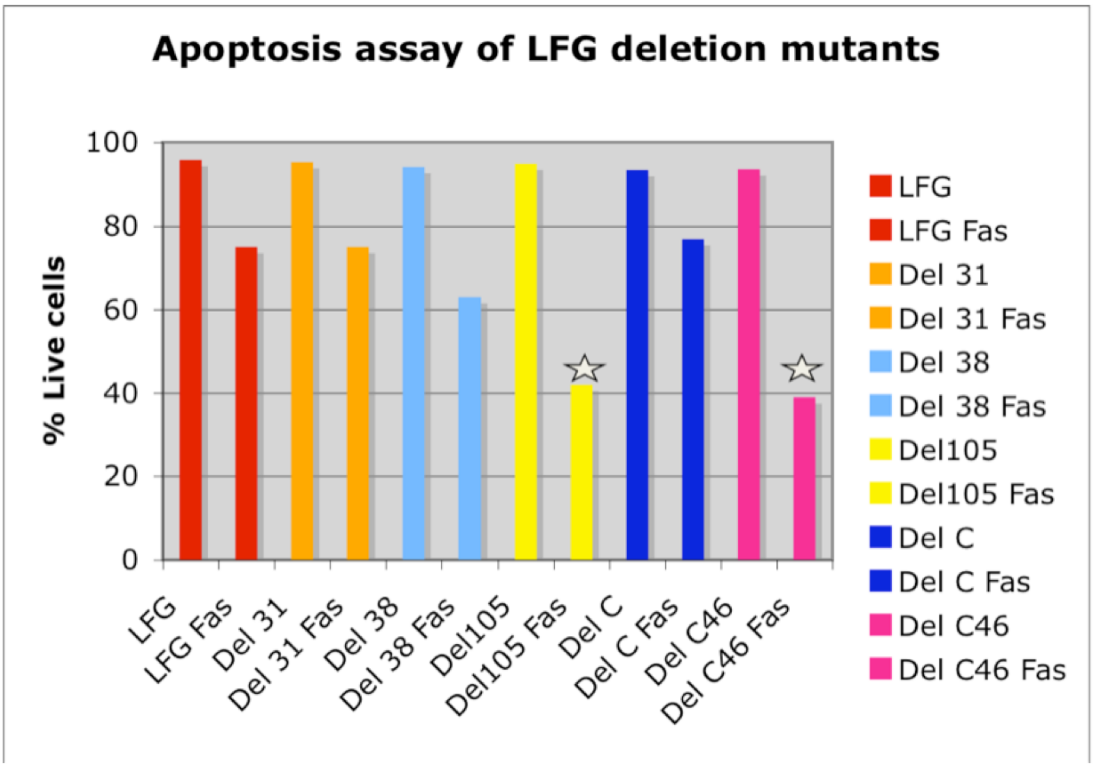

Figure 6.12- Apoptosis assay of LFG deletion mutants. Histograms representing the percentage of live cells with or without Fas treatment for 24 hours of wild type LFG and the deletion mutants. Apoptosis was measured by annexin V staining.

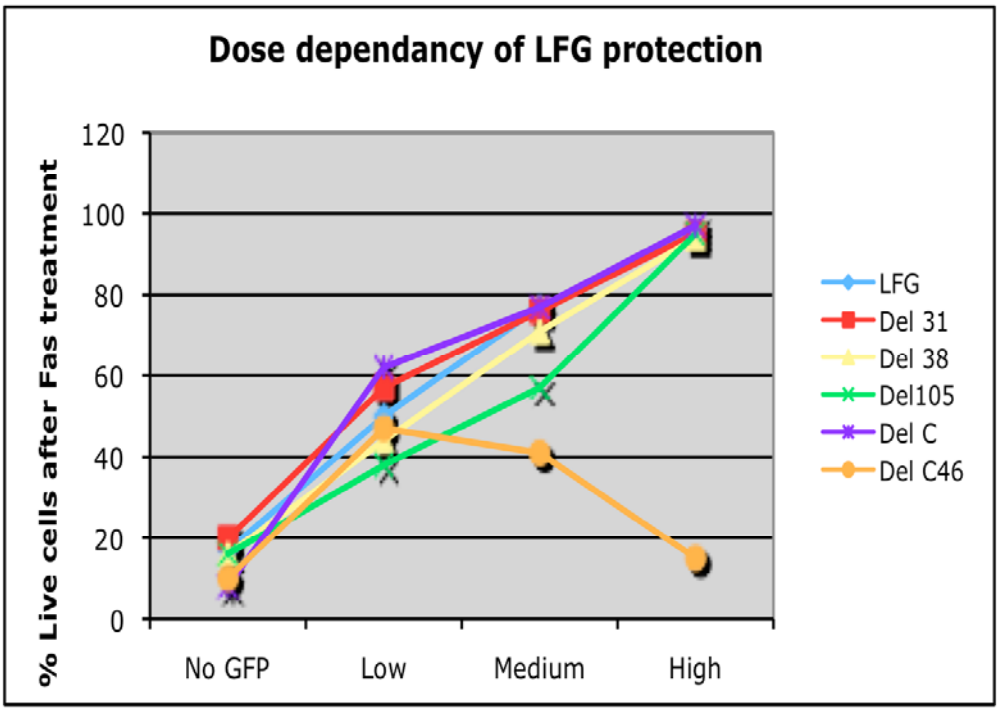

Figure 6.13- LFG protects from apoptosis in a dose dependent manner. The graph represents the percentage of live cells after Fas treatment of HeLa cells transduced with LFG or the different deletion mutants based on the level of GFP expression. Apoptosis was determined by annexin V staining.

CONCLUSSIONS AND DISCUSSION

We have taken several approaches to find out how LFG protects cells from Fas mediated apoptosis that allowed the collection of important information.

We demonstrated that LFG acts at the level of caspase 8 activation in the Fas apoptotic cascade. Our data has shown that in the presence of LFG the DISC is formed and FADD and caspase 8 are recruited, but the cleavage of caspase 8 is inhibited. One of the well-known inhibitors of caspase 8 activation is FLICE inhibitor protein (FLIP) that also gets recruited to the DISC and interferes with the autoproteolytical cleavage that occurs when two molecules of caspase 8 are in close proximity to each other. Therefore a reasonable hypothesis is that in the presence of LFG there are more FLIP molecules recruited to the DISC, blocking caspase 8 activation.

Our deletion mutant studies demonstrated that the only mutant that showed loss of protection from Fas mediated cell death, even at high levels of expression, was ΔC46 in which the deletion spanned a big part of the carboxy terminal part of LFG (aminoacids 270 to 316). Maybe the intracellular loop deleted in this mutant could be playing an important role in providing protection from apoptosis by constituting a binding site for other proteins to be recruited and start a signal transduction cascade that will result in the survival of the cell. The aminoacid sequence deleted in mutant ΔC46 corresponds to the most conserved portion in the family of cytoprotective proteins that LFG belongs to. Thus, perhaps it is not surprising that it plays an important role in LFG's antiapoptotic function.

The finding that LFG is ubiquitinated is also very interesting. We couldn't confirm the identity of the E3 Ubiquitin ligase but it would be worth repeating the experiments to verify that the ligase dead AIP4 was indeed inactive. However, the observation that LFG downregulated the protein levels of AIP4 is also intriguing. Michael Karin's group reported that AIP4, also known as Itch, plays a role in apoptosis mediated by TNF. Upon TNF stimulation Itch gets phosphorylated by Jun N terminal kinase (JNK); this phosphorylation activates Itch and results in FLIP ubiquitination and degradation leading to more caspase 8 activation and ultimately to cell death (Chang et al., 2006). An interesting hypothesis is that LFG may protect from apoptosis by downregulating Itch levels leading to less FLIP degradation. Therefore FLIP can be recruited to the DISC and block caspase 8 activation. A possible argument against this hypothesis is that our Δ38 mutant, that lacks the putative motif for the interaction with AIP4, still showed protection in the functional assay. However we haven't yet confirmed if the motif we deleted in our Δ38 mutant was indeed the interacting site for AIP4. Since we know that the last intracellular loop of LFG deleted in the ΔC46 mutant is essential for protection, testing the interaction between AIP4 and ΔC46 should give us the information we need to see if LFG's mechanism of action is through downregulation of Itch and caspase 8 inhibition by FLIP.

Chapter 6, in part is currently being prepared for submission for publication of the material. Hurtado de Mendoza, Tatiana; Perez-Garcia, Carlos G; Kroll, Todd; Hoong, Nien; O'Leary, Dennis and Verma, Inder M. The Antiapoptotic Protein

Lifeguard Plays a Role in Cerebellar Cell Survival. The dissertation author was the primary investigator and author of this material.

7

Additional findings in LFG knockdown mice

This chapter describes additional phenotypes presented by the siLFG mice. Histological analysis of the tissue collected from wild type and siLFG mice showed that lung, kidney, spleen, thymus and brain were among the organs affected by the reduction of LFG. The siLFG strain had a high mortality rate at birth, so we collected several newborn mice to try to determine the cause of death.

Lung

The most severe effects of LFG downregulation were seen in the lungs. Several animals died at P0 presumably of lung failure due to underdevelopment. Two degrees of severity were found: 1. The worst condition showed lungs that were never developed enough to start breathing and accumulated hyelin membranes in the air spaces; 2. A milder form showed lungs that were able to start breathing, but the air spaces were larger than wild type ones. Some of the mice that were found dead at P0 showed a dilation of the right atrium of the heart and at times hemorrhages in the lungs, which could be a consequence of asphyxia (Figure 7.1).

Some of the siLFG transgenic mice died prematurely at 4-5 weeks of age. Histological analysis also showed the same heart phenotype with blood in the lungs observed in mice that died at P0.

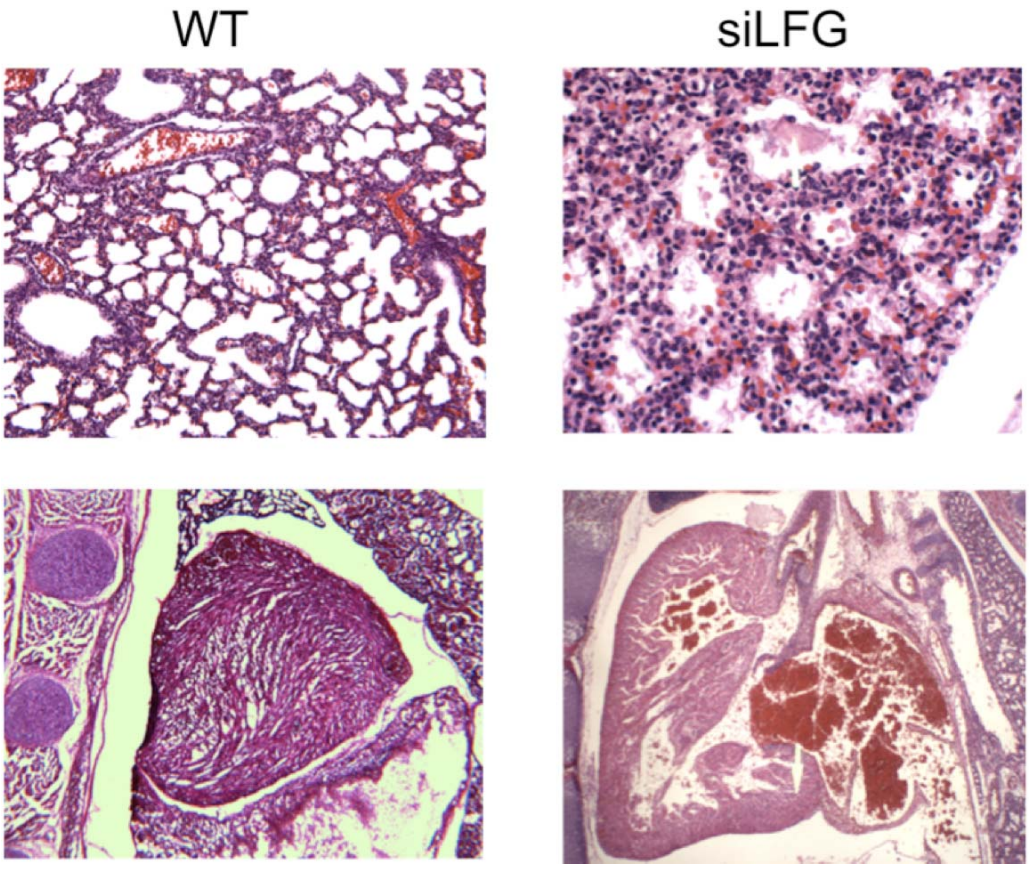

Figure 7.1- siLFG mice have underdeveloped lungs at birth. H&E staining of P0 wild type and siLFG lungs (top) and heart (bottom).

Kidney

The expression of LFG in kidneys significantly increases from P0 to P10 (Figure 7.2), suggesting that LFG may play a role in kidney development during this time frame. We observed an underdevelopment of the kidneys at P7 and P10 in siLFG mice, compared to age matched wild type mice. LFG knockdown kidneys had normal shape but their size and weight was reduced. Histological analysis by H & E staining revealed that kidneys from siLFG mice had a larger immature zone and closed tubules (Figure 7.3). Downregulation of LFG expression was confirmed by QPCR (Figure 7.4).

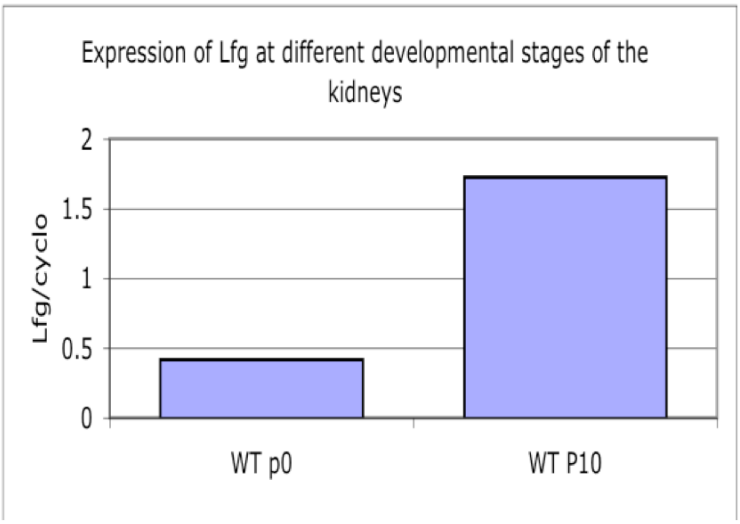

Figure 7.2- LFG expression in the kidneys. QPCR of kidney cDNA from wild type P0 and P10 mice. LFG levels were normalized to cyclophilin.

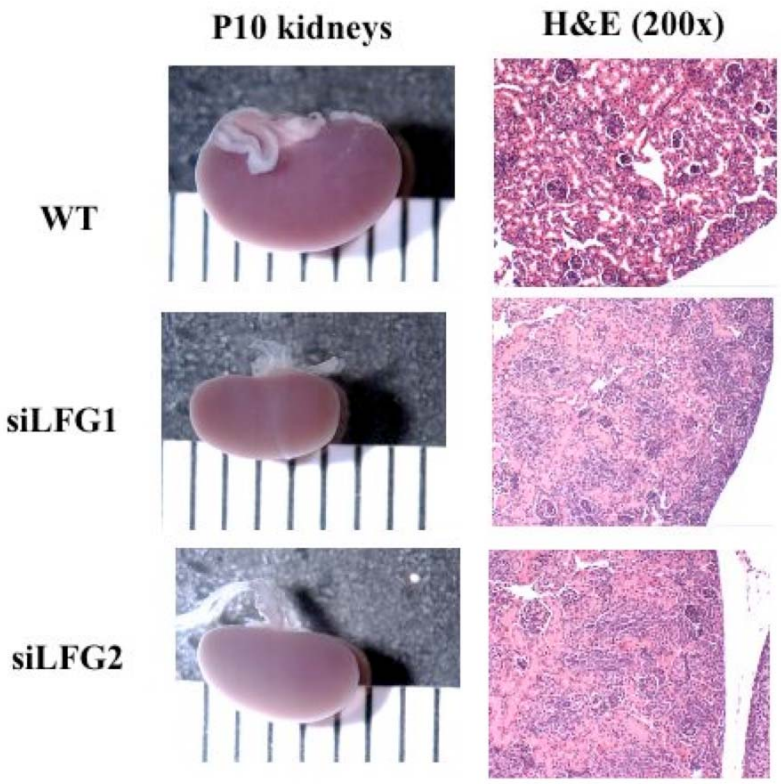

Figure 7.3- siLFG mice have underdeveloped kidneys. Photograph of P10 wild type and siLFG kidneys (left) and H&E staining of sagittal kidney sections (right).

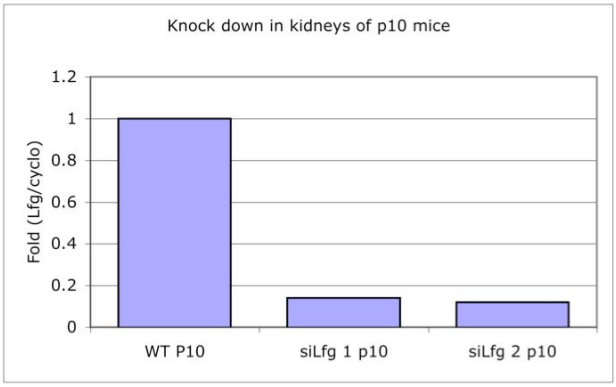

Figure 7.4- Validation of LFG knockdown in the kidney. QPCR showing fold reduction of LFG levels in siLFG mice compared to wild type. The level of LFG was normalized to that of cyclophilin.

Spleen and thymus

A developmental delay was also observed in the spleen. The development of follicles in wild type spleen initiates around P10 and by P14 those follicles are well defined. The siLFG mice at the ages of P10 and P14 showed less developed spleens compared to wild type and finally formed well defined follicles by P21 (Figure 7.5). Previous Northern blot experiments carried out in our laboratory showed no LFG expression in the spleen of adult mice. Thus, it was surprising to find a phenotype in this organ. To address this issue, we decided to perform QPCR on spleen cDNA samples from mice at several developmental time points between P0 and P21. We found LFG expression in the spleen but with a very high variability between mice of the same age (Figure 7.6). The same experiment was performed with cDNA from thymus, confirming the expression of LFG in this organ and also the extensive degree of variability among individuals (Figure 7.7).

TUNEL staining of siLFG and wild type newborn mice revealed a very significant increase in apoptosis in the thymus of mice with LFG downregulation, suggesting that LFG could have a role in T lymphocyte development (Figure 7.8).

.

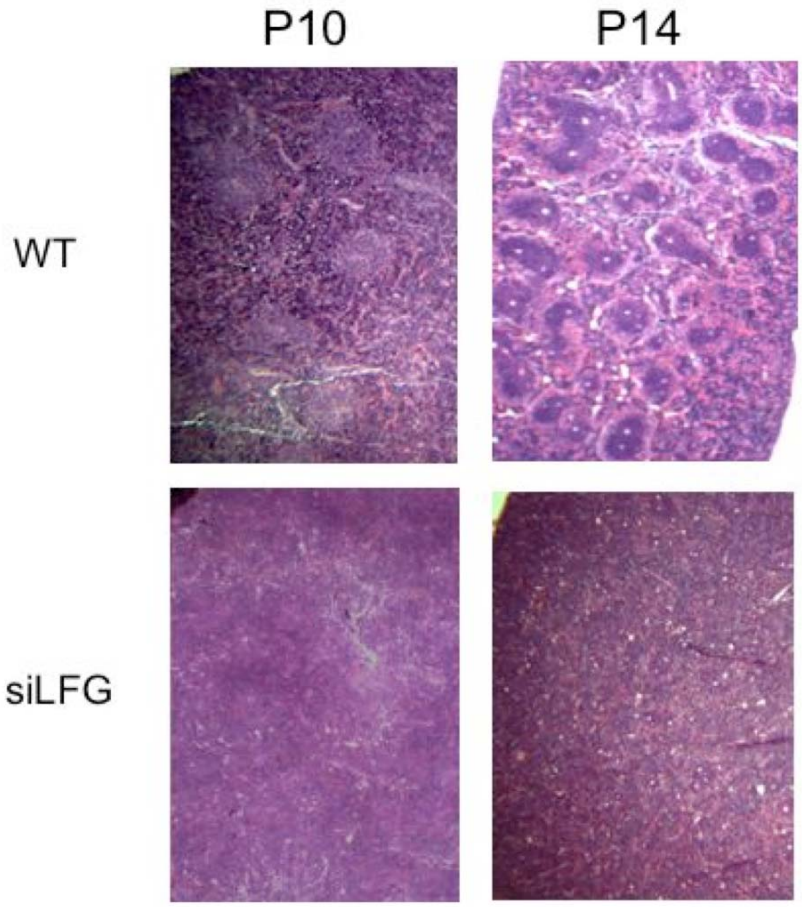

Figure 7.5- siLFG mice have delayed follicle formation in the spleen. H&E staining of wild type and siLFG spleen sections at P10 and P14.

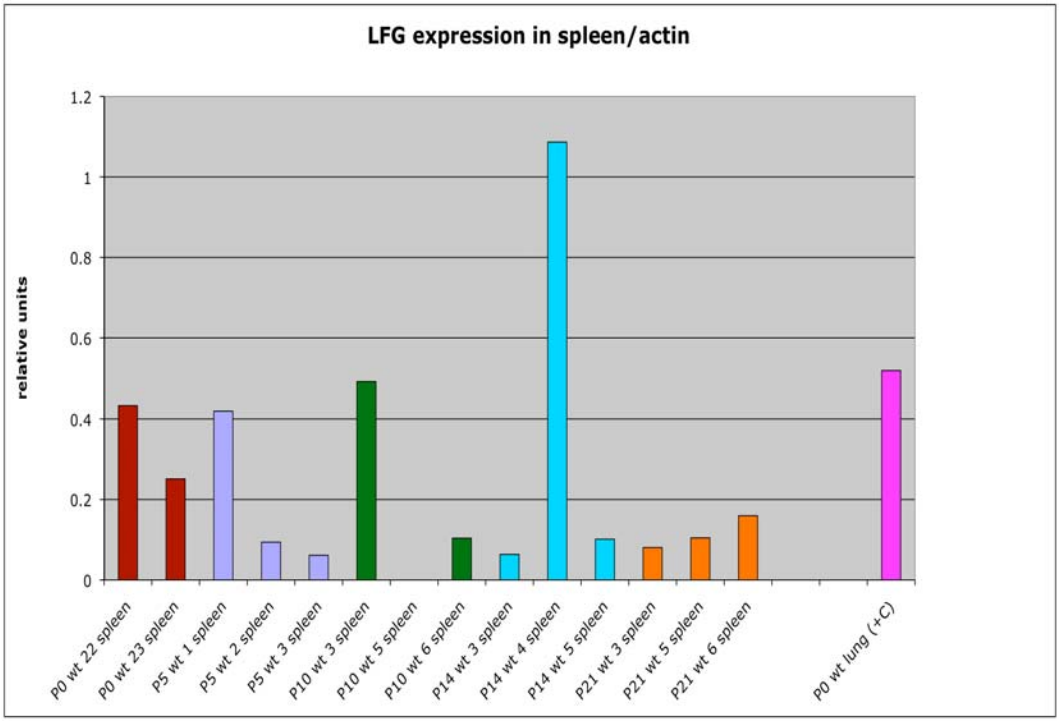

Figure 7.6- LFG expression in spleen by QPCR. Histogram of QPCR of LFG in spleen cDNA from different developmental stages as indicated. Lung cDNA was used as a positive control and LFG values were normalized to actin.

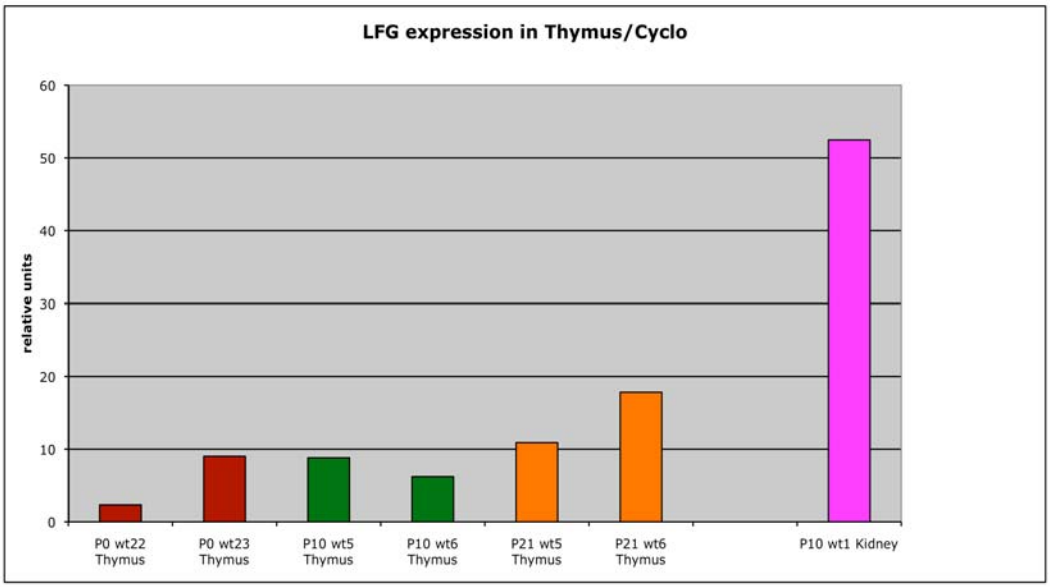

Figure 7.7- LFG expression in thymus by QPCR. Histogram of QPCR of LFG in thymus cDNA from different developmental stages as indicated. Kidney cDNA was used as a positive control and LFG values were normalized to cyclophillin.

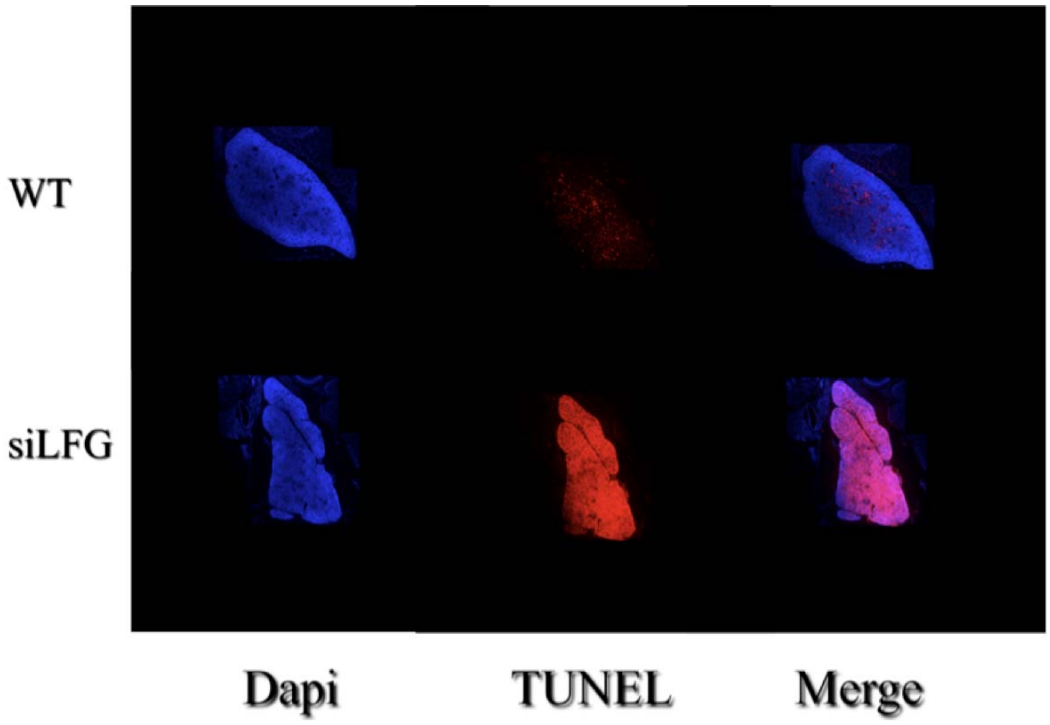

Figure 7.8- Increased apoptosis in siLFG P0 thymus. Sagittal sections of P0 thymus stained with Dapi (blue) and TUNEL (red).

Brain

LFG expression pattern and neuroanatomical analysis of the phenotype

The highest expression of LFG in adult mice is found in the brain. LFG *in situ* hybridization (ISH) was performed in brains from embryonic (E14.5, E16.5, E18.5) and postnatal (P0, P10) stages. Our results showed little or no expression during preplate splitting, although during late cortical plate formation (E18.5) the expression pattern of LFG is high in the developing cortical layers. Postnatally, LFG is expressed in all cortical layers (II-VI) with the exception of layer I; hippocampus (mainly CA3 and the granular cells of the dentate gyrus (DG)), piriform cortex and within the cerebellum, in the granular layer and Purkinje cells. So far the most extensive analysis was done in brains of P10 mice. ISH on brains from P10 wt and siLFG animals demonstrated successful downregulation of LFG expression in cerebellum, caudal cortex and the hippocampus (Figure 7.9).

Nissl staining showed apparently normal brain cortical cytoarchitecture, nevertheless the cerebellum presented reduced arborization and smaller size with loss of granular and Purkinje cells. The hippocampus was mostly normal except for the CA3 region that showed a splitting and lower cell density (Figures 7.10 and 7.11).

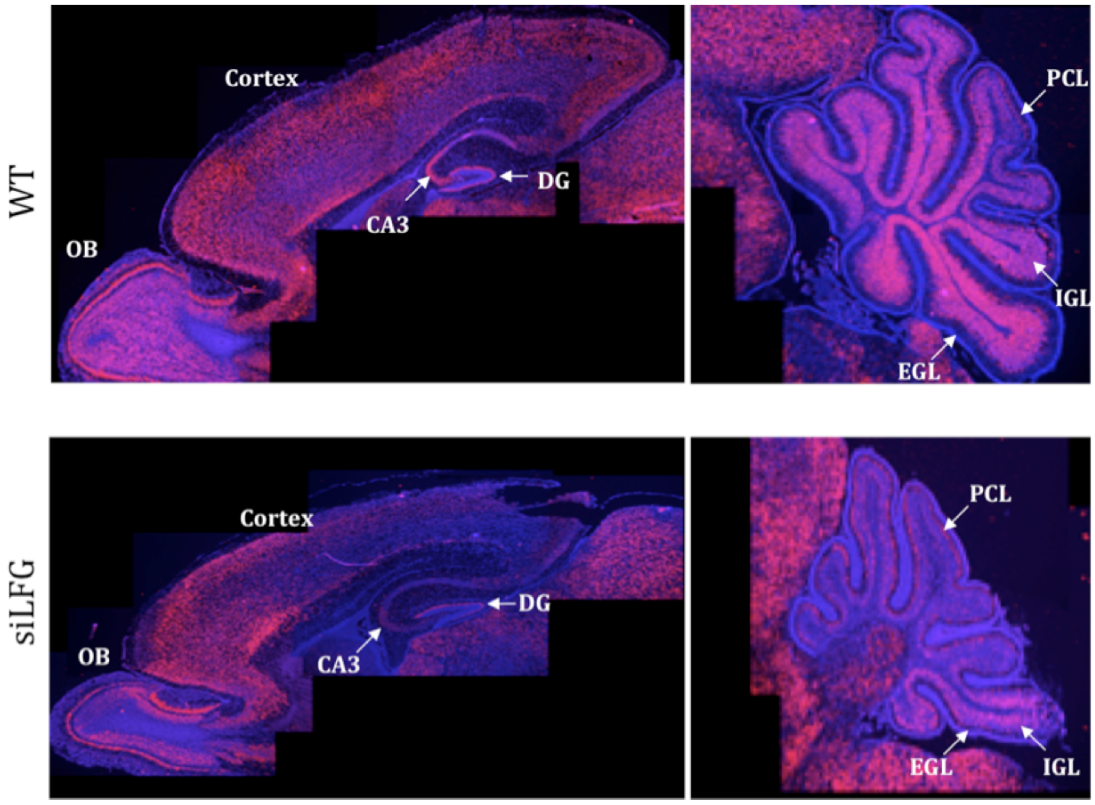

Figure 7.9- LFG expression pattern in the brain and knockdown validation. ISH sagittal sections from P10 wild type and siLFG brains, using the LFG probe (red) and counterstained with DAPI (blue).

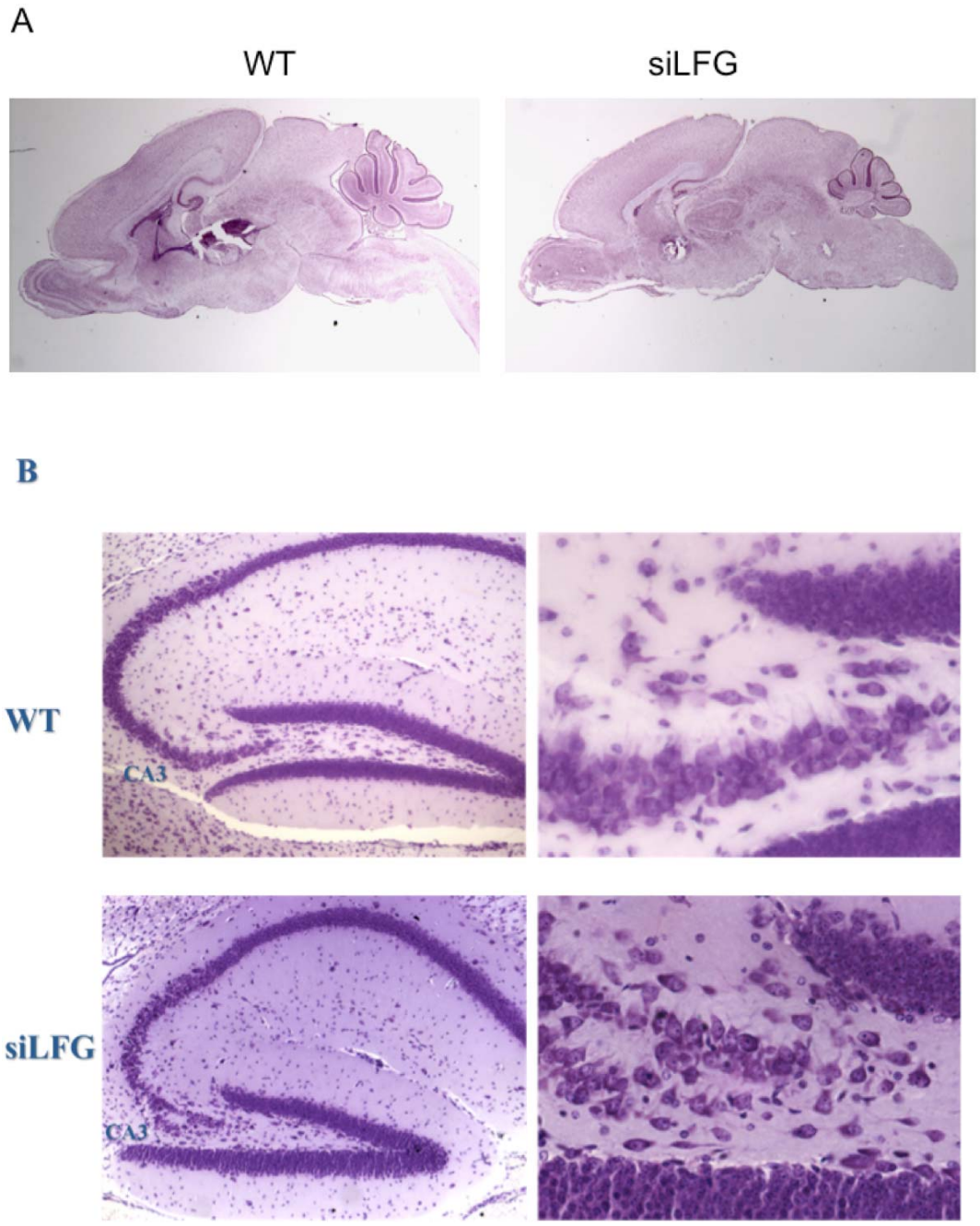

Figure 7.10- Cytoarchitechtural analysis of the brain by Nissl staining. Panoramic picture of cresyl violet stained sagittal sections of P5 wild type and siLFG brains (A). Nissl staining of sagittal sections of the hippocampus of wild type and siLFG mice at P35 (B).

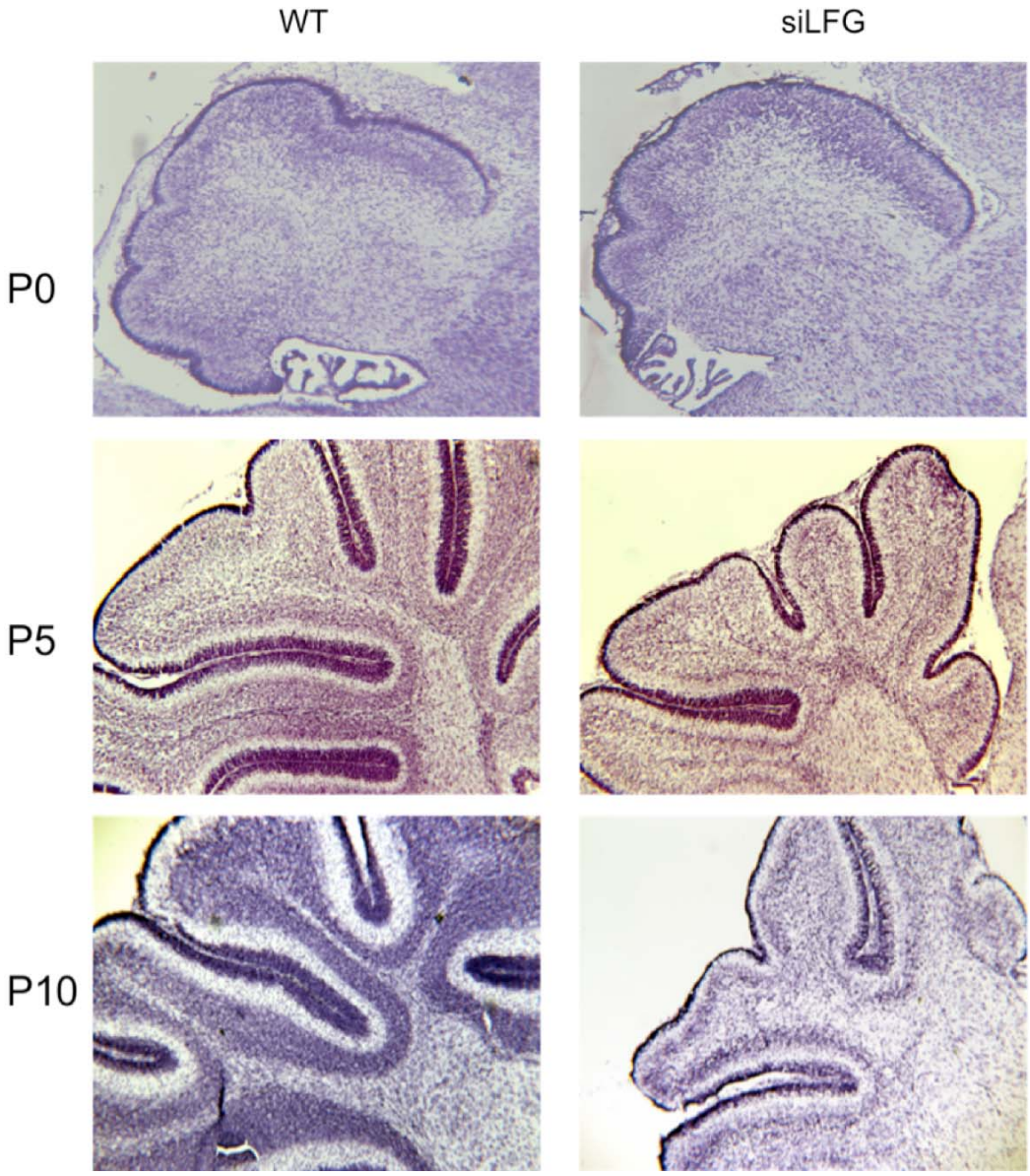

Figure 7.11- Cytoarchitechtural analysis of the cerebellum by Nissl staining. Cresyl violet stained sagittal sections of P0, P5 and P10 cerebella from wild type and siLFG mice.

Analysis of the cortical layers by *in situ* hybridization with layer-specific markers

The effects of LFG downregulation on cerebral cortex were investigated by ISH with specific probes for the different cortical layers. The results showed a reduction of several cortical layer markers such as ER81 and Tbr1 that are expressed in layers V and VI respectively. The layer IV marker RORβ was not affected in the siLFG mice. Reelin-positive GABAergic interneurons seemed to be especially sensitive to the donwregulation of LFG in the cortex (Figure 7.12).

The fact that the downregulation of LFG was much higher in the caudal cortex compared to the rostral cortex turned out to be a very useful control. If we look for example at the ER81 ISH we can see that in the siLFG mice ER81 expression is normal in the rostral cortex but the signal is very reduced in the medial and caudal part of the cortex, coinciding with the area where LFG expression was lower. In conclusion, the loss of LFG seemed to affect mostly deeper layers, such as V and VI, while the more superficial layers were less affected.

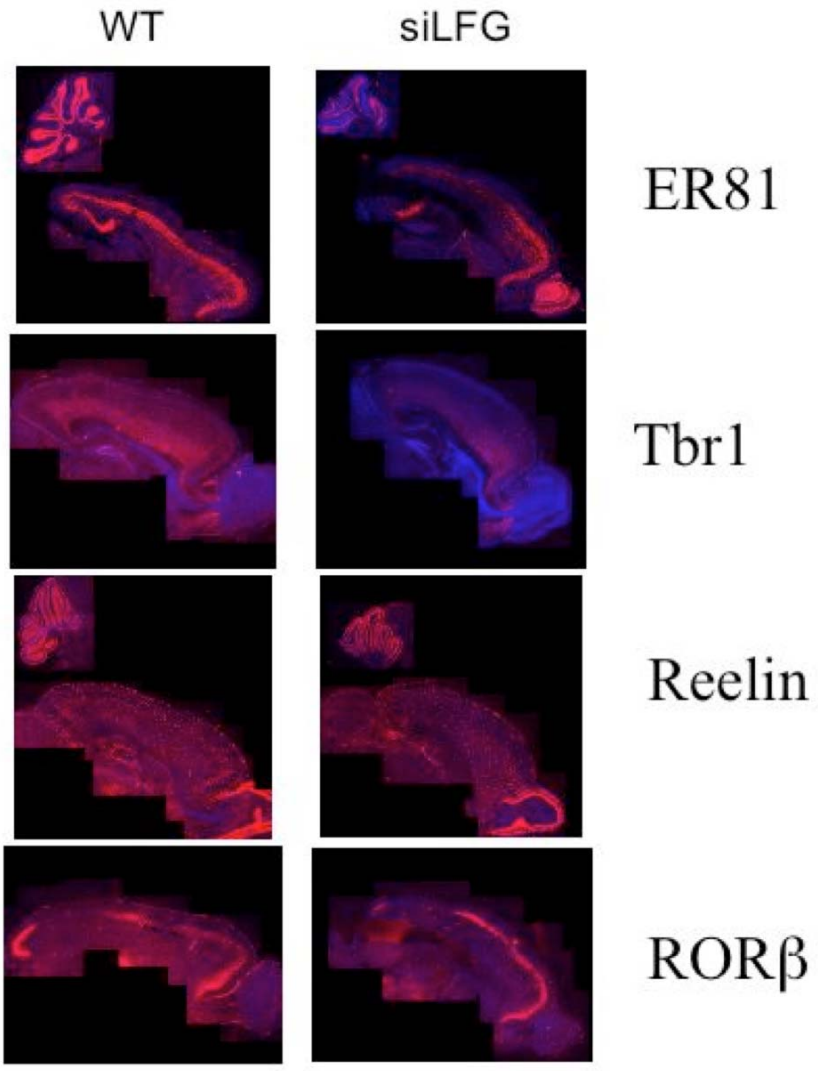

Figure 7.12- Analysis of cortical layers by ISH. ISH of P10 wild type and siLFG brain sagittal sections with the indicated probes (red) and counterstained with DAPI (blue).

siLFG mice have a predisposition for brain hemorrhages

Apart from the study of LFG's role in brain development, we studied the adult brain and examined several animals at 5 weeks of age. We noticed that 50% of the siLFG mice had hemorrhages in the brain, compared to none of the wild type. Sometimes the hemorrhages were localized to the area of the cerebellum with blood leaking into the hippocampus or other times smaller hemorrhages were found close to a blood vessel. Another observation was that the blood vessels of siLFG mice seemed to have an increased size and diameter (Figure 7.13).

Further analysis of the hemorrhagic brains was carried out by GFAP immunostaining, since astrocytes are known to be recruited to the sites of injury. The staining revealed an increase in GFAP positive astrocytes that localized around the blood vessels in the siLFG brains but not in the wild type ones (Figure 7.14).

A possible cause for the hemorrhages could be due to structural problems in the blood vessels of siLFG mice that can cause blood to leak out and produce the hemorrhage. To investigate this possibility we performed intravenous injection of FITC labeled tomato lectin together with Evans blue in order to see the structure of the blood vessels, that will be labeled by the lectin, and if these blood vessels are leaky by observing if the Evans blue stays inside the vessels or leaks out. Ten minutes after the injection we sacrificed the mice, harvested the brains and imaged by confocal microscopy. Lectin staining revealed a mostly normal structure and distribution of the blood vessels, but in some areas of some siLFG brains the blood vessels looked abnormal. Evans blue showed that some areas in the siLFG brains had a clear leak, while in other areas the Evans blue was confined to the blood vessel (Figure 7.15).

Chapter 7, in part will be prepared for submission for publication of the material. Sara Weiss contributed to this work. The dissertation author was the primary investigator and author of this material.

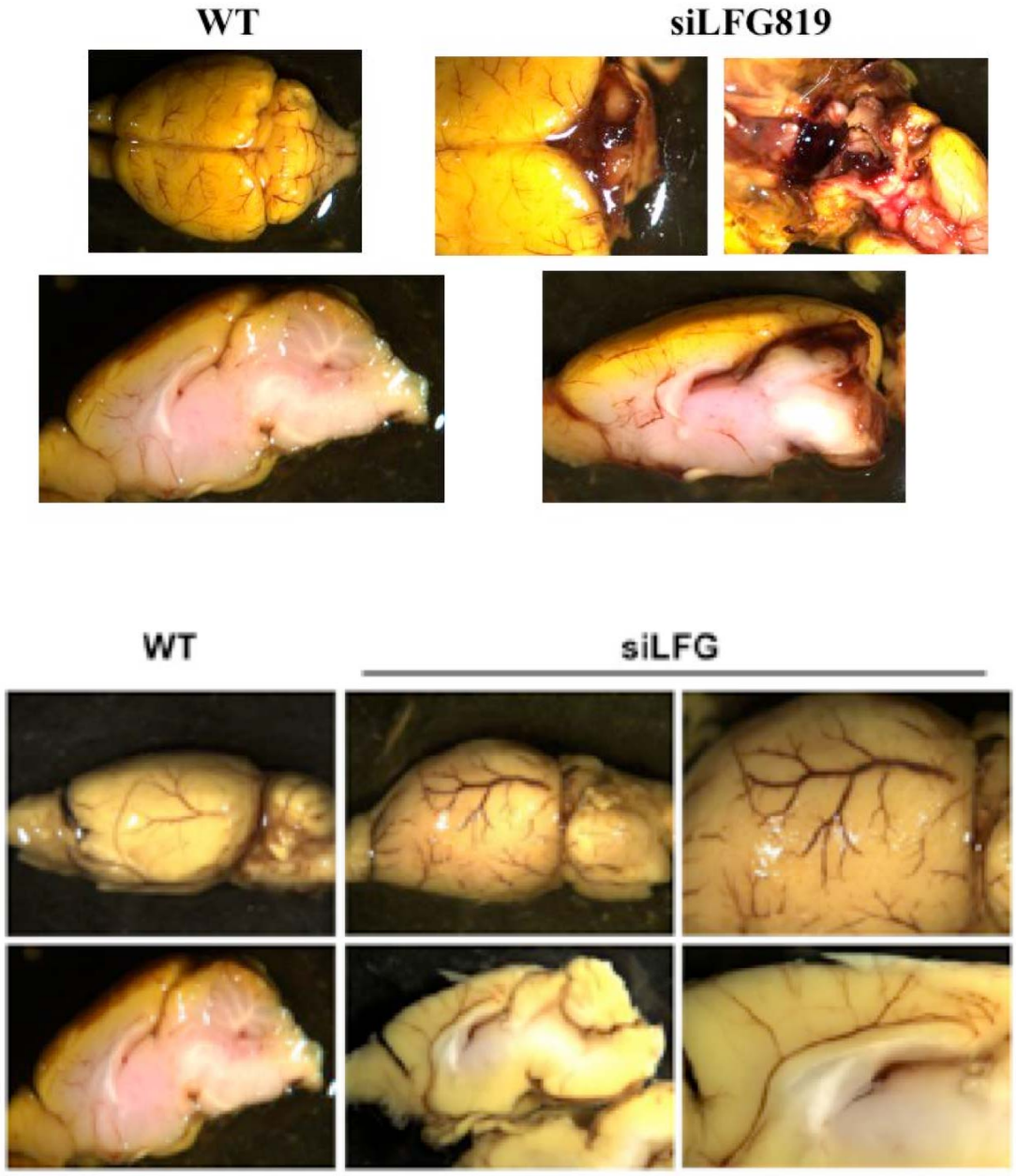

Figure 7.13- siLFG mice have brain hemorrhages and larger blood vessels. Pictures of wild type and siLFG brains to illustrate the hemorrhage and the larger blood vessel size of siLFG mice.

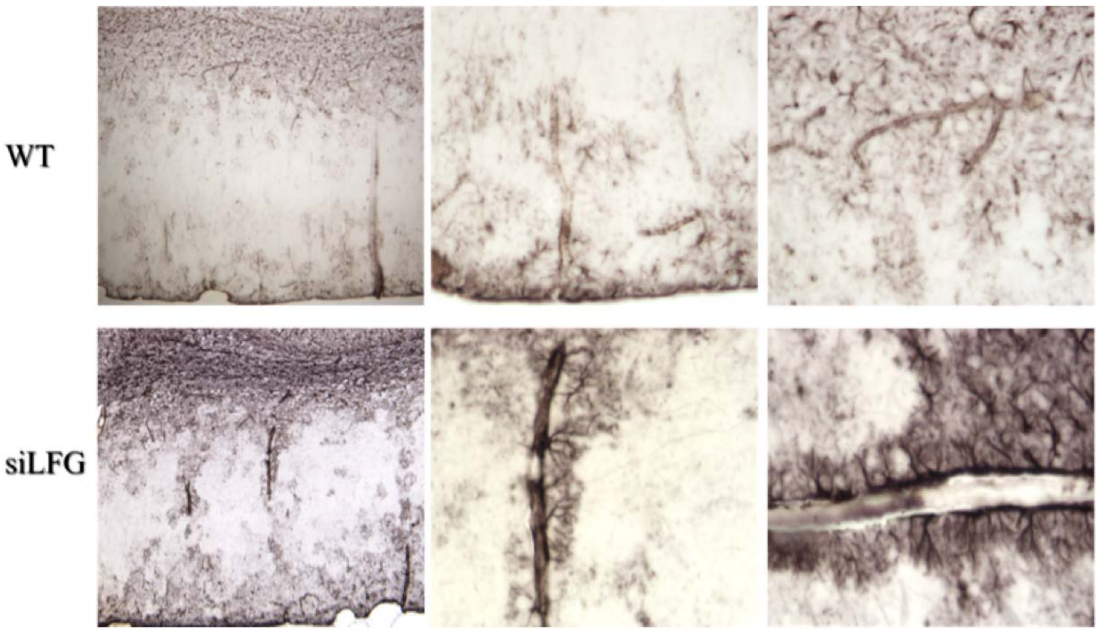

Figure 7.14- Astrocyte recruitment to blood vessels in siLFG mice. Sagittal sections of wild type and siLFG brains immunostained with GFAP.

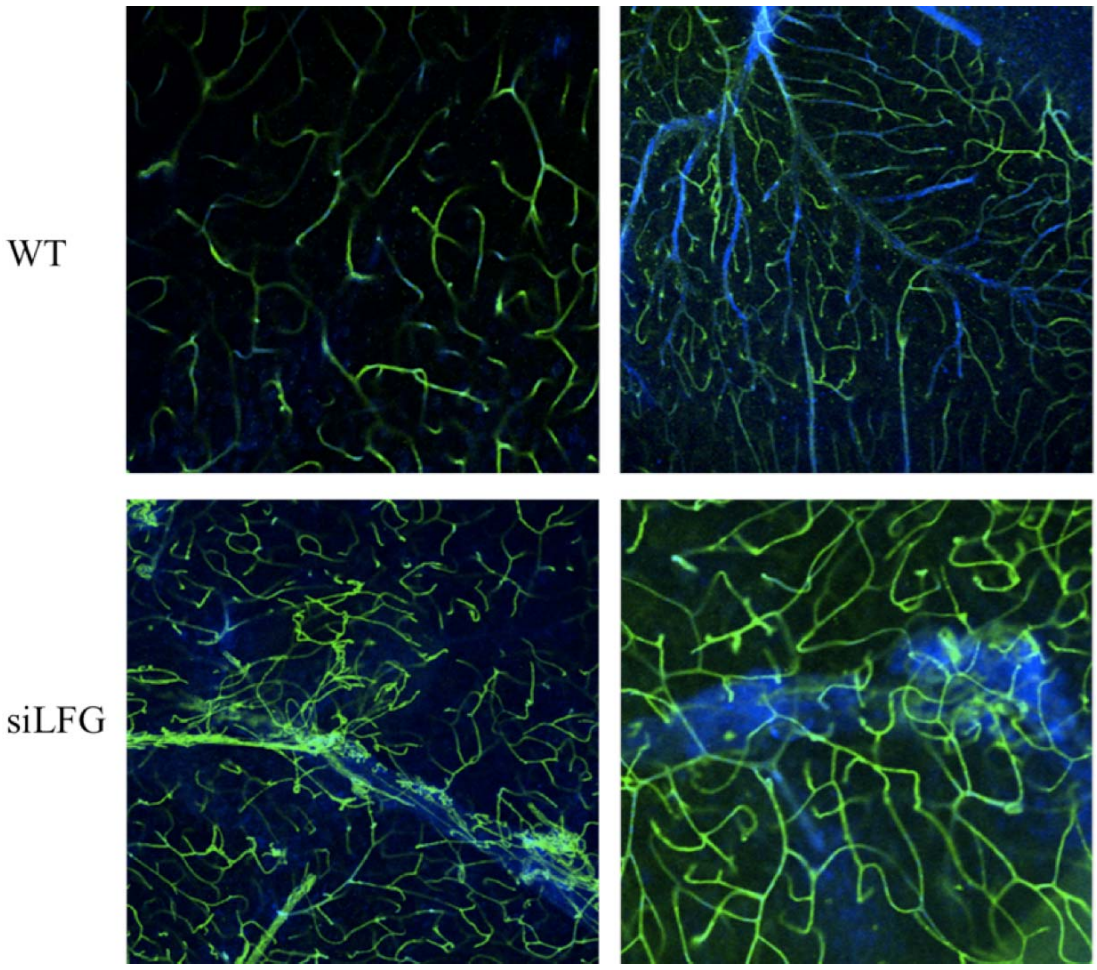

Figure 7.15- Analysis of blood vessel leakiness. Confocal images of brains from wild type and siLFG mice that were intravenously injected with FITC labeled tomato lectin (green) and Evans blue (blue).

Appendices

Materials and Methods

Cloning and validation of the short interfering RNAs (siRNAs)

The siRNA constructs were generated using a 94mer oligonucleotide that contains a 22 nucleotides sense and a 22 nucleotides antisense strand separated by a 9 nucleotides loop.

At the 5' end an XbaI site followed by a stretch of five adenines that serve as template for the Pol III promoter termination signal, and 25 nucleotides complementary to the 3' end of the mouse U6 pol III promoter. A PCR reaction using this 94 mer and a SP6 primer amplified a fragment containing the whole mouse U6 promoter and the siRNA sequences. XbaI and SpeI digestion allows ligation of the siRNA cassette into the NheI site located at the U3 region of a lentiviral vector containing an eGFP cassette driven by the mouse PGK promoter, as a transduction marker.

PCR conditions: 94 C for 3 minutes followed by 35 cycles of 94 C for 30 seconds, 55 C for 40 seconds and 72 C for 50 seconds.

Primer sequences (sense and antisense sequence in bold, loop underlined):

simLFG1- 5'-GCT GTC TAG ACA AAA A**GC CGT GTT CTT TGC AAC TTA CC**T CTC TTG AA**G GTA AGT TGC AAA GAA CAC GGC** AAA CAA GGC TTT TCT CCA AGG GAT A-3'; simLFG2- 5'-GCT GTC TAG ACA AAA A**GC CCT CAA CAT CTA CTT AGA CA**T CTC TTG AA**T GTC TAA GTA GAT GTT GAG GGC** AAA CAA GGC TTT TCT CCA AGG GAT A-3'; sihLFG1- 5'- GCT GTC TAG ACA AAA A**GC TGT GTT CTT TGC AAC CTA CC**T CTC

TTG AA**G GTA GGT TGC AAA GAA CAC AGC** AAA CAA GGC TTT TCT CCA AGG GAT A-3'; sihLFG5- 5'- GCT GTC TAG ACA AAA A**GC CCT CAA CAT TTA CCT AGA CA**T CTC TTG AA**T GTC TAG GTA AAT GTT GAG GGC** AAA CAA GGC TTT TCT CCA AGG GAT A-3'; siBACE and siGFP, (Singer et al., 2005) (Tiscornia et al., 2003).

The validation of the siRNA constructs was performed by calcium phosphate transfection of HEK293T cells together with a mouse LFG cDNA that contains a C' V5 tag or a human LFG cDNA that has a Flag tag in the N', in a 5:1 ratio followed by protein extraction and Western Blot using the V5 or Flag-M2 antibody (Invitrogen; Carlsbad, CA) (Sigma) and the p65 antibody (Santa Cruz) as a loading control.

Lentivirus production

Recombinant lentiviruses were produced by calcium phosphate transfection of HEK293T cells as previously described (Naldini et al., 1996b) (Naldini et al., 1996a). After 48 and 72 hours infectious lentiviruses were harvested and filtered through a 0.22 μm pore cellulose acetate filter and concentrated by ultracentrifugation (2h at 50,000g) followed by purification on a 20% sucrose gradient (2h at 46,000g) as described (Naldini et al., 1996a; Naldini et al., 1996b). The viral titer was assessed using an immunocapture p24-gag ELISA (alliance; DuPont-NEN) and by quantification of GFP positive cells after transduction of HEK293T cells by flow cytometry as previously described (Marr et al., 2003).

Generation of knockdown mice

The basic methodology has been described by our laboratory (Tiscornia et al., 2003). Briefly, 6 week-old B6D2 F1 females were superovulated by injecting 5 units of pregnant mare serum gonadotropin (Sigma), followed by injection of 5 units of human chorionic gonadotropin (Sigma) 48 hours later. At this time B6D2 F1 females are mated to B6D2 F1 males and the following day female oviducts are flushed with FHM medium (Specialty Media, Lavellette, NJ) in order to isolate fertilized eggs at the two-cell stage. Removal of the zona pellucida is performed by acidic tyrode treatment (Sigma) followed by transduction with 2,500 ng of p24 per ml in 5 μl of KSOM medium (Specialty Media) covered with light mineral oil. Forty-eight hours after transduction, blastocysts are transplanted into the uterus of ICR pseudopregnant females.

RNA Isolation, Reverse Transcription and Real-time PCR analysis

Total RNA was extracted using Trizol reagent (Invitrogen), followed by reverse transcription using SuperScript III First-strand Synthesis System (Invitrogen).

Quantitative PCR was performed using SYBR green in an ABI PRISM 7700 (Applied Biosystems).

Primer sequences are as follows:

mLFG1 5’-TGC CCT TCC AAT ACG TCC C-3’; GAA CAC ACC CGC TCC CAG T; mLFG2 5’-GGC TAA CCC CGG CTG GTA-3’; GCA AGC CAG AGT CAG GTA AGT TG; hLFG 5’- GTC ACC GTC TTC AGC TTC CAG-3’; AAG CAC GAA GAG CAC GCC; Cyclophilin 5’-GGC CGA TGA CGA GCC C-3’; TGT CTT

TGG AAC TTT GTC TGC AAA T; Actin 5'-TTC GTT GCC GGT CCA CA-3'; ACC AGC GCA GCG ATA TCG.

In situ hybridization

The full length LFG cDNA was cloned into pGEMTeasy and linearized by digestion with SpeI. The linear template was gel-purified and used to generate a riboprobe by *in vitro* transcription in the presence of [35S]-UTP. Other probes used were ER81, Tbr1, Reelin and RORβ. Radioactive *In situ* hybridization was performed as previously described (Liu et al., 2000).

Immunohistochemistry

Immunohistochemistry was performed as described by (Perez-Garcia et al., 2004) using the DAB colorimetric assay (Vector Laboratories).

Apoptosis induction and detection

Apoptosis was induced by incubation with 0.5 μg/ml of Fas agonist, CH11 for human cells or Jo2 for mouse cells. The incubation time was 24 hours except for the timepoint analysis in which the incubation times were 6, 8, 12 and 24 hours.

Apoptosis was detected by several methods:

TUNEL immunoassays were performed using the Cell death detection kit (Roche Molecular Biochemicals).

Annexin V staining followed by FACS analysis (BD Pharmingen).

CellTiter-Glo Luminescent Cell Viability assay that measures ATP as an index of metabolical activity in live cells (Promega).

Cerebellar slice cultures

Tissue slices were prepared from 11-day old wild type and LFG knockout mice. Cerebella were dissected in ice-cold oxygenated cerebrospinal fluid (ACSF) and cut sagittally with a vibratome at 400 μm. The ACSF consisted in 1mM $CaCl_2$, 10mM D-glucose, 4mM KCl, 5mM $MgCl_2$, 26mM $NaHCO_3$, 246mM sucrose and phenol red.

The slices were then transferred to six-well plates containing membrane inserts (Millicell CM, Millipore, Bedford, MA) and cultured in 75% MEM containing 25mM Hepes, 25% horse serum (Gibco, Grand Island, NY), 1mM glutamine, 5mg/ml glucose, penicillin (100 U/ml) and streptomycin (100 μg/ml) at 37 °C with 5% carbon dioxide as described by (Stoppini et al., 1991).

Slices were maintained in culture for five days with one change of media at day 3. On day 5 Fas agonistic antibody (Jo2) (0.5 μg/ml) was added to the culture media (BD Pharmingen). After 24 hours of incubation with Fas the slices were fixed and stained for TUNEL and calbindin according to the protocol of (Gogolla et al., 2006).

Slice imaging and statistical analysis

The slices were imaged with a Leica confocal microscope using the 488 and 568 excitation settings for calbindin and TUNEL respectively, with a 20X objective. For image quantification z-stacks of four images over 15 μm were taken. We analyzed

four representative images per mouse and per untreated or Fas treated condition. Within each image we defined two types of 3x3 fields: 1-The Purkinje field, based on the calbindin positive signal, 2-The internal granular layer field (IGL), adjacent to the Purkinje field with no calbindin positive cells. Three different 3x3 fields of each type were analyzed in each image to determine the number of TUNEL positive cells, making a total of 12 Purkinje fields and 12 IGL fields analyzed per mouse and per treatment. The statistical analysis was performed with the SigmaStat software and analyzed by two-way ANOVA followed by Tukey's *post hoc* test for multiple comparisons. ANOVA results were considered significant if $p < 0.05$.

Tissue preparation

All procedures were approved by the Institutional Animal Care Committee of the University of California San Diego. Mice were euthanized by Nembutal overdose and their brain was dissected. Brains were either fixed with Bouin and Paraffin embedded or fixed with 4%PFA followed by 30% sucrose and frozen in OCT.

Sagittal or coronal sections were cut using a microtome at 10μm for the Paraffin blocks or with a cryostat at 20μm for the frozen samples.

Analysis of brain vasculature and leakiness

Mice were intravenously injected with 100 μg of FITC tomato lectin (Vector Laboratories) and 1mg/ml Evans blue (Sigma). Fifteen minutes after injection their brain was harvested, sectioned with a brain matrix and analyzed by confocal microscopy.

Middle Cerebral Artery Occlusion (MCAO)

Transient focal cerebral ischemia was induced in wild type and LFG knockout mice. Middle cerebral artery occlusion (MCAO) was achieved by the intraluminal filament method. Briefly, a midline neck incision was made under a dissecting microscope; the right common carotid artery and external carotid artery (ECA) were isolated. The ECA was ligated with 6−0 silk suture distal from carotid bifurcation and ECA branch was then cut distal to ligation point. Another 6−0 silk suture was tied loosely around ECA close to the common carotid artery. A 6−0 monofilament nylon suture with heat-rounded tip was introduced into a small incision on ECA and advanced to the origin of the middle cerebral artery. The silk suture around the ECA stump was tied tightly to prevent bleeding and secure the nylon suture. Mice were subjected to 2 h of occlusion and cerebral infarction was determined at 24 h reperfusion by 2, 3, 5-triphenyltetrazolium chloride (TTC) histology. Slices were photographed, and images were analyzed with image-analysis software (Image J). Infarct volume in all slices was expressed as a percentage of the contralateral hemisphere after correcting for edema.

Bone marrow transplant and competitive repopulation assay

Murine total bone marrow hematopoietic progenitor donor cells were harvested from CD45.1 wild type or CD45.2 LFG null mice (background C57Bl6J) available through Jackson Laboratories (Bar Harbor, Maine). The donor cells were transplanted via tail vein injection, separated or mixed in a 1:1 ratio, into lethally irradiated RAG knockout C57Bl6J recipients (1100 rads; Cobalt-60 source) with a minimum cell dose

of 10^6 mononuclear cells per mouse. Transplanted mice were housed in micro-isolator housing for 5 weeks prior engraftment analysis. Peripheral blood was collected at 5, 10 and 15 weeks post transplant, stained with CD45.1, CD45.2, CD4, CD8, B220, Gr-1 and Mac-1 antibodies (BD Pharmingen) and analyzed by FACS.

Cell culture and Transfections

HeLa and 293T cells were cultured in Dulbecco's modified Eagle medium supplemented with 10% fetal calf serum (Hyclone). Transfections were performed by the calcium phosphate method or with Lipofectamine 2000 (Invitrogen).

Immunoprecipitations and Western blot

Cells were harvested in phophate buffer saline (PBS), pelleted, and resuspended in lysis buffer containing 20mM Tris-HCl, 1mM $CaCl_2$, 150mM NaCl, 1% Triton X-100 and protease inhibitors (Roche Molecular Biochemicals). After 30 minutes on ice the debris was pelleted at 15,000 rpm for 10 minutes and protein concentration of the supernatant was measured by Bradford assay (Biorad). Sample volume was determined for 1mg of protein and and brought up to twice the volume in 2x pulldown buffer containing 40mM Tris-HCl pH8, 500mM NaCl, 0.1% NP-40, 6mM EDTA and 6mM EGTA. Lysates were precleared with protein-G Sepharose (Amersham Pharmacia) for 1 hour at 4°C. Once precleared, the lysates were incubated with protein G and the corresponding IP antibody at 4°C overnight. The next day the lysates were washed three times in PBS and resuspended in SDS loading buffer, followed by heating at 95 °C for 10 minutes. Samples were resolved in 10% or 12%

Bis-Tris gels sing the Novex electrophoresis and transfer system. The gels were transferred to PVDF membranes (Immobilon P, Millipore), blocked in 5% milk or BSA in PBS containing 0.2% of Tween-20. Proteins were detected by chemoluminescence (Amersham).

Antibodies and Reagents

The following antibodies were used for this study: rabbit anti-LFG, generated by Imgenex, rabbit and mouse anti-Flag (Sigma), mouse anti-V5 (Invitrogen), mouse anti-Parvalbumin (Chemicon), rabbit and mouse anti-Calbindin (Swant), rabbit anti-Active Caspase 3 (Cell signaling), rabbit anti-GFAP (Neomarkers), rat anti-CD4, CD8, CD3, CD25, CD44, CD45.1, CD45.2, B220, Gr-1, Mac-1 (BD Pharmingen), human anti-Fas antibody CH11 (Upstate), mouse anti-Fas antibody Jo2 (BD Transduction Laboratories), anti-Fas 7C11 IgM (Immunotech), mouse anti-Caspase 8 (Cell Signaling), mouse anti-Caspase 3 (Cell signaling), mouse anti-FADD (BD Transduction Laboratories), mouse anti-AIP4 (Santa Cruz), rabbit anti-β Galactosidase (Abcam), mouse anti-IKK1 (BioSource International), mouse anti-Hemagglutinin (HA) (12CA5) (Roche Molecular Biochemicals), rabbit anti-Hsp70 (Cell Signaling), Alexa Fluor 488 goat anti-mouse IgG, Alexa Fluor 350 goat anti-rabbit, Alexa Fluor 594 goat anti-rabbit (Molecular Probes), anti-rabbit IgG-HRP, anti-mouse IgG-HRP, anti-mouse IgG1-HRP, anti-mouse IgG2b-HRP (Santa Cruz biotechnology), TTC (Sigma), FITC- Tomato Lectin (Vector Laboratories), Evans Blue (Sigma), Dexamethasone (Sigma).

References

Andressen, C., Gotzos, V., Berchtold, M.W., Pauls, T.L., Schwaller, B., Fellay, B., and Celio, M.R. (1995). Changes in shape and motility of cells transfected with parvalbumin cDNA. Exp Cell Res *219*, 420-426.

Bai, J., Ramos, R.L., Ackman, J.B., Thomas, A.M., Lee, R.V., and LoTurco, J.J. (2003). RNAi reveals doublecortin is required for radial migration in rat neocortex. Nat Neurosci *6*, 1277-1283.

Baurle, J., Hoshi, M., and Grusser-Cornehls, U. (1998). Dependence of parvalbumin expression on Purkinje cell input in the deep cerebellar nuclei. J Comp Neurol *392*, 499-514.

Beier, C.P., Wischhusen, J., Gleichmann, M., Gerhardt, E., Pekanovic, A., Krueger, A., Taylor, V., Suter, U., Krammer, P.H., Endres, M., *et al.* (2005). FasL (CD95L/APO-1L) resistance of neurons mediated by phosphatidylinositol 3-kinase-Akt/protein kinase B-dependent expression of lifeguard/neuronal membrane protein 35. J Neurosci *25*, 6765-6774.

Benayed, R., Gharani, N., Rossman, I., Mancuso, V., Lazar, G., Kamdar, S., Bruse, S.E., Tischfield, S., Smith, B.J., Zimmerman, R.A., *et al.* (2005). Support for the homeobox transcription factor gene ENGRAILED 2 as an autism spectrum disorder susceptibility locus. Am J Hum Genet *77*, 851-868.

Boatright, K.M., Renatus, M., Scott, F.L., Sperandio, S., Shin, H., Pedersen, I.M., Ricci, J.E., Edris, W.A., Sutherlin, D.P., Green, D.R., *et al.* (2003). A unified model for apical caspase activation. Molecular Cell *11*, 529-541.

Bourrat, F., and Sotelo, C. (1984). Postnatal development of the inferior olivary complex in the rat. III. A morphometric analysis of volumetric growth and neuronal cell number. Brain Res *318*, 241-251.

Broughton, B.R., Reutens, D.C., and Sobey, C.G. (2009). Apoptotic mechanisms after cerebral ischemia. Stroke *40*, e331-339.

Brunet, A., Bonni, A., Zigmond, M.J., Lin, M.Z., Juo, P., Hu, L.S., Anderson, M.J., Arden, K.C., Blenis, J., and Greenberg, M.E. (1999). Akt promotes cell survival by phosphorylating and inhibiting a Forkhead transcription factor. Cell *96*, 857-868.

Chang, L., Kamata, H., Solinas, G., Luo, J.L., Maeda, S., Venuprasad, K., Liu, Y.C., and Karin, M. (2006). The E3 ubiquitin ligase itch couples JNK activation to TNFalpha-induced cell death by inducing c-FLIP(L) turnover. Cell *124*, 601-613.

Corbo, J.C., Deuel, T.A., Long, J.M., LaPorte, P., Tsai, E., Wynshaw-Boris, A., and Walsh, C.A. (2002). Doublecortin is required in mice for lamination of the hippocampus but not the neocortex. J Neurosci *22*, 7548-7557.

Delhaye-Bouchaud, N., Geoffroy, B., and Mariani, J. (1985). Neuronal death and synapse elimination in the olivocerebellar system. I. Cell counts in the inferior olive of developing rats. J Comp Neurol *232*, 299-308.

Dempsey, P.W., Doyle, S.E., He, J.Q., and Cheng, G. (2003). The signaling adaptors and pathways activated by TNF superfamily. Cytokine & Growth Factor Reviews *14*, 193-209.

Doughty, M.L., De Jager, P.L., Korsmeyer, S.J., and Heintz, N. (2000). Neurodegeneration in Lurcher mice occurs via multiple cell death pathways. J Neurosci *20*, 3687-3694.

Drappa, J., Brot, N., and Elkon, K.B. (1993). The Fas protein is expressed at high levels on CD4+CD8+ thymocytes and activated mature lymphocytes in normal mice but not in the lupus-prone strain, MRL lpr/lpr. Proc Natl Acad Sci U S A *90*, 10340-10344.

Earnshaw, W.C., Martins, L.M., and Kaufmann, S.H. (1999). Mammalian caspases: structure, activation, substrates, and functions during apoptosis. Annual Review of Biochemistry *68*, 383-424.

Farah, C.A., Liazoghli, D., Perreault, S., Desjardins, M., Guimont, A., Anton, A., Lauzon, M., Kreibich, G., Paiement, J., and Leclerc, N. (2005). Interaction of microtubule-associated protein-2 and p63: a new link between microtubules and rough endoplasmic reticulum membranes in neurons. J Biol Chem *280*, 9439-9449.

Fernandez, M., Segura, M.F., Sole, C., Colino, A., Comella, J.X., and Cena, V. (2007). Lifeguard/neuronal membrane protein 35 regulates Fas ligand-mediated apoptosis in neurons via microdomain recruitment. J Neurochem *103*, 190-203.

Ghoumari, A.M., Wehrle, R., Bernard, O., Sotelo, C., and Dusart, I. (2000). Implication of Bcl-2 and Caspase-3 in age-related Purkinje cell death in murine organotypic culture: an in vitro model to study apoptosis. Eur J Neurosci *12*, 2935-2949.

Gogolla, N., Galimberti, I., DePaola, V., and Caroni, P. (2006). Staining protocol for organotypic hippocampal slice cultures. Nat Protoc *1*, 2452-2456.

Golstein, P. (2000). Signal transduction. FasL binds preassembled Fas.[see comment][comment]. Science *288*, 2328-2329.

Gratiot-Deans, J., Merino, R., Nunez, G., and Turka, L.A. (1994). Bcl-2 expression during T-cell development: early loss and late return occur at specific stages of commitment to differentiation and survival. Proc Natl Acad Sci U S A *91*, 10685-10689.

Hatten, M.E. (1990). Riding the glial monorail: a common mechanism for glial-guided neuronal migration in different regions of the developing mammalian brain. Trends Neurosci *13*, 179-184.

Jankowski, J., Holst, M.I., Liebig, C., Oberdick, J., and Baader, S.L. (2004). Engrailed-2 negatively regulates the onset of perinatal Purkinje cell differentiation. J Comp Neurol *472*, 87-99.

Janowsky, J.S., and Finlay, B.L. (1983). Cell degeneration in early development of the forebrain and cerebellum. Anat Embryol (Berl) *167*, 439-447.

Jensen, P., Zoghbi, H.Y., and Goldowitz, D. (2002). Dissection of the cellular and molecular events that position cerebellar Purkinje cells: a study of the math1 null-mutant mouse. J Neurosci *22*, 8110-8116.

Jung, A.R., Kim, T.W., Rhyu, I.J., Kim, H., Lee, Y.D., Vinsant, S., Oppenheim, R.W., and Sun, W. (2008). Misplacement of Purkinje cells during postnatal development in Bax knock-out mice: a novel role for programmed cell death in the nervous system? J Neurosci *28*, 2941-2948.

Kerr, J.F., Wyllie, A.H., and Currie, A.R. (1972). Apoptosis: a basic biological phenomenon with wide-ranging implications in tissue kinetics. British Journal of Cancer *26*, 239-257.

Kitao, Y., Hashimoto, K., Matsuyama, T., Iso, H., Tamatani, T., Hori, O., Stern, D.M., Kano, M., Ozawa, K., and Ogawa, S. (2004). ORP150/HSP12A regulates Purkinje cell survival: a role for endoplasmic reticulum stress in cerebellar development. J Neurosci *24*, 1486-1496.

Koizumi, H., Tanaka, T., and Gleeson, J.G. (2006). Doublecortin-like kinase functions with doublecortin to mediate fiber tract decussation and neuronal migration. Neuron *49*, 55-66.

Krammer, P.H. (2000). CD95's deadly mission in the immune system. Nature *407*, 789-795.

Le-Niculescu, H., Bonfoco, E., Kasuya, Y., Claret, F.X., Green, D.R., and Karin, M. (1999). Withdrawal of survival factors results in activation of the JNK pathway in neuronal cells leading to Fas ligand induction and cell death. Mol Cell Biol *19*, 751-763.

Li, H., Zhu, H., Xu, C.J., and Yuan, J. (1998). Cleavage of BID by caspase 8 mediates the mitochondrial damage in the Fas pathway of apoptosis. Cell *94*, 491-501.

Liu, Q., Dwyer, N.D., and O'Leary, D.D. (2000). Differential expression of COUP-TFI, CHL1, and two novel genes in developing neocortex identified by differential display PCR. J Neurosci *20*, 7682-7690.

Lossi, L., and Merighi, A. (2003). In vivo cellular and molecular mechanisms of neuronal apoptosis in the mammalian CNS. Prog Neurobiol *69*, 287-312.

Luo, J., Treubert-Zimmermann, U., and Redies, C. (2004). Cadherins guide migrating Purkinje cells to specific parasagittal domains during cerebellar development. Mol Cell Neurosci *25*, 138-152.

Luo, X., Budihardjo, I., Zou, H., Slaughter, C., and Wang, X. (1998). Bid, a Bcl2 interacting protein, mediates cytochrome c release from mitochondria in response to activation of cell surface death receptors. Cell *94*, 481-490.

Marr, R.A., Rockenstein, E., Mukherjee, A., Kindy, M.S., Hersh, L.B., Gage, F.H., Verma, I.M., and Masliah, E. (2003). Neprilysin gene transfer reduces human amyloid pathology in transgenic mice. J Neurosci *23*, 1992-1996.

Martin-Villalba, A., Herr, I., Jeremias, I., Hahne, M., Brandt, R., Vogel, J., Schenkel, J., Herdegen, T., and Debatin, K.M. (1999). CD95 ligand (Fas-L/APO-1L) and tumor necrosis factor-related apoptosis-inducing ligand mediate ischemia-induced apoptosis in neurons. J Neurosci *19*, 3809-3817.

Miale, I.L., and Sidman, R.L. (1961). An autoradiographic analysis of histogenesis in the mouse cerebellum. Exp Neurol *4*, 277-296.

Nagata, S. (1999). Fas ligand-induced apoptosis. Annual Review of Genetics *33*, 29-55.

Naldini, L., Blomer, U., Gage, F.H., Trono, D., and Verma, I.M. (1996a). Efficient transfer, integration, and sustained long-term expression of the transgene in adult rat brains injected with a lentiviral vector. Proc Natl Acad Sci U S A *93*, 11382-11388.

Naldini, L., Blomer, U., Gallay, P., Ory, D., Mulligan, R., Gage, F.H., Verma, I.M., and Trono, D. (1996b). In vivo gene delivery and stable transduction of nondividing cells by a lentiviral vector. Science *272*, 263-267.

Nishimura, Y., Ishii, A., Kobayashi, Y., Yamasaki, Y., and Yonehara, S. (1995). Expression and function of mouse Fas antigen on immature and mature T cells. J Immunol *154,* 4395-4403.

Perez-Garcia, C.G., Tissir, F., Goffinet, A.M., and Meyer, G. (2004). Reelin receptors in developing laminated brain structures of mouse and human. Eur J Neurosci *20,* 2827-2832.

Peter, M.E., and Krammer, P.H. (2003). The CD95(APO-1/Fas) DISC and beyond. Cell Death & Differentiation *10,* 26-35.

Rakic, P. (1971). Neuron-glia relationship during granule cell migration in developing cerebellar cortex. A Golgi and electronmicroscopic study in Macacus Rhesus. J Comp Neurol *141,* 283-312.

Raoul, C., Henderson, C.E., and Pettmann, B. (1999). Programmed cell death of embryonic motoneurons triggered through the Fas death receptor. J Cell Biol *147,* 1049-1062.

Raoul, C., Pettmann, B., and Henderson, C.E. (2000). Active killing of neurons during development and following stress: a role for p75(NTR) and Fas? Curr Opin Neurobiol *10,* 111-117.

Reimers, K., Choi, C.Y., Mau-Thek, E., and Vogt, P.M. (2006). Sequence analysis shows that Lifeguard belongs to a new evolutionarily conserved cytoprotective family. Int J Mol Med *18,* 729-734.

Rosenbaum, D.M., Gupta, G., D'Amore, J., Singh, M., Weidenheim, K., Zhang, H., and Kessler, J.A. (2000). Fas (CD95/APO-1) plays a role in the pathophysiology of focal cerebral ischemia. J Neurosci Res *61,* 686-692.

Rothenberg, E.V., and Taghon, T. (2005). Molecular genetics of T cell development. Annu Rev Immunol *23,* 601-649.

Schweitzer, B., Suter, U., and Taylor, V. (2002). Neural membrane protein 35/Lifeguard is localized at postsynaptic sites and in dendrites. Brain Research Molecular Brain Research *107*, 47-56.

Schweitzer, B., Taylor, V., Welcher, A.A., McClelland, M., and Suter, U. (1998). Neural membrane protein 35 (NMP35): a novel member of a gene family which is highly expressed in the adult nervous system. Mol Cell Neurosci *11*, 260-273.

Schweizer, A., Ericsson, M., Bachi, T., Griffiths, G., and Hauri, H.P. (1993a). Characterization of a novel 63 kDa membrane protein. Implications for the organization of the ER-to-Golgi pathway. J Cell Sci *104 (Pt 3)*, 671-683.

Schweizer, A., Rohrer, J., Jeno, P., DeMaio, A., Buchman, T.G., and Hauri, H.P. (1993b). A reversibly palmitoylated resident protein (p63) of an ER-Golgi intermediate compartment is related to a circulatory shock resuscitation protein. J Cell Sci *104 (Pt 3)*, 685-694.

Selimi, F., Doughty, M., Delhaye-Bouchaud, N., and Mariani, J. (2000). Target-related and intrinsic neuronal death in Lurcher mutant mice are both mediated by caspase-3 activation. J Neurosci *20*, 992-1000.

Siegel, R.M., Frederiksen, J.K., Zacharias, D.A., Chan, F.K., Johnson, M., Lynch, D., Tsien, R.Y., and Lenardo, M.J. (2000). Fas preassociation required for apoptosis signaling and dominant inhibition by pathogenic mutations.[see comment]. Science *288*, 2354-2357.

Singer, O., Marr, R.A., Rockenstein, E., Crews, L., Coufal, N.G., Gage, F.H., Verma, I.M., and Masliah, E. (2005). Targeting BACE1 with siRNAs ameliorates Alzheimer disease neuropathology in a transgenic model. Nat Neurosci *8*, 1343-1349.

Somia, N.V., Schmitt, M.J., Vetter, D.E., Van Antwerp, D., Heinemann, S.F., and Verma, I.M. (1999). LFG: an anti-apoptotic gene that provides protection from Fas-mediated cell death. Proc Natl Acad Sci U S A *96*, 12667-12672.

Sprent, J., and Kishimoto, H. (2002). The thymus and negative selection. Immunol Rev *185*, 126-135.

Stoppini, L., Buchs, P.A., and Muller, D. (1991). A simple method for organotypic cultures of nervous tissue. J Neurosci Methods *37*, 173-182.

Suzuki, K., Sakai, K., Koike, T (1999). Genes involved in programmed cell death of cerebellar granule neurons Neural Development, 176-179.

Tiscornia, G., Singer, O., Ikawa, M., and Verma, I.M. (2003). A general method for gene knockdown in mice by using lentiviral vectors expressing small interfering RNA. Proc Natl Acad Sci U S A *100*, 1844-1848.

Van Parijs, L., Biuckians, A., and Abbas, A.K. (1998). Functional roles of Fas and Bcl-2-regulated apoptosis of T lymphocytes. J Immunol *160*, 2065-2071.

Veis, D.J., Sorenson, C.M., Shutter, J.R., and Korsmeyer, S.J. (1993). Bcl-2-deficient mice demonstrate fulminant lymphoid apoptosis, polycystic kidneys, and hypopigmented hair. Cell *75*, 229-240.

Wallace, V.A. (1999). Purkinje-cell-derived Sonic hedgehog regulates granule neuron precursor cell proliferation in the developing mouse cerebellum. Curr Biol *9*, 445-448.

Wallach, D., Varfolomeev, E.E., Malinin, N.L., Goltsev, Y.V., Kovalenko, A.V., and Boldin, M.P. (1999). Tumor necrosis factor receptor and Fas signaling mechanisms. Annual Review of Immunology *17*, 331-367.

Watanabe, D., Suda, T., Hashimoto, H., and Nagata, S. (1995). Constitutive activation of the Fas ligand gene in mouse lymphoproliferative disorders. EMBO J *14*, 12-18.

Weber, C.H., and Vincenz, C. (2001). The death domain superfamily: a tale of two interfaces? Trends in Biochemical Sciences *26*, 475-481.

White, F.A., Keller-Peck, C.R., Knudson, C.M., Korsmeyer, S.J., and Snider, W.D. (1998). Widespread elimination of naturally occurring neuronal death in Bax-deficient mice. J Neurosci *18*, 1428-1439.

Wullner, U., Loschmann, P.A., Weller, M., and Klockgether, T. (1995). Apoptotic cell death in the cerebellum of mutant weaver and lurcher mice. Neurosci Lett *200*, 109-112.

Yuasa, S., Kitoh, J., Oda, S., and Kawamura, K. (1993). Obstructed migration of Purkinje cells in the developing cerebellum of the reeler mutant mouse. Anat Embryol (Berl) *188*, 317-329.

Zanjani, H.S., Vogel, M.W., Delhaye-Bouchaud, N., Martinou, J.C., and Mariani, J. (1996). Increased cerebellar Purkinje cell numbers in mice overexpressing a human bcl-2 transgene. J Comp Neurol *374*, 332-341.